Temporal order of clinical and biomarker changes in familial frontotemporal dementia

Adam M. Staffaroni PhD,[1] Melanie Quintana PhD,[2] Barbara Wendelberger PhD,[2] Hilary W. Heuer PhD,[1] Lucy L. Russell PhD,[3] Yann Cobigo PhD,[1] Amy Wolf MS,[1] Sheng-Yang Matt Goh MS,[1] Leonard Petrucelli PhD,[4] Tania F. Gendron PhD,[4] Carolin Heller BSc,[3] Annie L. Clark MS, [1] Jack Carson Taylor MS,[1] Amy Wise BA,[1] Elise Ong BS,[1] Leah Forsberg PhD,[5] Danielle Brushaber BS,[6] Julio C. Rojas MD PhD,[1] Lawren VandeVrede MD PhD,[1] Peter Ljubenkov MD,[1] Joel Kramer PsyD,[1] Kaitlin B. Casaletto PhD,[1] Brian Appleby MD,[7] Yvette Bordelon MD PhD,[8] Hugo Botha MD,[5] Bradford C. Dickerson MD,[9] Kimiko Domoto-Reilly MD,[10] Julie A. Fields PhD,[11] Tatiana Foroud PhD,[12] Ralitza Gavrilova MD,[5] Daniel Geschwind MD PhD,[8,13] Nupur Ghoshal MD PhD,[14] Jill Goldman MS MPhil,[15] Jonathon Graff-Radford MD,[5] Neill Graff-Radford MD,[16] Murray Grossman MD EdD,[17] Matthew GH Hall MS,[1] Ging-Yuek Hsiung MD MHSc,[18] Edward D. Huey MD,[15] David Irwin MD,[17] David T. Jones MD,[5] Kejal Kantarci MD,[5] Daniel Kaufer MD,[19] David Knopman MD,[5] Walter Kremers PhD,[6] Argentina Lario Lago PhD,[1] Maria I. Lapid MD,[11] Irene Litvan MD,[20] Diane Lucente MS,[9] Ian R. Mackenzie MD,[21] Mario F. Mendez MD PhD,[8] Carly Mester BA,[6] Bruce L. Miller MD,[1] Chiadi U. Onyike MD,[22] Rosa Rademakers PhD,[4,23,24] Vijay K. Ramanan MD PhD,[5] Eliana Marisa Ramos PhD,[8] Meghana Rao MPH,[5] Katya Rascovsky PhD,[17] Katherine P. Rankin PhD,[1] Erik D. Roberson MD PhD,[25] Rodolfo Savica MD PhD,[5] M. Carmela Tartaglia MD,[26] Sandra Weintraub PhD,[27] Bonnie Wong PhD,[9] David M Cash PhD,[3] Arabella Bouzigues MSc,[3] Imogen J Swift MSc,[3] Georgia Peakman MSc,[3] Martina Bocchetta PhD,[3] Emily G. Todd MRes,[3] Rhian S. Convery MSc,[3] James B. Rowe PhD,[28] Barbara Borroni MD,[29] Daniela Galimberti PhD,[30,31] Pietro Tiraboschi MD,[32] Mario Masellis MD PhD,[33] Elizabeth Finger MD,[34] John C. van Swieten MD PhD,[35] Harro Seelaar MD PhD,[35] Lize C. Jiskoot PhD,[35] Sandro Sorbi MD PhD,[36,37] Chris R. Butler PhD,[38,39] Caroline Graff PhD RN,[40,41] Alexander Gerhard MD,[42,43] Tobias Langheinrich MD,[42,44] Robert Laforce MD PhD,[45] Raquel Sanchez-Valle MD PhD,[46] Alexandre de Mendonça MD PhD,[47] Fermin Moreno MD,[48,49] Matthis Synofzik MD,[50,51] Rik Vandenberghe MD,[52,53,54] Simon Ducharme MD,[55,56] Isabelle Le Ber MD PhD,[57,58,59] Johannes Levin MD,[60,61,62] Adrian Danek MD,[60] Markus Otto MD,[63] Florence Pasquier MD PhD,[64,65,66] Isabel Santana MD PhD,[67,68] John Kornak PhD,[69] Bradley F. Boeve MD,[5] Howard J. Rosen MD[1], Jonathan D. Rohrer FRCP PhD,[3] Adam. L. Boxer MD PhD[1] and Frontotemporal Dementia Prevention Initiative (FPI) Investigators*

[1] University of California, San Francisco, Weill Institute for Neurosciences, Department of Neurology, Memory and Aging Center, San Francisco, CA
[2] Berry Consultants, Austin, TX
[3] Dementia Research Centre, Department of Neurodegenerative Disease, UCL Queen Square London
[4] Mayo Clinic, Department of Neuroscience, Jacksonville, FL, USA
[5] Mayo Clinic, Department of Neurology, Rochester, MN, USA
[6] Mayo Clinic, Department of Quantitative Health Sciences, Rochester, MN, USA
[7] Case Western Reserve University, Department of Neurology, Cleveland, OH, USA
[8] University of California, Los Angeles, Department of Neurology, Los Angeles, CA, USA
[9] Department of Neurology, Massachusetts General Hospital and Harvard Medical School, Boston MA
[10] University of Washington, Department of Neurology, Seattle, WA, USA
[11] Mayo Clinic, Department of Psychiatry and Psychology, Rochester, MN, USA

[12] Indiana University School of Medicine, National Centralized Repository for Alzheimer's, IN, USA
[13] Institute for Precision Health, David Geffen School of Medicine, University of California, Los Angeles, Los Angeles, CA, USA
[14] Departments of Neurology and Psychiatry, Washington University School of Medicine, Washington University, St. Louis, MO, USA
[15] Columbia University, Department of Neurology, New York, NY, USA
[16] Mayo Clinic, Department of Neurology, Jacksonville, FL, USA
[17] University of Pennsylvania, Department of Neurology, Philadelphia, PA, USA
[18] University of British Columbia, Division of Neurology, Vancouver, BC, CA
[19] University of North Carolina, Department of Neurology, Chapel Hill, NC, USA
[20] University of California, San Diego, Department of Neurosciences, La Jolla, CA, USA
[21] Department of Pathology, University of British Columbia. Vancouver, BC, CA
[22] Johns Hopkins University, Department of Psychiatry and Behavioral Sciences, Baltimore, MD, USA
[23] Applied and Translational Neurogenomics Group, VIB Center for Molecular Neurology, VIB, Antwerp, Belgium
[24] Department of Biomedical Sciences, University of Antwerp, Antwerp, Belgium
[25] University of Alabama at Birmingham, Department of Neurology, Birmingham, AL
[26] Tanz Centre for Research in Neurodegenerative Diseases, Division of Neurology, University of Toronto, Toronto, Ontario, Canada
[27] Northwestern University, Department of Neurology, Chicago, IL, USA
[28] Department of Clinical Neurosciences and Cambridge University Hospitals NHS Trust and Medical Research Council Cognition and Brain Sciences Unit, University of Cambridge, Cambridge, UK
[29] Centre for Neurodegenerative Disorders, Department of Clinical and Experimental Sciences, University of Brescia, Brescia, Italy
[30] Department of Biomedical, Surgical and Dental Sciences, University of Milan, Milan, Italy
[31] Fondazione IRCCS Ca' Granda, Ospedale Maggiore Policlinico, Milan, Italy
[32] Fondazione IRCCS Istituto Neurologico Carlo Besta, Milano, Italy
[33] Division of Neurology, Department of Medicine, Sunnybrook Health Sciences Centre; Hurvitz Brain Sciences Program, Sunnybrook Research Institute; University of Toronto, Toronto, Canada
[34] Department of Clinical Neurological Sciences, University of Western Ontario, London, Ontario Canada
[35] Department of Neurology, Erasmus Medical Centre, Rotterdam, Netherlands
[36] Department of Neurofarba, University of Florence, Italy
[37] IRCCS Fondazione Don Carlo Gnocchi, Florence, Italy
[38] Nuffield Department of Clinical Neurosciences, Medical Sciences Division, University of Oxford, Oxford, UK
[39] Department of Brain Sciences, Imperial College London, UK
[40] Center for Alzheimer Research, Division of Neurogeriatrics, Department of Neurobiology, Care Sciences and Society, Bioclinicum, Karolinska Institutet, Solna, Sweden
[41] Unit for Hereditary Dementias, Theme Aging, Karolinska University Hospital, Solna, Sweden
[42] Division of Neuroscience and Experimental Psychology, Wolfson Molecular Imaging Centre, University of Manchester, Manchester, UK.
[43] Departments of Geriatric Medicine and Nuclear Medicine, Center for Translational Neuro- and Behavioral Sciences, University Medicine Essen, Essen, Germany.
[44] Cerebral Function Unit, Manchester Centre for Clinical Neurosciences, Salford Royal NHS Foundation Trust, Salford, UK
[45] Clinique Interdisciplinaire de Mémoire, Département des Sciences Neurologiques, CHU de Québec, and Faculté de Médecine, Université Laval, QC, Canada
[46] Alzheimer's disease and Other Cognitive Disorders Unit, Neurology Service, Hospital Clínic, Institut d'Investigacións Biomèdiques August Pi I Sunyer, University of Barcelona, Barcelona, Spain
[47] Faculty of Medicine, University of Lisbon, Lisbon, Portugal
[48] Cognitive Disorders Unit, Department of Neurology, Donostia University Hospital, San Sebastian, Gipuzkoa, Spain
[49] Neuroscience Area, Biodonostia Health Research Institute, San Sebastian, Gipuzkoa, Spain
[50] Department of Neurodegenerative Diseases, Hertie-Institute for Clinical Brain Research and Center of Neurology, University of Tübingen, Tübingen, Germany

[51] Center for Neurodegenerative Diseases (DZNE), Tübingen, Germany
[52] Laboratory for Cognitive Neurology, Department of Neurosciences, KU Leuven, Leuven, Belgium
[53] Neurology Service, University Hospitals Leuven, Belgium
[54] Leuven Brain Institute, KU Leuven, Leuven, Belgium
[55] Douglas Mental Health University Institute, Department of Psychiatry, McGill University, Montreal Canada
[56] McConnell Brain Imaging Centre, Montreal Neurological Institute, Department of Neurology & Neurosurgery, McGill University, Montreal Canada
[57] Sorbonne Université, Paris Brain Institute – Institut du Cerveau – ICM, Inserm U1127, CNRS UMR 7225, AP-HP - Hôpital Pitié-Salpêtrière, Paris, France
[58] Centre de référence des démences rares ou précoces, IM2A, Département de Neurologie, AP-HP - Hôpital Pitié-Salpêtrière, Paris, France
[59] Département de Neurologie, AP-HP - Hôpital Pitié-Salpêtrière, Paris, France
[60] Neurologische Klinik und Poliklinik, Ludwig-Maximilians-Universität, Munich, Germany
[61] Center for Neurodegenerative Diseases (DZNE), Munich, Germany
[62] Munich Cluster of Systems Neurology, Munich, Germany
[63] Department of Neurology, University of Ulm, Ulm, Germany
[64] Univ Lille, France
[65] Inserm 1172, Lille, France
[66] CHU, CNR-MAJ, Labex Distalz, LiCEND Lille, France
[67] University Hospital of Coimbra (HUC), Neurology Service, Faculty of Medicine, University of Coimbra, Portugal
[68] Center for Neuroscience and Cell Biology, Faculty of Medicine, University of Coimbra, Coimbra, Portugal
[69] University of California, San Francisco, Department of Epidemiology and Biostatistics, San Francisco, CA

Word Count: 4,119/4,000

Co-Corresponding Authors:
Adam M. Staffaroni, PhD
Assistant Professor

Adam L. Boxer, MD, PhD
Professor

University of California, San Francisco
Weill Institute for Neurosciences, Department of Neurology, Memory and Aging Center
675 Nelson Rising Lane, Suite 190
San Francisco, CA 94158
Phone: 415-502-7201; Fax: 415.476.1816
Emails: adam.staffaroni@ucsf.edu, adam.boxer@ucsf.edu

Abstract (150/150 words)

Unlike familial Alzheimer's disease, we have been unable to accurately predict symptom onset in presymptomatic familial frontotemporal dementia (f-FTD) mutation carriers, which is a major hurdle to designing disease prevention trials. We developed multimodal models for f-FTD disease progression and estimated clinical trial sample sizes in *C9orf72*, *GRN,* and *MAPT* mutation carriers. Models included longitudinal clinical and neuropsychological scores, regional brain volumes, and plasma neurofilament light chain (NfL) in 796 carriers and 412 non-carrier controls. We found that the temporal ordering of clinical and biomarker progression differed by genotype. In prevention-trial simulations employing model-based patient selection, atrophy and NfL were the best endpoints, whereas clinical measures were potential endpoints in early symptomatic trials. F-FTD prevention trials are feasible but will likely require global recruitment efforts. These disease progression models will facilitate the planning of f-FTD clinical trials, including the selection of optimal endpoints and enrollment criteria to maximize power to detect treatment effects.

Key words: Frontotemporal lobar degeneration*, C9orf72, GRN, MAPT*, disease progression, neurofilament light chain, neuroimaging, neuropsychology, clinical trials

178 Frontotemporal dementia (FTD), marked by impairments in behavior, language, and
179 sometimes motor function, is a common form of early-onset dementia.[1] Approximately
180 20-30% of FTD is caused by autosomal dominant mutations (familial, or f-FTD), usually
181 in one of three genes: chromosome 9 open reading frame 72 (*C9orf72)*, progranulin
182 (*GRN),* or microtubule-associated protein tau (*MAPT)*.[2] FTD is uniformly fatal, and there
183 are no approved therapies; however, a growing number of new treatments targeting
184 *C9orf72, GRN,* and *MAPT* are moving into clinical trials.[3,4] Experience from Alzheimer's
185 disease (AD), spinal muscular atrophy (SMA),[5] and amyotrophic lateral sclerosis (ALS)[6]
186 suggests treating FTD will be most successful if treatment is initiated early in the
187 disease course, ideally prior to the onset of symptoms. Such a disease prevention
188 approach has been implemented in the Dominantly Inherited Alzheimer's Network Trials
189 Unit (DIAN-TU; https://dian.wustl.edu/our-research/clinical-trial/) platform clinical trial for
190 dominantly inherited AD (DIAD) by including presymptomatic mutation carriers.[7]
191 Prevention trials in DIAD have also been facilitated by fluid and molecular PET imaging
192 biomarkers that allow for the measurement of treatment-related changes in AD
193 pathologies and neurodegeneration.[8]
194
195 There are many challenges to performing f-FTD clinical trials.[9] Although the clinical
196 manifestations of the f-FTD mutations are similar, the biology and neuropathology
197 associated with *C9orf72, GRN,* and *MAPT* mutations are vastly different.[2] Unlike AD,[10]
198 little is known about the ontogeny of biomarker and clinical changes in f-FTD that could
199 be used to determine enrollment criteria or identify the best clinical trial endpoints at
200 different disease stages. Also, the age at which symptoms present is variable even

201 within a family (e.g., onset in the thirties vs. seventies in one family),[11] making it difficult
202 to identify the individuals in late presymptomatic stages most likely to benefit from
203 therapies. For example, in *GRN*, familial age of onset only explains 14% of the
204 variability in individual age at symptom onset.[12]
205
206 F-FTD is rare, with only hundreds of mutation carriers known to exist worldwide.[12]
207 Therefore, to prepare for f-FTD trials, the FTD Prevention Initiative (FPI,
208 www.thefpi.org), an international collaboration focused on organizing f-FTD prevention
209 trials, combined data from the two largest f-FTD natural history studies worldwide:
210 ALLFTD in North America (www.allftd.org), and GENFI in Europe and Canada
211 (www.genfi.org).[13] In rare neurogenetic diseases such as f-FTD, the FDA has promoted
212 the use of innovative approaches such as disease progression models (DPM) for
213 selecting clinical trial endpoints, determining enrollment criteria, and analyzing the
214 effects of novel interventions that might lead to deviations from expected disease
215 progression,[14] and such models have been employed successfully in DIAN-TU.[7] We
216 developed Bayesian DPMs that jointly model the best known measures of f-FTD global
217 clinical status, neuropsychological performance, brain volume, and active
218 neurodegeneration (plasma neurofilament light chain [NfL]) to model latent "Disease
219 Age (DA)," which forecasts presymptomatic mutation carriers' proximity to symptom
220 onset and enables comprehensive quantification of disease progression. We then
221 conducted simulations of prevention and early symptomatic treatment trials, exploring
222 the use of DA, plasma NfL, and clinical measures as inclusion criteria to prioritize the

223 recruitment of presymptomatic participants towards those most likely to exhibit
224 measurable disease progression during a trial.
225

226 Results

227 Subject Characteristics

228 Demographic and clinical data are presented in Tables 1 and S1. Of the 796 mutation
229 carriers, *C9orf72* was the most common mutation (43.6%), followed by *GRN* (35.3%)
230 and *MAPT* (21.1%). Across all three genetic groups, most participants were
231 presymptomatic (CDR®+NACC-FTLD-Global=0, 54.4%). Most symptomatic participants
232 presented with behavioral variant FTD (bvFTD, 68.6%), followed by primary progressive
233 aphasia (PPA, 12.7%), which was driven largely by *GRN* (33.8% of symptomatic *GRN*).
234 The average number of visits per mutation carrier was 2.1 (SD=1.1). The models
235 incorporated 412 non-carrier family controls. A subset of participants had available NfL
236 (n=981, 1,948 observations) and MRI data (n=882, 1,896 observations).
237

238 Disease Progression Models

239 *Overview*

240 When ALLFTD and GENFI participants were modeled separately, rates of progression
241 were very similar between consortia on all measures (Figures 1, S1); subsequent
242 models combined all participants. To understand the temporal ordering of biomarker
243 and clinical changes, disease progression curves were graphed in relation to predicted
244 DA (Figure 2).
245

246 *MR imaging and plasma NfL*

247 In *C9orf72*, MRI was the first biomarker to change (Figures 2, 3, & Extended Data
248 Figure 1; Tables 2, S2-S5), with visual inspection of the DPM curves suggesting that
249 brain volumes deviate from controls up to 40 years before expected onset. Thalamic
250 volume in *C9orf72* was significantly lower than controls in the -40 to -10 epoch, with the
251 largest effect size of all regions of interest (ROIs) (Extended Data Figure 1 & Table S5).
252 Voxelwise quantification also underscored the early thalamic involvement (Extended
253 Data Figure 2, Figure S2). In addition to the thalamus, most ROIs were smaller than
254 controls (Extended data figure 2, Tables S5) and other mutation carriers (Table S6) in
255 the -40 to -10 epoch. In the -10 to 0 epoch, the temporal lobe showed the largest effect
256 size (Extended Data Figure 1), and it was the first ROI to deviate from controls (Table
257 S4; deviated at DA = -6.1, 95%CI:-9.4,-3.2) by one standard deviation (SD), followed
258 closely by parietal (DA = -6.1, 95%CI:-9.2,-3.2) and frontal (DA = -4.9, 95%CI:-7.5,-2.7)
259 lobes. The largely overlapping credible intervals indicate these differences in temporal
260 ordering are not statistically significant. The longitudinal rate of volume loss was
261 relatively stable across the across epochs in *C9orf72* compared to the other genetic
262 groups (Table S4). Visual inspection of the DPM curves suggested mean NfL values in
263 *C9orf72* begin to deviate from controls approximately 30 years before estimated onset.
264 NfL levels in *C9orf72* were significantly higher than controls in all DA epochs and
265 became elevated one SD above controls three years before estimated onset (95%CI:-
266 0.7,-5.8).

267

268 In *GRN*, visual inspection suggested NfL begins to deviate from controls about 15 years
269 prior to symptom onset, followed by MRI 5-10 years prior to onset (Figures 2, S1).
270 Baseline plasma NfL concentrations in *GRN* were significantly elevated relative to
271 controls in all DA epochs (Figure 3, Table S5) and elevated compared to all other
272 genetic groups in the symptomatic phase (Table S6). NfL concentrations become
273 elevated by one SD compared to controls 4.9 years prior to onset (95%CI:-3.4,-7). *GRN*
274 also displayed the most rapid rates of NfL increase in the symptomatic epoch (Figures
275 1&2, Table S4). The frontal and temporal lobes were the first brain regions to differ from
276 controls by one SD in the DPM (-1.1 and -1.2 years before estimated onset,
277 respectively). The insula was significantly atrophied compared to controls in the -40 to -
278 10 epoch (Extended Data Figure 1, Table S5), and all ROIs had smaller mean volumes
279 than controls in the -10 to 0 epoch, except the striatum (p=0.057). In the symptomatic
280 stage, volume loss in all ROIs was more rapid than the other genetic groups, with the
281 frontal, temporal, medial temporal, insular, and striatal ROIs losing volume most rapidly
282 (Figure S3, Table S4).
283
284 Medial temporal atrophy was the first observed biomarker change in *MAPT*, diverging
285 from controls ~10 years before symptoms based on visual inspection (Figure 2), and
286 reaching one SD below controls 1.8 years before onset (95%CI:-3.2,-0.5). The medial
287 temporal lobe was the only region with significant volume loss compared to controls in
288 the presymptomatic phase (Extended Data Figure 1, Table S5). The remaining temporal
289 regions and insula were the next regions to become atrophied by one SD compared to
290 controls (Table S4), with overlapping credible intervals. In the symptomatic stage,

291 frontal, temporal and medial temporal, insular, and striatal regions showed the greatest
292 degree of cross-sectional atrophy (Extended Data Figure 1, Figure S4, Table S5).
293 Longitudinally, the medial temporal lobe (MTL), followed by the remainder of the
294 temporal lobe, striatum, and insular regions were the regions to lose volume most
295 rapidly in the symptomatic phase (Table S4). NfL levels began to diverge from controls
296 closer to symptom onset in *MAPT* than *C9orf72* or *GRN*, with mean values showing
297 significant elevations during the symptomatic but not presymptomatic epochs (Extended
298 Data Figure 1, Tables S5-6), and average values did not reach one SD above controls
299 until 4.6 years *after* estimated symptom onset (95%CI:7.1,2.4).
300
301 We conducted a voxelwise sensitivity analysis in each DA epoch to complement the
302 coarse-grained ROIs used in the DPMs and to illustrate the findings were not dependent
303 on the DPMs. Results of this sensitivity analysis (Extended Data Figure 2, Figures S2-
304 S4) supported the patterns observed using ROIs.
305
306 *Global Ratings and Clinical Measures*
307 Visual inspection of the curves revealed a rapid CDR®+NACC-FTLD-SB increase after
308 symptom onset, and all genetic groups had cross-sectional elevations in CDR®+NACC-
309 FTLD-SB prior to symptom onset (Figure 3, Table S5); note that statistical comparisons
310 of this measure should be interpreted with caution given that controls were defined as
311 having a baseline CDR®+NACC-FTLD=0 (as is typical in most clinical dementia
312 research studies) and thus have no variance due to this selection process. Similar to the
313 MRI results, *GRN* exhibited the most rapid CDR®+NACC-FTLD-SB changes following

314 symptom onset (Figure 2, Table S4). Visual inspections of the curves indicated that
315 neuropsychological and Revised Self-Monitoring Scale (RSMS) impairments relative to
316 controls were generally observed only after symptom onset for all genetic groups
317 (Figure 2 & Table S5), and no measure reached one SD worse than controls until after
318 symptom onset (Table S4). In direct statistical comparison, *C9orf72* expansion carriers
319 performed worse than controls on Trails A and B at all DA epochs (Table S5). *GRN*
320 performed worse than controls on Trails A at all epochs, and worse than controls on
321 Trails B in the -10 to 0 epoch. *MAPT* mutation carriers exhibited impairments in the
322 Figure Copy in the -10 to 0 epoch, with a trend towards impairment on the Multilingual
323 Naming Test (MINT) in this epoch. Longitudinally, the most rapid change in the
324 symptomatic stage relative to controls was observed for Trails A & B in *C9orf72*, Trails
325 A, MINT, and Benson Copy in *GRN*, and the MINT and Trails B in *MAPT* (Table S4).
326
327 Raw values were modeled. The same pattern of findings was observed (Figure S5) in a
328 sensitivity analysis adjusting for nuisance covariates (details in online methods).
329
330 *Patient-level Estimates*
331 DA estimates at baseline ranged from -40 to 21. The precision of individual DA
332 estimates depends on the proximity to symptom onset and follow-up duration. In
333 mutation carriers with at least one post-baseline visit who were >10 years from
334 expected onset, the average uncertainty of the DA estimate (95%CI) was +/-14.6 years.
335 For those -10 to 0 years from onset, this uncertainty decreased to +/-5.5 years, and
336 after onset, the average uncertainty of the estimate was +/-0.9 years. To better

337 understand the impact of level of impairment, rate of progression, and model priors (i.e.,
338 years since onset) on estimated DA, individual patient-level data were examined
339 (Extended Data Figure 3). With increasing DA, performance is increasingly impaired
340 across multiple measures, and there is a greater tendency for progressive impairment
341 from baseline to final observations. In those furthest from onset, when most scores tend
342 to be within normal limits, prior information about their age has a large influence on
343 estimated DA. Examining cases that the model estimated to be presymptomatic (DA<0)
344 despite a CDR®+NACC-FTLD-SB>0, these participants tend to perform in the average
345 range across other measures and stay stable or show improvements over time.
346

347 **Application to Clinical Trials**

348 The DPM curves suggest that clinical trial endpoint selection might differ by genetic
349 group and disease stage (Figure 2). To explore this further, simulation studies based on
350 the natural history data were conducted to estimate the sample sizes required to
351 measure a 50% reduction in various potential endpoints for two- and four-year
352 presymptomatic prevention trials and 1.5 and two-year early symptomatic treatment
353 trials (Table 3; 1:1 randomized parallel design; details in online methods). Prevention
354 trial designs included only participants with a CDR®+NACC-FTLD-Global = 0 at
355 baseline. Simulations explored the use of baseline NfL and DA as additional inclusion
356 criteria to define a high-risk population most likely to show clinical change over the
357 course of the trial, thereby increasing power. Sample size estimates for prevention trials
358 were generally lowest when using biomarkers (NfL or MRI) as the outcome. For
359 example, a two-year prevention trial requiring a DA within five years of onset would

360 require sample sizes of 52 total participants for *GRN* (MRI Frontal), 108 for *MAPT* (MRI
361 MTL), and 424 for *C9orf72* (MRI Temporal) if MRI is used as an endpoint. Based on the
362 estimated number of eligible participants from the FPI dataset (assuming no additional
363 recruitment efforts), two-year trials appear to be feasible for *GRN* if MRI is used as the
364 outcome, whereas a four-year trial would be required for *MAPT*. Additional recruitment
365 would be required for a *C9orf72* prevention trial to be sufficiently powered to detect a
366 50% treatment effect.
367
368 Symptomatic trial simulations included all participants with a CDR®+NACC-FTLD-
369 Global=1 and subsets of high-risk participants with a CDR®+NACC-FTLD-Global of 0 or
370 0.5 defined based on elevated NfL (log(NfL) > 3.0) or an estimated DA within 2.5 years
371 of onset (Table 3). Based on these simulations, it would be feasible to power trials for all
372 three genetic groups using the CDR®+NACC-FTLD-SB and neuropsychological tests,
373 measures most likely to be approvable by regulatory bodies as clinically meaningful
374 endpoints.[15] For example, within a population having a CDR®+NACC-FTLD-Global=1
375 or a DA within 2.5 years of onset in those with a CDR®+NACC-FTLD-Global<1, the
376 estimated sample sizes using CDR®+NACC-FTLD-SB as the primary endpoint for a
377 two-year trial were 68 total participants for *GRN*, 120 for *MAPT*, and 124 for *C9orf72*.
378

379 ## Discussion

380 We present the efforts of the international FTD Prevention Initiative (FPI) to establish
381 the largest known cohort of f-FTD cases worldwide, gathered from North American
382 (ALLFTD) and European/Canadian (GENFI) natural history studies. We harmonized

383 clinical, neuropsychological, biofluid, and neuroimaging measurements to build DPMs
384 that allow direct comparisons of effect sizes for mean values and rates of change
385 between the best available measures for characterizing FTD. The DPMs revealed
386 important insights about the earliest manifestations of f-FTD and the temporal ordering
387 of biomarker and clinical changes. Across all three FTD mutation carrier groups,
388 regional brain atrophy and plasma NfL elevations were the first measurable
389 manifestations of disease, potentially developing 10 to 40 years before the earliest
390 clinical features. Neuropsychological changes typically occurred later,
391 contemporaneous with the emergence of informant-reported symptoms (CDR®+NACC-
392 FTLD-SB). The genetic groups displayed differences in patterns of disease progression
393 that are relevant for clinical care and clinical trial planning. The striking concordance in
394 disease progression between the two independent North American and European
395 cohorts supports the validity of the models, suggesting that the natural history of the
396 disease is strongly determined by pathogenic mutations and that global clinical trials of
397 f-FTD therapies are feasible. Finally, we leveraged the DPMs and natural history data to
398 simulate prevention and treatment clinical trial scenarios, including candidate participant
399 selection criteria and primary endpoints, to provide evidence for the feasibility of running
400 presymptomatic prevention trials and symptomatic treatment trials in f-FTD.
401
402 The validity of our DPM models is supported by the results of previous studies focusing
403 on individual biomarkers or clinical measures in f-FTD. Because the models incorporate
404 both new and some previously analyzed historical data, we were able to replicate and
405 extend the results of previous studies. We also directly compared the relative utility of

406 different assessments at different stages of disease. Consistent with previous MRI
407 studies demonstrating brain atrophy can be detected in presymptomatic f-FTD,[16–19] MRI-
408 measured brain atrophy was the first biomarker to change in *C9orf72* and *MAPT*, but
409 our models revealed that NfL elevations preceded atrophy by a few years in *GRN*. In
410 *C9orf72,* the thalamus and most other brain regions were smaller than controls 10 to 40
411 years prior to onset, supporting the hypothesis that *C9orf72* repeat expansions may
412 affect early brain development.[19,20] Also consistent with prior work, the most rapid rates
413 of atrophy occurred in *GRN* with widespread brain involvement within 10 years of
414 onset.[21,22] Despite differences in analytic methods, and the inclusion of a much larger
415 dataset, the DPMs developed in this study allowed us to replicate the findings of earlier,
416 smaller analyses. In an earlier MRI study, Rohrer and colleagues[17] defined expected
417 disease onset based on each genetic group's mean age of onset rather than using
418 model derived DA employed here. Similar to the previous study, we detected medial
419 temporal atrophy in *MAPT* 15 years prior to onset followed by atrophy of the insula.
420 Temporal lobe atrophy in presymptomatic *MAPT* has been consistently reported,[16,18,23]
421 and the insula may be a common region of early atrophy in *MAPT*.[24]
422
423 We and others have previously shown that NfL concentrations are elevated in the
424 plasma[25–27] and CSF[28,29] of symptomatic FTD patients compared to other neurological
425 conditions. In the current study, we verified that the genotype-related patterns of plasma
426 NfL elevation that were measured in two different laboratories, in two independent f-
427 FTD cohorts, were very similar and for the purposes of DPM, could be combined. In
428 *C9orf72,* NfL levels began to deviate from controls approximately 30 years prior to onset

429 and remained significantly elevated compared to controls in all presymptomatic epochs.
430 In *GRN*, NfL levels begin to increase 15 years prior to onset and were elevated
431 compared to controls in the late presymptomatic stages. In contrast, NfL levels begin to
432 increase just proximal to symptom onset in *MAPT,* and presymptomatic *MAPT* mutation
433 carriers did not show increased levels compared to controls. In the symptomatic stage,
434 NfL levels rose more than twice as fast in *GRN* than the other genetic groups. These
435 results extend previous fluid biomarker studies showing NfL concentrations become
436 elevated early in f-FTD, are harbingers of symptom onset, and rise most rapidly in
437 *GRN*.[25,27,30–32]
438
439 Paralleling the biomarker findings, global disease severity (CDR®+NACC-FTLD-SB)
440 and neuropsychological measures declined more rapidly in *GRN* than *C9orf72* or *MAPT*
441 mutation carriers. Although *GRN* was previously shown to have the longest disease
442 course in an international f-FTD cohort,[12] disease duration in that study was determined
443 based on clinical interview rather than the data-driven approach taken in the current
444 study; moreover, the *C9orf72* sample in the prior study had a higher proportion of
445 participants with ALS or FTD with motor neuron disease than the current study (30.3% v
446 13.1%), and these diagnoses were associated with more rapid disease progression.[12,33]
447 Neuropsychological impairments relative to age-matched controls were typically
448 observed after symptom onset in all groups, although abnormalities on a few measures
449 were detected in the presymptomatic stages. These findings add to prior studies
450 suggesting that cognitive changes can be detected in the presymptomatic phases of f-
451 FTD and that there are genotype-specific cognitive profiles.[34–37] Future work should

452 continue to explore the development and validation of novel neuropsychological
453 measures for early detection and monitoring, including digital cognitive tests and
454 cognitive composite scores (e.g. GENFI-COG) that may improve early detection and
455 reduce sample size estimates.[37]
456
457 An overarching aim of this study was to develop models that inform the design of f-FTD
458 clinical trials. Simulation studies were conducted to estimate the sample sizes
459 necessary to power prevention and early symptomatic treatment trials. These studies
460 also explored the use of NfL and DA estimates as inclusion criteria to enroll
461 presymptomatic mutation carriers at heightened risk for clinical progression during a
462 trial. The simulations revealed important information that will be directly applicable to
463 clinical trial design. First, using NfL and MRI biomarkers as surrogate endpoints for
464 prevention trials would allow trials to be conducted with many fewer participants than
465 clinical measures. Second, prevention trials appear most feasible for *MAPT* and *GRN*
466 relative to the estimated number of eligible participants based on our dataset, however,
467 given that *C9orf72* is the most common mutation causing FTD and ALS, recruiting the
468 estimated sample sizes may be feasible. Third, using estimated DA to select high-risk
469 presymptomatic participants for trial enrollment leads to a sizeable reduction in sample
470 sizes. This reduction in sample size must be balanced against the reduction in number
471 of eligible participants (of that DA), but these simulations show that *GRN* and *MAPT*
472 trials enrolling presymptomatic participants within five years of estimated onset would
473 be feasible based on the estimated number of eligible participants from our current
474 dataset. Fourth, clinical measures perform very well in the early symptomatic trial

475 simulations, and sample sizes for trials using the CDR®+NACC-FTLD-SB as a primary
476 outcome are feasible for all three genetic groups. Not only was this measure statistically
477 powerful for measuring change, but given that it reflects informant-reported clinical
478 status, it could also be considered a clinically meaningful outcome and approvable
479 endpoint from a regulatory perspective.[15]
480
481 The clinical trial simulations included in this study used standard, two-arm, parallel-
482 group clinical trial designs. Future work to explore innovative trial designs and analysis
483 methods may enable trials with smaller samples sizes and/or increased power for
484 smaller (but clinically meaningful) treatment effects. With the incorporation of a
485 treatment effect parameter, the DPM-predicted versus post-treatment progression could
486 potentially be used as a primary endpoint in clinical trials to estimate the slowing in
487 disease progression across multiple endpoints.[7,38] In rare diseases such as f-FTD
488 analysis methods may also simulate data from natural history participants to generate
489 "synthetic" participants to decrease sample sizes and reduce allocation to placebo as
490 has been encouraged in recent FDA guidance.[14] Additionally, platform trials based on
491 DPMs allow multiple therapies to be tested simultaneously with comparisons made to a
492 shared placebo group further improving trial efficiency in rare populations.[39]
493
494 There are important limitations to this work. Known genetic modifiers of f-FTD disease
495 progression were not included, such as specific mutations (for *MAPT*) and *TMEM106B*,
496 a modifier of penetrance in *GRN.*[2,40] We were also limited in the clinical measures that
497 we could include in the analysis to those that were readily harmonizable between

498 ALLFTD and GENFI, excluding a variety of promising novel measures that were not
499 available in both cohorts.[34,35] Future models will likely be improved by including a more
500 exhaustive collection of measures and biomarkers[41] and approaches accounting for
501 heterogeneity in f-FTD features.[42] Because disease onset was defined as
502 CDR®+NACC-FTLD-SB=0.5, non-carrier controls by definition had CDR®+NACC-
503 FTLD-SB=0 at baseline, which reduced the variance in this measure, thereby potentially
504 overestimating the effect size relative to other measures where there was more
505 variance in the controls. Because abnormal global status may reflect other brain
506 pathologies in the controls that could potentially obscure important findings, we believe
507 that the requirement for CDR®+NACC-FTLD-SB=0 in controls was appropriate.
508
509 The DPMs produced for the current study have additional limitations related to less
510 informative clinical data at early stages of disease and missing data at late stages of
511 disease. In subjects estimated to be within 10 years of symptom onset, the accuracy is
512 +/- 5.5 years, which approaches the accuracy of familial age of onset-based estimates
513 which are useful in DIAD,[43] but not possible in most f-FTD syndromes.[12] However,
514 individuals furthest from onset are typically within normal limits on all contributing
515 measures forcing the model to rely heavily on prior information about participants'
516 chronological age to estimate DA. This results in considerable uncertainty around exact
517 DA in those furthest from expected onset (e.g., +/-14 years in the -40 to -10 epoch). To
518 visually assess how the weight of evidence (number of measures that changed over the
519 range of visits) related to each subject's DA, we color coded measurements in each
520 individual mutation carrier in Figure S6. This revealed that in more severely impaired

521 mutation carriers at later DA, there was more missing data, particularly MRI. This
522 suggests an important limitation to the use of MRI as an outcome in symptomatic
523 mutation carriers: data may be missing because scans are harder to acquire in
524 advanced patients, possibly because they either cannot travel to research centers or
525 they cannot lie still in a MRI scanner. Such informative missing data also impacts the
526 DPMs, potentially biasing the models towards a smaller standard deviation from normal;
527 this is a limitation and a direction for future research. Finally, the current study is limited
528 by the lack of racial and ethnic diversity of the sample. Improving the diversity of
529 participants in FTD research is an urgent priority,[44] however, it should be noted that in
530 genetic f-FTD there are known founder effects for *C9orf72*[45] and *GRN* mutations[46] with
531 European ancestry, leading to strong associations with particular racial and ethnic
532 groups.
533
534 In conclusion, these DPMs will facilitate the planning of f-FTD clinical trials, including
535 selection of optimal endpoints and enrollment criteria to maximize power to detect
536 treatment effects.[14] Brain atrophy and plasma NfL elevations are measurable years prior
537 to symptom onset, paving the way for using these biomarkers in clinical trials of agents
538 that could prevent or delay the clinical manifestations of f-FTD. The models also
539 highlight the challenges of conducting adequately powered trials in rare f-FTD
540 populations and provide a roadmap for development of new biomarkers and clinical
541 endpoints that may improve power to detect effects in presymptomatic stages of
542 disease and create a renewed sense of urgency to identify eligible trial participants
543 outside of Europe and North America.

Acknowledgements

Data collection and dissemination of the data presented in this manuscript was supported by the ALLFTD Consortium (U19: AG063911, funded by the National Institute on Aging and the National Institute of Neurological Diseases and Stroke) and the former ARTFL & LEFFTDS Consortia (ARTFL: U54 NS092089, funded by the National Institute of Neurological Diseases and Stroke and National Center for Advancing Translational Sciences; LEFFTDS: U01 AG045390, funded by the National Institute on Aging and the National Institute of Neurological Diseases and Stroke). The manuscript has been reviewed by the ALLFTD Executive Committee for scientific content. The authors acknowledge the invaluable contributions of the study participants and families as well as the assistance of the support staffs at each of the participating sites. This work is also supported by the Association for Frontotemporal Degeneration (including the FTD Biomarkers Initiative), the Bluefield Project to Cure FTD, Larry L. Hillblom Foundation [2018-A-025-FEL (AMS)], the National Institutes of Health [AG038791 (ALB), AG032306 (HJR), AG016976 (WAK), AG062677 (RCP), AG019724 (BLM), AG058233 (SEL), AG072122 (WAK), P30 AG062422 (BLM), K12 HD001459 (NG), K23AG061253 (AMS), AG062422 (RCP), K24AG045333 (HJR)], and the Rainwater Charitable Foundation. Samples from the National Centralized Repository for Alzheimer Disease and Related Dementias (NCRAD), which receives government support under a cooperative agreement grant [U24 AG021886 (TF)] awarded by the National Institute on Aging (NIA), were used in this study.

566 This work was also supported by the Medical Research Council UK GENFI grant
567 [MR/M023664/1 (JDR)], the Bluefield Project, the National Institute for Health Research
568 including awards to Cambridge and UCL Biomedical Research Centres, and the JPND
569 GENFI-PROX grant (2019–02248). Several authors of this publication are members of
570 the European Reference Network for Rare Neurologic Diseases, project No. 739510.
571 JDR and LLR are also supported by the NIHR UCL/H Biomedical Research Centre, the
572 Leonard Wolfson Experimental Neurology Centre (LWENC) Clinical Research Facility,
573 and the UK Dementia Research Institute, which receives its funding from UK DRI Ltd,
574 funded by the UK Medical Research Council, Alzheimer's Society and Alzheimer's
575 Research UK. JDR is also supported by the Miriam Marks Brain Research UK Senior
576 Fellowship and has received funding from an MRC Clinician Scientist Fellowship
577 (MR/M008525/1) and the NIHR Rare Disease Translational Research Collaboration
578 (BRC149/NS/MH). MB is supported by a Fellowship award from the Alzheimer's
579 Society, UK (AS-JF-19a-004-517). RC/CG are supported by a Frontotemporal Dementia
580 Research Studentships in Memory of David Blechner funded through The National
581 Brain Appeal (RCN 290173). J.B.R. is supported by NIHR Cambridge Biomedical
582 Research Centre (BRC-1215-20014; The views expressed are those of the authors and
583 not necessarily those of the NIHR or the Department of Health and Social Care); The
584 Wellcome Trust (220258) The Cambridge Centre for Parkinson-plus; The Medical
585 Research Council (SUAG/092 G116768); ILB is supported by ANR-PRTS PREV-
586 DemAls, PHRC PREDICT-PGRN and several authors of this publication are members
587 of the European Reference Network for Rare Neurological Diseases - Project ID No
588 739510. JL is funded by the Deutsche Forschungsgemeinschaft (DFG, German

589 Research Foundation) under Germany's Excellence Strategy within the framework of
590 the Munich Cluster for Systems Neurology (EXC 2145 SyNergy – ID 390857198). RS-V
591 was funded at the Hospital Clinic de Barcelona by Instituto de Salud Carlos III, Spain
592 (grant code PI20/00448 to RSV) and Fundació Marató TV3, Spain (grant code
593 20143810 to RSV). MLS has been supported by the German Federal Ministry of
594 Education and Research (BMBF) by a grant given to the German FTLD Consortium
595 (FKZ O1GI1007A), and by the German Research Foundation DFG (SCHR 774/5-1).
596 MM was, in part, funded by the UK Medical Research Council, the Italian Ministry of
597 Health and the Canadian Institutes of Health Research as part of a Centres of
598 Excellence in Neurodegeneration grant, and also Canadian Institutes of Health
599 Research operating grants (Grant #s: MOP- 371851 and PJT-175242) and funding from
600 the Weston Brain Institute to Mario Masellis. R.L. is sup-ported by the Canadian
601 Institutes of Health Research and the Chaire de Recherche sur les Aphasies Primaires
602 Progressives Fondation Famille Lemaire. C.G. is supported by the Swedish
603 Frontotemporal Dementia Initiative Schörling Foundation, Swedish Research Council,
604 JPND Prefrontals, 2015–02926,2018–02754, Swedish Alzheimer Foundation, Swedish
605 Brain Foundation, Karolinska Institutet Doctoral Funding, KI Strat-Neuro, Swedish
606 Dementia Foundation, and Stockholm County Council ALF/Region Stockholm. J.L. is
607 supported by Germany's Excellence Strategy within the framework of the Munich
608 Cluster for Systems Neurology (German Research Foundation, EXC 2145 Synergy
609 390857198). The Dementia Research Centre is supported by Alzheimer's Research
610 UK, Alzheimer's Society, Brain Research UK, and The Wolfson Foundation. This work
611 was supported by the National Institute for Health Research UCL/H Biomedical

Research Centre, the Leonard Wolfson Experimental Neurology Centre Clinical Research Facility, and the UK Dementia Research Institute, which receives its funding from UK DRI Ltd, funded by the UK Medical Research Council, Alzheimer's Society, and Alzheimer's Research UK.

Author Contributions Statement

A.M.S., M.Q., and B.W. had full access to the data in the study and take responsibility for the integrity of the data and the accuracy of the data analysis. A.M.S., M.Q., B.W., H.W.H., L.R., H.J.R., J.D.R., and A.L.B. were responsible for concept development and design. A.M.S., M.Q., and B.W. conducted statistical analyses. M.Q. and B.W. developed the custom code for the disease progression models. L.P., T.F.G., and C.H. processed the neurofilament light chain data. Y.C., A.W., and S.Y.M.G. processed the neuroimaging data. A.M.S., M.Q. and B.W. drafted the manuscript. A.M.S., M.Q., B.W., H.W.H, L.R., H.J.R., J.D.R, and A.L.B critically revised the manuscript. A.L.B. supervised the research. B.F.B, H.J.R, J.D.R, & A.L.B obtained funding. All authors contributed to acquisition, analysis, or interpretation of data or revision of the manuscript.

Competing Interest Statement

Appleby B - receives research support from CDC, NIH, Ionis, Alector, and the CJD Foundation. He has provided consultation to Acadia, Ionis, and Sangamo.

Boccheta M – nothing to disclose

Boeve B – has served as an investigator for clinical trials sponsored by EIP Pharma, Alector and Biogen. He receives royalties from the publication of a book entitled Behavioral Neurology of Dementia (Cambridge Medicine, 2009, 2017). He serves on the Scientific Advisory Board of the Tau Consortium. He receives research support from NIH, the Mayo Clinic Dorothy and Harry T. Mangurian Jr. Lewy Body Dementia Program and the Little Family Foundation.

Bordelon Y – nothing to disclose

Botha H – receives research support from NIH.

Boxer A – receives research support from NIH, the Tau Research Consortium, the Association for Frontotemporal Degeneration, Bluefield Project to Cure Frontotemporal Dementia, Corticobasal Degeneration Solutions, the Alzheimer's Drug Discovery Foundation and the Alzheimer's Association. He has served as a consultant for Aeovian, AGTC, Alector, Arkuda, Arvinas, Boehringer Ingelheim, Denali, GSK, Life Edit, Humana, Oligomerix, Oscotec, Roche, TrueBinding and Wave, and received research support from Biogen, Eisai and Regeneron.

Brushaber D – nothing to disclose

Cobigo Y – Nothing to disclose

Dickerson B – Dr. Dickerson is a consultant for Acadia, Alector, Arkuda, Biogen, Denali, Eisai, Genentech, Lilly, Merck, Novartis, Takeda, Wave Lifesciences. Dr. Dickerson receives royalties from Cambridge University Press, Elsevier, Oxford University Press. Dr. Dickerson receives grant funding from the NIA, NINDS, NIMH, and the Bluefield Foundation.

Domoto-Reilly K – receives research support from NIH, and serves as an investigator for a clinical trial sponsored by Lawson Health Research Institute.

Ducharme S - has participated or is currently participating in clinical trials of anti-dementia drugs sponsored by the following companies: Biogen, Ionis Pharmaceuticals, Wave Life Sciences, and Janssen. He has received speaking honorarium/advisory fees from the following companies: Eisai, Biogen, Innodem Neurosciences, NeuroCatch. Dr. Ducharme receives salary support from the Fond de Recherche du Québec – Santé.

Faber K – receives research support from NIH

Fields J – receives research support from NIH

Foroud T – receives research support from NIH

Forsberg L – receives research support from NIH.

Gavrilova R – receives research support from NIH

Gendron T – receives research support from NIH

Ghoshal N - has participated or is currently participating in clinical trials of anti-dementia drugs sponsored by the following companies: Bristol Myers Squibb, Eli Lilly/Avid Radiopharmaceuticals, Janssen Immunotherapy, Novartis, Pfizer, Wyeth, SNIFF (The Study of Nasal Insulin to Fight Forgetfulness) study, and A4 (The Anti-Amyloid Treatment in Asymptomatic Alzheimer's Disease) trial. She receives research support from Tau Consortium and Association for Frontotemporal Dementia and is funded by the NIH.

Goh SYM – Nothing to disclose

Goldman, JS – is serving as a consultant to the Novartis Alzheimer's Prevention Advisory Board. She receives research support from NIH, HDSA, New York State Department of Health (RFA # 1510130358)

Graff-Radford J – receives research support from the NIH and is on the editorial board of *Neurology*.

Graff-Radford N – receives royalties from UpToDate, has participated in multicenter therapy studies by sponsored by Biogen, TauRx, AbbVie, Novartis and Lilly. He receives research support from NIH.

Grossman M - receives grant support from NIH, Avid and Piramal; participates in clinical trials sponsored by Biogen, TauRx, and Alector; serves as a consultant to Bracco and UCB; and serves on the Editorial Board of *Neurology*.

Hall MGH – nothing to disclose

Heuer H – nothing to disclose

Hsiung G-Y – has served as an investigator for clinical trials sponsored by AstraZeneca, Eli Lilly, and Roche / Genentech. He receives research support from Canadian Institutes of Health Research and the Alzheimer Society of British Columbia.

Huey E – receives research support from NIH

Irwin D – receives support from NIH, Brightfocus Foundation and Penn Institute on Aging.

Jones D- – receives research support from NIH and the Minnesota Partnership for Biotechnology and Medical Genomics

Kantarci K - served on the Data Safety Monitoring Board for Takeda Global Research & Development Center, Inc.; data monitoring boards of Pfizer and Janssen Alzheimer Immunotherapy; research support from the Avid Radiopharmaceuticals, Eli Lilly, the Alzheimer's Drug Discovery Foundation and NIH

Kerwin, D has served on an Advisory Board for AbbVie and as site PI for studies funded by Roche/Genentech, AbbVie, Avid, Novartis, Eisai, Eli Lilly and UCSF.

Knopman D - serves on the DSMB of the DIAN-TU study, is a site PI for clinical trials sponsored by Biogen, Lilly and the University of Southern California, and is funded by NIH.

Kornak J - – has provided expert witness testimony for Teva Pharmaceuticals in *Forest Laboratories Inc. et al. v. Teva Pharmaceuticals USA, Inc.*, Case Nos. 1:14-cv-00121 and 1:14-cv-00686 (D. Del. filed Jan. 31, 2014 and May 30, 2014) regarding the drug Memantine; for Apotex/HEC/Ezra in *Novartis AG et al. v. Apotex Inc*., No. 1:15-cv-975 (D. Del. filed Oct. 26, 2015, regarding the drug Fingolimod. He has also given testimony on behalf of Puma Biotechnology in *Hsingching Hsu et al*, *vs*. *Puma Biotechnology, INC*., *et al*. 2018 regarding the drug Neratinib. He receives research support from the NIH.

Kramer J – receives royalties from Pearson Inc.

Kremers W - receives research funding from AstraZeneca, Biogen, Roche, DOD and NIH.

Lapid M – receives research support from the NIH.

Levin J - reports speaker fees from Bayer Vital, Biogen and Roche, consulting fees from Axon Neuroscience and Biogen, author fees from Thieme medical publishers and W. Kohlhammer GmbH medical publishers, non-financial support from Abbvie and compensation for duty as part-time CMO from MODAG, outside the submitted work.

Litvan I– receives research support from the National Institutes of Health grants: 2R01AG038791-06A, U01NS100610, U01NS80818, R25NS098999; U19 AG063911-1 and 1R21NS114764-01A1; the Michael J Fox Foundation, Parkinson Foundation, Lewy Body Association, CurePSP, Roche, Abbvie, Biogen, Centogene. EIP-Pharma, Biohaven Pharmaceuticals, Novartis, Brain Neurotherapy Bio and United Biopharma SRL - UCB. She was a member of the Scientific Advisory Board of Lundbeck and is a Scientific advisor for Amydis and Rossy Center for Progressive Supranuclear Palsy

University of Toronto. She receives her salary from the University of California San Diego and as Chief Editor of Frontiers in Neurology.

Ljubenkov P - is a site primary investigator for clinical trials by Alector, AbbVie, and Woolsey. He serves as an advisor for Retrotrope. He receives research and salary support from the NIH-NIA and the Alzheimer's Association- Part the Cloud partnership

Lucente D - receives research support from NIH

Mackenzie I – receives research funding from Canadian Institutes of Health Research, Alzheimer's Association US, NIH, Weston Brain Institute.

Masellis - MM reports grant funding from the Canadian Institutes of Health Research relating to this work. MM reports grants from the Canadian Institutes of Health Research, Woman's Brain Health Initiative, Brain Canada, Ontario Brain Institute, Weston Brain Institute and Washington University, outside of this submitted work. MM has received personal fees for serving on a Scientific Advisory Committee for Ionis Pharmaceuticals, Alector Pharmaceuticals, Wave Life Sciences, and Biogen Canada, outside of this submitted work. MM has received royalties from Henry Stewart Talks, outside of this submitted work. MM is a clinical trial site investigator for Roche, and Alector Pharmaceuticals, outside of this submitted work.

McGinnis S – has served as an investigator for clinical trials sponsored by AbbVie, Allon Therapeutics, Biogen, Bristol-Myers Squibb, C2N Diagnostics, Eisai Inc., Eli Lilly and Co., Genentech, Janssen Pharmaceuticals, Medivation, Merck, Navidea Biopharmaceuticals, Novartis, Pfizer, and TauRx Therapeutics. He receives research support from NIH.

Mendez M - receives research support from NIH.

Miller B – Dr. Miller is Director and Internal Advisor of The Bluefield Project to Cure FTD, Co-Director and Scientific Advisor Tau Consortium, Co-Director of the Global Brain Health Institute (GBHI) – Co-Director, Medical Advisor for The John Douglas French Foundation, Scientific advisor for The Larry L. Hillblom Foundation, Scientific Advisor for Association for Frontotemporal Degeneration, Scientific Advisor for National Institute for Health Research Cambridge Biomedical Research Centre and its subunit, the Biomedical Research Unit in Dementia, External Advisor to University of Washington ADRC , Stanford University ADRC, Arizona Alzheimer's Disease Center (ADC). Massachusetts Alzheimer Disease Research Center, and scientific advisor to The Buck Institute for Research on Aging. Serves as Editor-in-Chief for Neurocase, on the editorial board of ALS/FTD Journal (Taylor & Francis), Section Editor for Frontiers, and editor for PLOS Medicine. He receives royalties from Cambridge University Press, Guilford Publications, Inc., Johns Hopkins Press, Oxford University Press, Taylor & Francis Group, Elsevier, Inc., and Up-to-Date.

Ong E – reports no disclosures.

Onyike CU - receives research funding from the NIH, Lawton Health Research Institute, National Ataxia Foundation, Alector Inc., and Transposon, Inc. He is also supported by the Robert and Nancy Hall Brain Research Fund, the Jane Tanger Black Fund for Young-Onset Dementias, and the gift from Joseph Trovato. He is a consultant with Alector, Inc. and Acadia Pharmaceuticals.

Petrucelli L – receives research support from NIH.

Quintana M – is an employee of Berry Consultants, LLC where she serves as a consultant to numerous pharmaceutical and device companies

Rademakers R – receives research funding from NIH and the Bluefield Project to Cure Frontotemporal Dementia. RR is on the Scientific Advisory Board of Arkuda Therapeutics and receives royalties from progranulin-related patent. She is also on the Scientific Advisory Board of the Fondation Alzheimer.

Ramanan V – reports no disclosures.

Ramos E – receives research support from NIH.

Rankin K – receives research support from NIH and NSF, and serves on a Medical Advisory Board for Eli Lilly.

Rascovsky K – receives research support from NIH.

Roberson ED – receives research support from NIH, Bluefield Project to Cure Frontotemporal Dementia, Alzheimer's Association, BrightFocus Foundation, Biogen, and Alector, has served as a consultant for AGTC and on a DSMB for Lilly, and owns intellectual property related to tau.

Rohrer JD - has served on a Medical Advisory Board and had a consultancy agreement with Alector, Arkuda Therapeutics, Wave Life Sciences, and Prevail Therapeutics, and had a consultancy agreement also with UCB, AC Immune, Astex Pharmaceuticals, Biogen, Takeda and Eisai.

Rojas JC – receives research support from NIH and is a site PI for clinical trials sponsored by Eli-Lilly and Eisai.

Rosen HJ – has received research support from Biogen Pharmaceuticals, has consulting agreements with Wave Neuroscience and Ionis Pharmaceuticals, and receives research support from NIH.

Rowe J - has research grants unrelated to the current work from AstraZeneca, Janssen, Lilly, GSK via the Dementias Platform UK; and has provided consultancy unrelated to

the current work, to Asceneuron, Astex, Curasen, UCB, SV Health, WAVE and Alzheimer Research UK.

Russell LR – nothing to disclose

Sanchez-Valle R - receives personal fees from Wave pharmaceuticals for attending Advisory board meetings, personal fees from Roche diagnostics, Janssen and Neuraxpharm for educational activities, and research grants to her institution from Biogen and Sage Therapeutics outside the submitted work.

Savica R- receives support from the National Institute on Aging, the National Institute of Neurological Disorders and Stroke, the Parkinson's Disease Foundation, and Acadia Pharmaceuticals

Staffaroni AM – received research support from the NIA/NIH, the Bluefield Project to Cure FTD, and the Larry L. Hillblom Foundation. He has provided consultation to Passage Bio and Takeda.

Tartaglia M.C. has served as an investigator for clinical trials sponsored by Biogen, Avanex, Green Valley, and Roche / Genentech, Bristol Myers Squibb, Eli Lilly/Avid Radiopharmaceuticals, Janssen. She receives research support from Canadian Institutes of Health Research.

Tatton N – was employed by the Association for Frontotemporal Degeneration and is now employed by Alector.

Taylor J – nothing to disclose

VandeVrede L – receives research support from the Alzheimer's Association, American Academy of Neurology, American Brain Foundation, and the NIH, and has provided consultation for Retrotope.

Weintraub S – receives research support from the NIH

Wendelberger B – is an employee of Berry Consultants, LLC where she serves as a consultant to numerous pharmaceutical and device companies

Wong B – receives research support from the NIH

Table 1. Characteristics of the study participants

Characteristic	All Carriers	*C9orf72+*	*GRN+*	*MAPT+*	Non-Carriers	p-value	Pairwise Comparisons
Sample Size	796	347	281	168	412		
ALLFTD Sample Size	275	127	68	80	161		
GENFI Sample Size	521	220	213	88	251		
Age - yr (mean(SD))	50.2 (13.9)	51.2 (13.7)	52.2 (13.7)	44.9 (13.3)	45.9 (13.0)	<0.001	(NC = *MAPT*) < (*C9*=*GRN*)
Female - n (%)	447 (56.1%)	188 (54.2%)	167 (59.4%)	92 (54.8%)	239 (58.0%)	0.51	
Education - yr	14.4 (3.2)	14.5 (3.0)	14.2 (3.4)	14.7 (3.0)	14.8 (2.9)	0.07	
Visits (total number)	2.1 (1.1)	2.0 (1.0)	2.1 (1.1)	2.5 (1.2)	2.2 (1.1)	<0.001	*(C9=GRN,*NC*=GRN,C9*<NC*)< MAPT*
N with 1 visit	292	135	114	43	137		
N with 2 visits	233	120	68	45	106		
N with 3 visits	158	53	57	48	118		
N with ≥4 visits	113	39	42	32	51		
Total number of observations	1,695	690	592	413	910		
Follow-up Length (if > 1 visit) - yr	2.0 (0.9)	1.9 (0.9)	2.1 (0.9)	2.2 (0.9)	2.2 (0.8)	<0.001	*C9< (GRN = MAPT = NC)*
Race - n (%)							
White	776 (97.5%)	342 (98.6%)	274 (97.5%)	160 (95.2%)	404 (98.0%)	0.11	
Non-White^	19 (2.4%)	4 (1.2%)	7 (2.5%)	8 (4.8%)	6 (1.5%)		
Unknown	1 (0.1%)	1 (0.3%)	0	0	2 (0.5%)		
CDR®+NACC-FTLD Global- n (%)							
0	433 (54.4%)	171 (49.3%)	168 (59.8%)	94 (56.0%)	412 (100%)	0.03^^	*C9<GRN*, *C9=MAPT*, *GRN=MAP*T
0.5	127 (16.0%)	61 (17.6%)	39 (13.9%)	27 (16.1%)	NA	0.45	
≥ 1	236 (29.7%)	115 (33.1%)	74 (26.3%)	47 (28.0%)	NA	0.16	
Estimated Years Since Onset*	4.4 (4.7)	5 (4.7)	2.7 (2.4)	6 (7.8)	NA	<0.001	*GRN< C9, GRN < MAPT, C9 = MAPT*
Symptomatic Diagnoses - n (%)							
bvFTD	162 (68.6%)	85 (73.9%)	38 (51.4%)	39 (83.0%)	NA	<0.001	GRN < (*C9 = MAPT)*
PPA	30 (12.7%)	4 (3.5%)	25 (33.8%)	1 (2.1%)	NA	<0.001	(*C9 = MAPT*) < *GRN*
CBS	2 (0.9%)	--	2 (2.7%)	--	NA	0.13	
PSP	3 (1.3%)	1 (0.9%)	1 (1.4%)	1 (2.1%)	NA	0.78	
ALS	4 (1.7%)	4 (3.5%)	--	--	NA	0.14	
FTD-MND	11 (4.7%)	11 (9.6%)	--	--	NA	0.002	(*GRN=MAPT*) < *C9*
MCI	4 (1.7%)	2 (1.7%)	1 (1.4%)	1 (2.1%)	NA	1.0	
AD Dementia	5 (2.1%)	1 (0.9%)	3 (4.1%)	1 (2.1%)	NA	0.35	
Other**	4 (1.7%)	3 (2.6%)	1 (1.4%)	1 (2.1%)	NA	NA	
Missing	9 (3.8%)	4 (3.5%)	2 (2.7%)	3 (6.4%)	NA	NA	

Note. Demographics were calculated using baseline values. Demographic variables and other participant characteristics were compared across genetic groups and controls using regression with pairwise group contrasts for most variables. Sex, race, CDR®+NACC-FTLD, and diagnostic categories were compared using chi-square with Bonferroni-adjusted pairwise comparisons when the omnibus test was significant. For chi-square tests in which any bins were < 10, the Fisher's exact test was used. All tests were two-sided. Symptomatic clinical diagnoses were calculated in those with a CDR®+NACC FTLD Global ≥ 1

^ Due to the small number of non-White participants in this sample, a single bin was used to protect participants' identities.

^^ Controls not included in pairwise comparisons for CDR®+NACC FTLD

*Median (IQR) of baseline values for symptomatic cases based on clinician-reported age of onset.

**Other diagnoses include dementia not otherwise specified (n=2) or the clinician marked "other" without entering additional information.

Abbreviations: CDR®+NACC-FTLD: Clinical Dementia Rating Scale plus National Alzheimer's Coordinating Center Frontotemporal Lobar Degeneration Module; bvFTD: Behavioral Variant Frontotemporal Dementia; PPA: Primary Progressive Aphasia; CBS: Corticobasal Syndrome; PSP: Progressive Supranuclear Palsy Syndrome; ALS: Amyotrophic Lateral Sclerosis; MND: Motor Neuron Disease; MCI: Mild Cognitive Impairment; AD: Alzheimer's Disease

928 **Table 2. Baseline descriptive statistics of measures for each genetic group at**
929 **three epochs.**
930

Mutation Status	Outcome Measure		Disease Age Epoch		
			-40 to -10 YSO	-10 to 0 YSO	0+ YSO
Age-Matched Controls	N (prop) at baseline		229 (0.56)	85 (0.21)	98 (0.24)
	Mean Age (SD) at baseline		36.8 (7.7)	52.6 (6.7)	61.6 (7.7)
	Mean Raw Score (SD; Range)	CDR®+ NACC FTLD SB	0 (0; 0-0)	0 (0; 0-0)	0 (0; 0-0)
		Trails A (Total time in Seconds)	22.76 (8.03; 8-78)	26.36 (9.39; 12-61)	31.07 (14.67; 12-89)
		Trails B (Total time in Seconds)	53.81 (21.93; 19-187)	62.06 (29.48; 27-202)	73.63 (30.43; 31-167)
		MINT (Total Correct)	29.92 (1.75; 24-32)	29.94 (1.62; 26-32)	29.95 (1.92; 25-32)
		MRI Frontal/TIV	7.07 (0.48; 5.39-8.21)	6.68 (0.41; 5.83-7.55)	6.33 (0.45; 5.27-7.28)
		MRI Temporal/TIV	4.76 (0.29; 3.76-5.62)	4.54 (0.22; 4.07-5.03)	4.24 (0.28; 3.46-4.79)
		MRI Medial Temporal (MTL)/TIV	1.03 (0.06; 0.81-1.22)	1.02 (0.06; 0.89-1.19)	0.97 (0.07; 0.8-1.13)
		NfL (log)	1.67 (0.43; 0.38-3.27)	2.05 (0.38; 1.06-2.94)	2.42 (0.43; 1.71-3.76)
C9orf72	N (prop) at baseline		135 (0.39)	63 (0.18)	149 (0.43)
	Mean Age (SD) at baseline		38.3 (8.8)	54.6 (8.2)	61.5 (9)
	Mean Raw Score (SD; Range)	CDR®+ NACC FTLD SB	0.19 (0.57; 0-3)	0.31 (0.69; 0-3.5)	8.32 (6.23; 0-22)
		Trails B (Total time in Seconds)	58.92 (21.85; 28-151)	84 (45.61; 23-300)	168.25 (88.4; 35-300)
		MRI Temporal/TIV	4.58 (0.29; 3.95-5.22)	4.16 (0.32; 3.43-4.71)	3.76 (0.46; 2.29-4.78)
		NfL (log)	1.89 (0.48; 0.94-3.89)	2.58 (0.6; 1.72-4.76)	3.31 (0.85; 1.54-5.54)
	Mean Standardized Units from Control (SD; Range)	CDR®+ NACC FTLD SB	---	---	---
		Trails B	0.23 (1; -1.18-4.43)	0.74 (1.55; -1.32-8.07)	3.11 (2.91; -1.27-7.44)
		MRI Temporal/TIV	-0.62 (1; -2.79-1.56)	-1.75 (1.43; -5.04-0.76)	-1.71 (1.65; -6.92-1.94)
		NfL (log)	0.51 (1.11; -1.68-5.1)	1.37 (1.57; -0.85-7.06)	2.07 (1.96; -2.01-7.18)
GRN	N (prop) at baseline		125 (0.44)	72 (0.26)	84 (0.3)
	Mean Age (SD) at baseline		41 (10.3)	58.2 (7.5)	63.7 (8.8)
	Mean Raw Score (SD; Range)	CDR®+ NACC FTLD SB	0.08 (0.26; 0-2)	0.31 (0.71; 0-3)	9.19 (6.53; 0-24)
		Trails A (Total time in Seconds)	25.37 (9.2; 9-63)	30.57 (10.73; 16-81)	72.12 (46.48; 23-150)
		MRI Frontal/TIV	7.03 (0.52; 5.39-8.93)	6.4 (0.52; 5.25-7.48)	5.15 (0.92; 2.62-7.77)
		NfL (log)	1.87 (0.43; 0.82-3.34)	2.45 (0.56; 1.57-4.27)	4.04 (0.65; 2.14-5.35)
	Mean Standardized Units from Control (SD; Range)	CDR®+ NACC FTLD SB	---	---	---
		Trails A	0.33 (1.15; -1.71-5.01)	0.45 (1.14; -1.1-5.82)	2.8 (3.17; -0.55-8.11)
		MRI Frontal/TIV	-0.08 (1.09; -3.49-3.89)	-0.68 (1.26; -3.46-1.92)	-2.59 (2.02; -8.18-3.18)
		NfL (log)	0.46 (1; -1.95-3.84)	1.04 (1.45; -1.25-5.79)	3.74 (1.49; -0.62-6.75)
MAPT	N (prop) at baseline		69 (0.41)	37 (0.22)	62 (0.37)
	Mean Age (SD) at baseline		34.1 (9.2)	46.3 (9.5)	56.1 (8.6)
	Mean Raw Score (SD; Range)	CDR®+ NACC FTLD SB	0.15 (0.48; 0-2.5)	0.39 (0.76; 0-3)	7.9 (6.51; 0-24)
		MINT (Total Correct)	29.88 (1.8; 25-32)	29.16 (3; 17-32)	21.22 (8.04; 1-32)
		MRI MTL/TIV	1.05 (0.06; 0.87-1.16)	0.98 (0.07; 0.77-1.08)	0.72 (0.14; 0.46-1.04)
		NfL (log)	1.69 (0.45; 0.39-2.53)	1.98 (0.55; 0.93-3.44)	3.04 (0.55; 1.93-5.1)
	Mean Standardized Units from Control (SD; Range)	CDR®+ NACC FTLD SB	---	---	---
		MINT	-0.02 (1.03; -2.82-1.19)	-0.48 (1.85; -7.98-1.27)	-4.56 (4.2; -15.12-1.07)
		MRI MTL/TIV	0.41 (1.04; -2.7-2.15)	-0.69 (1.29; -4.46-1.15)	-3.33 (1.86; -6.87-1.04)
		NfL (log)	0.04 (1.03; -2.95-1.98)	-0.19 (1.45; -2.91-3.63)	1.45 (1.26; -1.11-6.17)

931
932 Note. Baseline raw and standardized values for several measures are displayed for controls and mutation
933 carriers at three Disease Age Epochs. Each participant was assigned to a Disease Age epoch based on
934 the estimated Disease Age at their first visit. Clinical and imaging measures were selected by choosing
935 the "best" measure for each genetic group based on when they became elevated compared to controls
936 and the rate of longitudinal change (descriptive statistics for all modeled measures are displayed in
937 Supplemental Table S2). Raw imaging measures are presented as percentage of total intracranial volume
938 to account for head size. Mean standardized units from controls indicates the number of standard
939 deviations from the control group.
940
941 *Abbreviations: Prop: Proportion; CDR®+NACC FTLD SB: Clinical Dementia Rating Scale plus National*
942 *Alzheimer's Coordinating Center's Frontotemporal Lobar Degeneration Module Sum of Boxes; Trail B:*
943 *Trail Making Test, Part B; MINT: Multilingual Naming Test; MRI: magnetic resonance imaging; TIV: Total*
944 *intracranial volume; NfL (log): Log-transformed plasma neurofilament light chain*
945

Table 3. Clinical trial sample size estimates

Pre-symptomatic prevention trial (CDR®+NACC-FTLD Global = 0)										
			Primary endpoint - Sample Size Estimates (50% Treatment Effect)							
Genetic Group	**Estimated number of eligible participants**	**Inclusion Criteria**	**CDR®+NACC-FTLD-SB**		**Neuropsychological Tests**		**NfL (log)**		**MRI Volume**	
			2 Yrs	4 Yrs	2 Yrs	4 Yrs	2 Yrs	4 Yrs	2 Yrs	4 Yrs
C9orf72 MRI=Temporal NP = Trails B	171	All CDR 0	>10000	4994	>10000	6784	3397	699	1639	394
	13	CDR 0 & NfL (log) > 3	582	334	1113	386	>10000	638	537	173
	38	CDR 0 & DA > -5	508	224	657	184	527	153	424	119
	20	CDR 0 & DA > -2.5	266	111	364	96	439	123	402	102
GRN MRI=Frontal NP=Trails A	168	All CDR 0	3144	1526	3844	1576	684	271	826	459
	7	CDR 0 & NfL (log) > 3	250	179	250	140	158	51	71	46
	26	CDR 0 & DA -5	297	182	267	130	99	**30**	52	**27**
	10	CDR 0 & DA -2.5	182	104	159	79	84	26	37	**24**
MAPT MRI=MTL NP=MINT	94	All CDR 0	7073	2733	>10000	3741	3059	802	1492	526
	4	CDR 0 & NfL (log) > 3	283	188	373	220	>10000	501	147	72
	19	CDR 0 & DA -5	362	190	641	265	595	149	108	39
	14	CDR 0 & DA -2.5	191	97	311	134	438	117	72	**24**
Early symptomatic treatment trial (All CDR®+NACC-FTLD Global = 1 enriched with 0 and 0.5 participants)										
			Primary endpoint - Sample Size Estimates (50% Treatment Effect)							
Genetic Group	**Estimated number of eligible participants**	**Inclusion Criteria**	**CDR®+NACC-FTLD-SB**		**Neuropsychological Tests**		**NfL (log)**		**MRI Volume**	
			1.5 Yrs	2 Yrs	1.5 Yrs	2 Yrs	1.5 Yrs	2 Yrs	1.5 Yrs	2 Yrs
C9orf72 MRI=Temporal NP = Trails B	94	ALL CDR 0.5 and 1	188	129	340	203	811	483	639	367
	37	All CDR 1 & (CDR 0 & 0.5 if NfL > 3)	161	115	370	222	1806	782	645	358
	83	All CDR 1 & (CDR 0 & 0.5 if DA > -2.5)	176	124	400	207	740	423	678	360
	67	All CDR 1 & (CDR 0 & 0.5 if DA > 0)	117	**79**	275	161	628	384	669	359
GRN MRI=Frontal NP=Trails A	67	ALL CDR 0.5 and 1	**76**	**66**	115	**79**	133	**76**	**44**	**30**
	33	All CDR 1 & (CDR 0 & 0.5 if NfL > 3)	97	84	124	92	182	110	49	**36**
	48	All CDR 1 & (CDR 0 & 0.5 if DA > -2.5)	79	68	105	74	127	75	**36**	**26**
	38	All CDR 1 & (CDR 0 & 0.5 if DA > 0)	**39**	**32**	62	**41**	124	72	**32**	**22**
MAPT MRI=MTL NP=MINT	43	ALL CDR 0.5 and 1	175	136	300	196	845	437	124	74
	11	All CDR 1 & (CDR 0 & 0.5 if NfL > 3)	89	66	138	91	1719	769	95	59
	43	All CDR 1 & (CDR 0 & 0.5 if DA > -2.5)	164	120	244	163	779	419	109	63
	31	All CDR 1 & (CDR 0 & 0.5 if DA > 0)	96	66	150	104	627	359	83	48

Note. Sample size estimates (total n for a trial) are first presented for pre-symptomatic prevention trials in which all enrolled participants are presymptomatic based on CDR®+NACC-FTLD = 0. Within each genetic group, sample sizes are estimated for trials enrolling all presymptomatic participants as well as three additional scenarios in which NfL or Disease Age are used to enroll high-risk participants likely to be proximal to symptom onset. In the bottom half of the table, estimates are presented for an early symptomatic trial in which all participants with a CDR®+NACC-FTLD Global = 1 are eligible, and those with CDR®+NACC-FTLD < 1 are included based on different inclusion criteria. The estimated number of eligible participants refers to the number of participants in the current dataset that meet the specified inclusion criteria. For each genetic group, we select a representative MRI and neuropsychological measures (displayed in the first column). Bolded cells indicate that the sample size estimates are less than or within 15 participants of the number eligible. All trial designs assume 1:1 randomization treatment vs. control, 10% attrition per year, and have a primary analysis of a change from baseline in the primary endpoint. Additional details of the assumptions underlying these simulations can be found in Table S9.

Abbreviations: CDR®+NACC-FTLD-SB/CDR: Clinical Dementia Rating Scale plus National Alzheimer's Coordinating Center's Frontotemporal Lobar Degeneration Module Sum of Boxes; NfL(log): Log-transformed plasma neurofilament light chain; MRI: magnetic resonance imaging; NP: Group-specific neuropsychological measure; Trails A/B: Trail Making Test, Parts A & B; MTL: Medial Temporal Lobe; MINT: Multilingual Naming Test; DA = Disease Age

Figure Captions (main text figures)

Figure 1. Raw data points overlaid on model estimated fit

Panels A, C, E, and G display raw data points for mutation carriers (blue) and non-carrier controls (gold) for several representative measures as a function of model estimated Disease Age, with a loess fit to each group displayed using thick solid lines. In these panels, raw outcomes are plotted, and mutation carriers are color coded based on whether they were enrolled through ALLFTD or GENFI. These panels highlight the consistency in progression regardless of cohort. Panels B, D, F, and H display raw data points colored by mutation as a function of disease age. In these panels, the overall fit for each group was derived from the Bayesian disease progression model and is displayed using thick solid lines. Shaded areas indicate the 95% credible interval of the estimate. Age-related changes in controls are observed in panels C-H. Figures for all modeled measures are included in Supplemental Figure S1.

Abbreviations: CDR®+NACC FTLD SB: Clinical Dementia Rating Scale plus National Alzheimer's Coordinating Center's Frontotemporal Lobar Degeneration Module Sum of Boxes; Trails B: Trail Making Test, Part B (total time displayed in seconds); NfL (log): Log-transformed plasma neurofilament light chain; TIV: Total intracranial volume.

Figure 2. Temporal ordering of clinical and biomarker changes in F-FTD

These figures display the empirically derived model-estimated curves in each genetic group. In all figures, model estimated time from onset (years) is on the x-axis. The left y-axis indicates the number of standard deviations (SD) of abnormality compared to controls. The right y-axis indicates CDR®+NACC FTLD Box Score units to provide a context for understanding the degree of clinical impairment associated with changes in the other biomarkers and to provide a raw estimate corresponding to the standardized CDR®+NACC FTLD Box Score (black line). Panels A-C display the mean curves for the CDR®+NACC FTLD Box Score, NfL, and a selected imaging and clinical measure for each genetic group, based on which measure is first elevated by one standard deviation from controls and the measure's rate of longitudinal progression. All clinical, imaging, and fluid biomarkers are displayed in the remaining panels (D-I). The shaded areas indicate the 95% credible interval of the estimate. These figures suggest brain atrophy and elevations in neurofilament light chain levels are detectable prior to symptom onset, and that each mutation shows a unique cascade of biomarker changes.

Abbreviations: CDR®+NACC FTLD SB: Clinical Dementia Rating Scale plus National Alzheimer's Coordinating Center's Frontotemporal Lobar Degeneration Module Sum of Boxes; Trail B: Trail Making Test, Part B; MINT: Multilingual Naming Test; RSMS: Revised Self Monitoring Scale; MRI: magnetic resonance imaging; NfL (log): Log-transformed plasma neurofilament light chain; Stand: Standard

Figure 3. Comparison of mutation carriers with controls at three epochs of disease age

Cross-sectional baseline differences between mutation carriers and controls are presented as effect sizes (omega squared). Bolded cells indicate statistical significance ($p < .05$). Comparisons in which mutation carriers are more impaired than controls at an omega squared > 0.00 are colored, with darker shades illustrating larger effect sizes. CDR®+NACC FTLD SB scores and log-transformed NfL levels are presented for all genetic groups. Clinical and imaging measures were selected for each genetic group based on how early they deviated from controls in the disease progression model and rate of longitudinal progression. Note that statistical comparisons for the CDR®+NACC FTLD SB should be interpreted with caution given that controls were defined as having a baseline CDR®+NACC-FTLD=0 and thus have no variance due to this selection process. A similar figure including all modeled measures can be found in the extended data figures (Extended Data Fig 1).

References

1. Knopman, D. S. & Roberts, R. O. Estimating the number of persons with frontotemporal lobar degeneration in the US population. *J. Mol. Neurosci.* **45**, 330–335 (2011).
2. Greaves, C. V & Rohrer, J. D. An update on genetic frontotemporal dementia. *J. Neurol.* **266**, 2075–2086 (2019).
3. Tsai, R. M. & Boxer, A. L. Therapy and clinical trials in frontotemporal dementia: past, present, and future. *J. Neurochem.* **138**, 211–221 (2016).
4. Boeve, B. F., Boxer, A. L., Kumfor, F., Pijnenburg, Y. & Rohrer, J. D. Advances and controversies in frontotemporal dementia: diagnosis, biomarkers, and therapeutic considerations. *Lancet. Neurol.* **21**, 258–272 (2022).
5. Mercuri, E. *et al.* Nusinersen versus Sham Control in Later-Onset Spinal Muscular Atrophy. *N. Engl. J. Med.* **378**, 625–635 (2018).
6. Miller, T. *et al.* Phase 1-2 Trial of Antisense Oligonucleotide Tofersen for SOD1 ALS. *N. Engl. J. Med.* **383**, 109–119 (2020).
7. Bateman, R. J. *et al.* The DIAN-TU Next Generation Alzheimer's prevention trial: Adaptive design and disease progression model. *Alzheimers. Dement.* **13**, 8–19 (2017).
8. Salloway, S. *et al.* A trial of gantenerumab or solanezumab in dominantly inherited Alzheimer's disease. *Nat Med* **27**, 1187–1196 (2021).
9. Boxer, A. L. *et al.* New directions in clinical trials for frontotemporal lobar degeneration: Methods and outcome measures. *Alzheimer's Dement.* **16**, 131–143 (2020).
10. Bateman, R. J. *et al.* Clinical and Biomarker Changes in Dominantly Inherited Alzheimer's Disease. *N. Engl. J. Med.* **367**, 795–804 (2012).
11. Leverenz, J. B. *et al.* A novel progranulin mutation associated with variable clinical presentation and tau, TDP43 and alpha-synuclein pathology. *Brain* **130**, 1360–1374 (2007).
12. Moore, K. M. *et al.* Age at symptom onset and death and disease duration in genetic frontotemporal dementia: an international retrospective cohort study. *Lancet Neurol.* **19**, 145–156 (2020).
13. Rohrer, J. D. & Boxer, A. L. The Frontotemporal Dementia Prevention Initiative: Linking Together Genetic Frontotemporal Dementia Cohort Studies. *Adv. Exp. Med. Biol.* **1281**, 113–121 (2021).
14. U.S. Food & Drug Administration. *Human Gene Therapy for Neurodegenerative Diseases. Draft Guidance for Industry. FDA-2020-D-2101.*
15. Rentz, D. M. *et al.* Building clinically relevant outcomes across the Alzheimer's disease spectrum. *Alzheimer's Dement. Transl. Res. Clin. Interv.* **7**, e12181 (2021).
16. Staffaroni, A. M. *et al.* Rates of Brain Atrophy across Disease Stages in Familial Frontotemporal Dementia Associated with MAPT, GRN, and C9orf72 Pathogenic Variants. *JAMA Netw. Open* **3**, e2022847–e2022847 (2020).
17. Rohrer, J. D. *et al.* Presymptomatic cognitive and neuroanatomical changes in genetic frontotemporal dementia in the Genetic Frontotemporal dementia Initiative (GENFI) study: a cross-sectional analysis. *Lancet Neurol.* **14**, 253–262 (2015).
18. Chen, Q. *et al.* Rates of lobar atrophy in asymptomatic MAPT mutation carriers. *Alzheimer's Dement. Transl. Res. Clin. Interv.* **5**, 338–346 (2019).
19. Lee, S. E. *et al.* Network degeneration and dysfunction in presymptomatic C9ORF72 expansion carriers. *NeuroImage Clin.* **14**, 286–297 (2017).
20. Caverzasi, E. *et al.* Gyrification abnormalities in presymptomatic *c9orf72* expansion carriers. *J. Neurol. Neurosurg. Psychiatry* **90**, 1005–1010 (2019).
21. Whitwell, J. L. *et al.* Brain atrophy over time in genetic and sporadic frontotemporal dementia: a study of 198 serial magnetic resonance images. *Eur. J. Neurol.* **22**, 745–52 (2015).

22. Rohrer, J. D. *et al.* Distinct profiles of brain atrophy in frontotemporal lobar degeneration caused by progranulin and tau mutations. *Neuroimage* **53**, 1070–6 (2010).
23. Chu, S. A. *et al.* Brain volumetric deficits in MAPT mutation carriers: a multisite study. *Ann. Clin. Transl. Neurol.* **8**, 95–110 (2021).
24. Young, A. L. *et al.* Characterizing the Clinical Features and Atrophy Patterns of MAPT-Related Frontotemporal Dementia With Disease Progression Modeling. *Neurology* **97**, e941-52 (2021).
25. van der Ende, E. L. *et al.* Serum neurofilament light chain in genetic frontotemporal dementia: a longitudinal, multicentre cohort study. *Lancet. Neurol.* **18**, 1103–1111 (2019).
26. Illán-Gala, I. *et al.* Plasma Tau and Neurofilament Light in Frontotemporal Lobar Degeneration and Alzheimer Disease. *Neurology* **96**, e671–e683 (2021).
27. Gendron, T. F. *et al.* Comprehensive cross-sectional and longitudinal analyses of plasma neurofilament light across FTD spectrum disorders. *Cell Reports Med.* **3**, (2022).
28. Bridel, C. *et al.* Diagnostic Value of Cerebrospinal Fluid Neurofilament Light Protein in Neurology: A Systematic Review and Meta-analysis. *JAMA Neurol.* **76**, 1035–1048 (2019).
29. Scherling, C. S. *et al.* Cerebrospinal fluid neurofilament concentration reflects disease severity in frontotemporal degeneration. *Ann. Neurol.* **75**, 116–126 (2014).
30. Rojas, J. C. *et al.* Plasma Neurofilament Light for Prediction of Disease Progression in Familial Frontotemporal Lobar Degeneration. *Neurology* **7**, (2021).
31. Panman, J. L. *et al.* Modelling the cascade of biomarker changes in GRN-related frontotemporal dementia. *J. Neurol. Neurosurg. Psychiatry* (2021). doi:10.1136/jnnp-2020-323541
32. Saracino, D. *et al.* Plasma NfL levels and longitudinal change rates in C9orf72 and GRN-associated diseases: from tailored references to clinical applications. *J. Neurol. Neurosurg. Psychiatry* (2021). doi:10.1136/jnnp-2021-326914
33. Glasmacher, S. A., Wong, C., Pearson, I. E. & Pal, S. Survival and Prognostic Factors in C9orf72 Repeat Expansion Carriers: A Systematic Review and Meta-analysis. *JAMA Neurol.* **77**, 367–376 (2020).
34. Moore, K. *et al.* A modified Camel and Cactus Test detects presymptomatic semantic impairment in genetic frontotemporal dementia within the GENFI cohort. *Appl. Neuropsychol. Adult* 1–8 (2020). doi:10.1080/23279095.2020.1716357
35. Staffaroni, A. M. *et al.* Assessment of executive function declines in presymptomatic and mildly symptomatic familial frontotemporal dementia: NIH-EXAMINER as a potential clinical trial endpoint. *Alzheimers. Dement.* **16**, 11–21 (2020).
36. Barker, M. S. *et al.* Recognition memory and divergent cognitive profiles in prodromal genetic frontotemporal dementia. *Cortex.* **139**, 99–115 (2021).
37. Poos, J. M. *et al.* Cognitive composites for genetic frontotemporal dementia: GENFI-Cog. *Alzheimers. Res. Ther.* **14**, 10 (2022).
38. Quintana, M. *et al.* Bayesian model of disease progression in GNE myopathy. *Stat. Med.* **38**, 1459–1474 (2019).
39. Paganoni, S. *et al.* Adaptive Platform Trials to Transform Amyotrophic Lateral Sclerosis Therapy Development. *Ann. Neurol.* **91**, 165–175 (2022).
40. Pottier, C. *et al.* Potential genetic modifiers of disease risk and age at onset in patients with frontotemporal lobar degeneration and GRN mutations: a genome-wide association study. *Lancet Neurol.* **17**, 548–558 (2018).
41. van der Ende, E. L. *et al.* A data-driven disease progression model of fluid biomarkers in genetic frontotemporal dementia. *Brain* **145**, 1805–1817 (2022).
42. Staffaroni, A. M. *et al.* Individualized atrophy scores predict dementia onset in familial frontotemporal lobar degeneration. *Alzheimer's Dement.* **16**, 37–48 (2020).

43. Oxtoby, N. P. *et al.* Data-driven models of dominantly-inherited Alzheimer's disease progression. *Brain* **141**, 1529–1544 (2018).
44. Onyike, C. U., Shinagawa, S. & Ellajosyula, R. Frontotemporal Dementia: A Cross-Cultural Perspective. *Adv. Exp. Med. Biol.* **1281**, 141–150 (2021).
45. Mok, K. *et al.* Chromosome 9 ALS and FTD locus is probably derived from a single founder. *Neurobiol. Aging* **33**, 209.e3–8 (2012).
46. van der Zee, J. *et al.* A Belgian ancestral haplotype harbours a highly prevalent mutation for 17q21-linked tau-negative FTLD. *Brain* **129**, 841–852 (2006).

Online Methods

Participants

Participants included 796 carriers of pathogenic mutations in the *C9orf72, GRN,* or *MAPT* genes and 412 non-carrier controls from families with a known mutation in one of these genes. Participants were enrolled through Advancing Research and Treatment for Frontotemporal Lobar Degeneration (ARTFL; NCT02365922) and Longitudinal Evaluation of Familial Frontotemporal Dementia Subjects (LEFFTDS; NCT02372773),[47] which recently combined into the ARTFL/LEFFTDS Longitudinal Frontotemporal Lobar Degeneration (ALLFTD; NCT04363684) study. These studies enrolled participants through a consortium of 18 centers across the US and Canada between 2015 and 2020. Participants were also enrolled through the Genetic Frontotemporal Initiative (GENFI), which involves 25 research centers across Europe and Canada. GENFI 2 participants from the 5th Data Freeze (2015-2019) were included. All participants were required to have completed the Clinical Dementia Rating Scale (CDR®) plus Behavioral and Language Domains from the National Alzheimer's Coordinating Center (NACC) FTLD module (CDR®+NACC-FTLD). GENFI 1 (2012 - 2015) participants were excluded because the CDR®+NACC-FTLD was not collected during that study period. Some participants in GENFI 2 and ALLFTD cohorts underwent longitudinal evaluations, and all available data were included. ALLFTD participants received travel compensation and remuneration up to $100 based on the study they participated in. For GENFI, Travel, accommodations, or other reasonable expenses are offered to the participants to cover any costs they incur in order to attend the research visits. The ALLFTD study was approved through the Trial Innovation Network (TIN) at Johns Hopkins University. Local ethics committees at each of the sites approved the study, and all participants provided written informed consent or assent with proxy consent.

ALLFTD Inclusion/Exclusion Criteria Relevant to this study:
<u>Inclusion criteria</u>: Participants must be a member of a family with a known pathogenic mutation in the *GRN* or *MAPT* genes, or with a pathogenic expansion in the *C9orf72* gene. The participant does not have to know their own genetic status but must be at least 18 years of age. The predominant phenotype in most families is cognitive or behavioral. However, families may present with motor-dominant syndromes without exclusion. Participants must have a reliable informant who personally speaks with or sees that subject at least weekly. Participants are sufficiently fluent in English to

complete all measures. Participants must be willing and able to consent to the protocol and undergo yearly evaluations over three years. Participants must be willing and able to undergo neuropsychological testing (at least at baseline visit) and have no contraindication to MRI imaging. Non-carrier family controls were included in the current study if they were clinically normal at baseline, defined by a CDR®+NACC-FTLD Global Score = 0.

Exclusion criteria: Known presence of a structural brain lesion (e.g., tumor, cortical infarct). Presence of another neurologic disorder that could impact findings (e.g., multiple sclerosis).

GENFI Inclusion/Exclusion Criteria Relevant to this study:
Inclusion Criteria: Participants are at least 18 years old. Participants must be a member of a family with a known pathogenic mutation in the *GRN* or *MAPT* genes, or with a pathogenic expansion in the *C9orf72* gene. If the participant is cognitively impaired, there must be an available caregiver that can escort them. The participant must have an identified informant. The participant must be fluent in the language of their country of assessment. Non-carrier family controls were included in the current study if they were clinically normal at baseline, defined by a CDR®+NACC-FTLD Global Score = 0.

Exclusion criteria: Participant has another medical or psychiatric illness that would interfere in completing assessments. Participant is pregnant. Local MRI and lumbar puncture contraindications. The predominant phenotype in most families is cognitive or behavioral. However, families may present with motor-dominant syndromes without exclusion.

Genetic Testing
ALLFTD participants had genetic testing at the University of California, Los Angeles using published methods.[48] GENFI participants were genotyped at their local sites according to previous methods.[17] Briefly, in ALLFTD and GENFI, DNA samples were screened using targeted sequencing of a custom panel of genes previously implicated in neurodegenerative diseases, including *GRN* and *MAPT*. The presence of hexanucleotide repeat expansions in *C9orf72* was detected in ALLFTD using both fluorescent and repeat-primed PC and in GENFI using repeat-primed PCR.

Clinical Assessment
The ALLFTD and GENFI multidisciplinary assessments includes neurological history and examination and collateral interview.[17] Documented years since onset, which was entered as prior in the model, was based on clinical interview.

The CDR®+NACC-FTLD module is an eight-domain rating scale based on informant report.[49–51] A Global Score was calculated to categorize disease severity as presymptomatic (0), questionable or mild symptoms of neurodegenerative disease (0.5), or clear symptoms of dementia (1, 2, or 3).[49] A sum of the eight box scores

(CDR®+NACC-FTLD-SB) was also calculated; this score ranges from 0 –24, with higher scores indicating greater functional impairment.[49]

A subset of neuropsychological tests from the Uniform Data Set (UDS) Neuropsychological Battery, version 3.0 was available for both consortia: Trail Making Test Parts A & B, the Multilingual Naming Test (Boston Naming Test in GENFI), Number Span Forward and Backward (Digit Span in GENFI), Benson Figure Copy and Delayed Recall, and Animal Fluency. Conversion tables from the UDS Crosswalk study were used to harmonize Number Span/Digit Span and the MINT/BNT.[52] Upon review of neuropsychological test scores in the controls, one outlier score was removed. As a sensitivity analysis to consider the impact of additional demographic covariates (i.e., sex, education, language), statistical harmonization of the neuropsychological data was conducted using a W-score approach,[42,53] which is a standardized score controlled for nuisance covariates. Regression models were built using baseline neuropsychological test scores in the non-carrier controls, with separate models in each consortium. All regressions included sex and education. In the GENFI cohort, primary language was included as an additional categorical covariate. Next, in all participants at every time point, the difference between their actual score and predicted score (based on regression conducted in controls) was divided by the standard deviation of the control group to derive a standardized estimate compared to controls with the same demographic background.

Neuroimaging

Image Acquisition

Details of image acquisition, processing, and harmonization can be found below and have been published elsewhere.[54] ALLFTD participants were scanned at 3T on MRI scanners (scanner types are displayed in Supplemental Table S7). T1-weighted images from ALLFTD were acquired as Magnetization Prepared Rapid Gradient Echo (MP-RAGE) images using the following parameters: 240x256x256 matrix; about 170 slices; voxel size = 1.05x1.05x1.25 mm^3; flip angle, TE and TR varied by vendor. A standard imaging protocol was used across all centers, managed, and reviewed for quality by a core group at the Mayo Clinic, Rochester.

GENFI participants underwent volumetric T1-weighted MRI using the standard GENFI protocol.[17,55] A variety of 1.5T and 3T scanners were used across the sites: Siemens Trio, Siemens Skyra, Siemens Prisma, Philips, and General Electric. The scan protocols were designed at the start of the GENFI study to ensure that there was adequate matching between the scanners and the quality of the images. T1-weighted images from GENFI were acquired using the following parameters: 256x256x208 matrix; 208 slices; voxel size = 1.1 mm isotropic, flip angle = 8°, TE and TR varied by vendor. All scans were quality checked and those with movements or artifacts were removed. Furthermore, if any participants displayed moderate to severe vascular disease or any other brain lesions, they were also excluded from the analysis.

Image Processing

The same image processing steps were performed on ALLFTD and GENFI data. Before any prepossessing of the images, all T1-weighted images were visually inspected for quality control. Images with excessive motion or image artifact were excluded. T1-weighted images underwent bias field correction using N3 algorithm.[56] The segmentation was performed using SPM12 (Wellcome Trust Center for Neuroimaging, London, UK, http://www.fil.ion.ucl.ac.uk/spm) unified segmentation.[57] A customized group template was generated from the segmented gray and white matter tissues and cerebrospinal fluid by non-linear registration template generation using the Large Deformation Diffeomorphic Metric Mapping framework.[58] Subjects' native space gray and white matter were geometrically normalized to the group template, modulated, and then smoothed in the group template. The applied smoothing used a Gaussian kernel with 8~mm full width half maximum. Every step of the transformation was carefully inspected from the native space to the group template.

Regional volume estimates were calculated from individual subjects' smoothed, modulated grey matter in template space, by taking the mean of all voxels in several a priori regions of interest (ROIs)[59] by taking the mean of all voxels within the following regions: Frontal, Temporal, Medial Temporal (consisting of amygdala, hippocampus, entorhinal cortex, and parahippocampal gyrus ROIs), Parietal, and Occipital Lobes, Striatum, Insula, Thalamus, and Cerebellum. Volume estimates were then represented as percentage of total intracranial volume. To understand the effects of scanner and to present voxelwise maps, a W-score was created at each voxel to represent volume relative to controls after adjusting for covariates. First, a multivariable linear model was fit for each voxel in a reference group that consisted of the first available scan for non-carrier family controls. Predictors in this model were total intracranial volume (TIV) and scanner platform.[42,53] Next, for each voxel of every available MRI in the study, the same model was fit, entering TIV and scanner, using the coefficients from the reference group to extract a residual. This residual was then divided by the standard deviation of the residuals in the reference group. Therefore, the W-score represents the gray matter content at that voxel as the number of standard deviations away from the expected mean for a reference group, accounting for TIV and scanner platform. We then created a mean W-score value for each ROI and entered it into the model as a sensitivity analysis. Mean W-scores at each voxel in mutation carriers are also presented in supplemental figures.

Plasma Neurofilament Light Chain (NfL)

ALLFTD Methods

Plasma NfL light concentrations were measured at the Mayo Clinic in Jacksonville using the Quanterix single-molecule array technology (Simoa) @ NF-Light Advantage Kit (Cat#103186, Lot 501992) and the HD-X instrument according to the instructions provided. Samples were tested in duplicate using kits from the same lot. In addition to the two quality control samples provided with the kit, all assays included five inter-assay controls. Prior to each assay, plasma samples were thawed, mixed thoroughly by low-speed vortexing, centrifuged at 10,000 g for five minutes, and transferred to 96-well plates that were then sealed to minimize sample evaporation. Samples were diluted four times by the instrument. If levels of NfL in a sample exceeded the upper limit of the

calibration curve, the sample was retested at a higher dilution. Across all assays, the percent coefficient of variations of the mean NfL concentration for the inter-assay controls were below 10%.

GENFI Methods

Plasma NfL concentrations were measured at baseline with Simoa, using the commercially available Simoa Neurology 4-Plex A kit (Quanterix, Lexington, MA, Cat# 102153). Plasma samples were thawed at room temperature (one cycle), mixed thoroughly, and centrifuged at 14,000g for 3 minutes. The supernatant was loaded onto a Quanterix HD-1 Analyzer with a 1:4 specified dilution. Measures were completed in duplicate over a total of six batches, each with an eight-point calibration curve tested in triplicate and two controls tested in duplicate. Plasma concentrations were interpolated from the calibration curve within the same batch and corrected for the dilution. All samples were quantifiable within the dynamic range of 0.69 to 2,000 pg/mL and with an average coefficient of variation below 10%. Instrument operators were blinded to clinical and genetic information.

Prior publications

Prior publications have included some of the data included in these models, including publications describing MRI,[16,18,23,42,54,60–62] NfL,[25,27,30] and clinical data.[12,31,35,37,41,51,54] For full lists of publications from these consortia see https://www.allftd.org/publications and https://www.genfi.org/publications/. This study is the first comprehensive effort to combine clinical, imaging, and plasma biomarker data across consortia.

Statistical Analyses

All available data were included in the statistical analyses. Complete cases were not required, and no imputation was conducted. Statistical tests were two-sided.

Participant characteristics

Demographic variables and other participant characteristics (Table 1) were compared across genetic groups and controls using regression with pairwise group contrasts for most variables. Sex, race, CDR®+NACC-FTLD, and diagnostic categories were compared using chi-square with Bonferroni-adjusted pairwise comparisons when the omnibus test was significant. For chi-square tests in which any bins were < 10, the Fisher's exact test was used.

Disease Progression Model

Disease progression models were built using a Bayesian mixed effects framework, with the goal of estimating a single latent disease stage parameter for each person, which we refer to as Disease Age. The disease progression model is a joint model of all 20 measures listed in Supplemental Table S8. Disease Age is the estimated difference between an individual's chronological age and the age of symptom onset (defined for this study as a CDR®+NACC-FTLD-SB = 0.5). This estimate is positive for symptomatic cases and negative for presymptomatic cases. The model included priors based on an individual's time from expected symptom onset. In symptomatic cases, we used the

clinician's estimate of time from symptom onset, sampled from a normal distribution with a small amount of error (SD=4) to acknowledge the imperfection of this estimate. For presymptomatic cases and non-carrier controls, we used the mean age of the mutation group as a prior, sampled from a normal distribution with more noise (SD=10). The prior standard deviations of 4 and 10 were chosen to be relatively non-informative. For a subject with an observed clinician's estimate of time since symptom onset, there is a 95% prior probability that the true age of onset was within +/- 8 years of the clinician's estimate. For a subject whose onset has not yet been observed, there is a 95% prior probability that the true age of onset was within +/- 20 years of the mean estimated age of onset from the same mutation group.

Disease age was then estimated from a joint analysis of all available clinical, neuropsychological, imaging, and NfL data. Simultaneously, overall disease progression of each endpoint was modeled as a function of latent disease age with several parameters, including expected value at "normal," total decline, endpoint and mutation-specific rate and timing of progression. To account for variability in values of each endpoint at healthy across subjects, we included subject-specific random effects that were correlated across similar endpoints (see Grouping variable in Table S8).

First, models were built separately in each cohort. Visual inspection suggested sufficient alignment between disease progression of all endpoints across the two consortia and subsequent models combined both cohorts within a single analysis. A detailed description of the approach follows:

<u>Latent Disease Stage Disease Progression Model</u>

- Model each endpoint, $k = 1{:}K$, for each subject, $i = 1{:}N$, for each visit, $j = 1{:}J_i$, as a function of latent disease stage. Where $Y_{i,j,k}$ is the value of the endpoint k for subject i at visit j, and $X_{i,j}$ is the age for subject i at visit j.

- Disease age was defined as years since onset (YSO): age at visit minus age at onset, $D_{i,j} = X_{i,j} - \alpha_i$. Age at onset is a latent variable that is estimated for each subject.

- The observed value $Y_{i,j,k}$ was assumed to be distributed normally with a subject and endpoint-specific mean and endpoint-specific variance that is a function of the mean.

$$Y_{i,j,k} \sim N\left(\mu_{i,j,k}, \sigma_k^2\right)$$
$$\mu_{i,j,k} = f_{i,k}\left(D_{i,j}\right)$$

- The subject and endpoint-specific mean decay function, $f_{i,k}(x)$, followed an exponential decay as a function of disease age with location and scale parameters that are mutation specific. Mutations are denoted $m = 1{:}4$ for *C9orf72*, *GRN*, *MAPT*, and non-carriers respectively, m_i is an indicator of the mutation (m=1:4) for subject i.

$$f_{i,k}(D_{i,j}) = (\delta_{0,k} + \delta_{0,k,i}) + \frac{\delta_{1,k} - \delta_{0,k}}{1 + \exp(\theta_{k,m_i} + \beta_{k,m_i} * D_{i,j})}$$

Model parameters and prior distributions for each parameter are described below.

<u>Model Components and prior distributions</u>

- $\delta_{0,k}$: Value of the endpoint at normal/healthy state. Normal prior distribution with mean fixed based on expected value of endpoint at a normal state (see Table S8) and SD of 10.

- $\delta_{1,k}$: Worst value for the endpoint (floor). Normal prior distribution with mean fixed based on expected worst value of the endpoint (see Table S8) and SD of 10.

- $\delta_{0,k,i}$: Subject and endpoint-specific random effects in value of the endpoint at normal state that are correlated across similar endpoints (see Table S8 for groupings). Random effects are standardized based on the estimated endpoint-specific variability across subjects at normal, $\sigma^2_{\delta_{0,k}}$, and have a hierarchical prior distribution with subject-specific standardized mean for each group, g, of endpoints, $\mu_{\delta_0,g,i}$, and group-specific variability across endpoints within a subject, $\sigma^2_{\mu_{\delta_{0,g}}}$.

$$\frac{\delta_{0,k,i}}{\sigma_{\delta_{0,k}}} \sim N\left(\mu_{\delta_0,g_k,i}, \sigma^2_{\mu_{\delta_{0,g_k}}}\right); i = 1{:}N; k = 1{:}K$$

$$\mu_{\delta_0,g,i} \sim N(0,1); g = 1{:}G;$$

$$1/\sigma^2_{\delta_{0,k}} \sim Gamma(0.1,0.1); k = 1{:}K;$$

$$1/\sigma^2_{\mu_{\delta_{0,g}}} \sim Gamma(0.1,0.1); g = 1{:}G$$

Hyper-prior distributions for the endpoint-specific variability across subjects at normal and the group-specific variability across endpoints in that group within a subject have a mean value of 1 on the precision and a SD of 10.

- $\theta_{k,m}$: Endpoint and mutation-specific overall location of mean decay function. Location parameter was set for endpoint, $k = 1$, that corresponds to CDR®+NACC-FTLD-SB so that the model is anchored to assume that a disease age of 0 corresponds to a value on CDR®+NACC-FTLD-SB of 0.5. For all other endpoints, we placed a non-informative prior distribution on the location parameter.

$$\theta_{k,m} \sim N(0,10^2); k = 2{:}K; m = 1{:}4.$$

In particular, $1/(1 + \exp(\theta_{k,m}))$, provides the percentage of the total decline of the endpoint at “onset” (DA =0). A value of 1 implies the endpoint is fully declined, a value of 0.5 implies 50% of the total decline. Under the above non-

informative prior, 95% of the distribution of $1/(1+\exp(\theta_{k,m}))$ is between 0 (<.00001) and 1 (>.99999) with a median value of 0.50.

- $\beta_{k,m}$: Endpoint and mutation-specific overall slope of mean decay function. For all endpoints and mutations, we placed a non-informative prior distribution on the scale parameter.

$$\beta_{k,m} \sim N(0,10^2); k = 1:K; m = 1:4.$$

- α_i: Age at onset per subject
  - If value was observed within the dataset, we assumed that the prior distribution of a subjects age of onset was normal with a mean of the observed value and a SD of 4.
  - If value was not observed within the dataset, we assumed that the prior distribution of a subjects age of onset was normal with a mean of the imputed value (imputed as the mutation and study-specific mean from all observed ages of onset) and a SD of 10.

$$\alpha_i \sim N(\mu_{\alpha,i}, \sigma^2_{\alpha,i});$$

$\mu_{\alpha,i}$: Imputed or observed age of onset per subject

$\sigma_{\alpha,i}$:4 if observed 10 if imputed

- σ_k^2: Endpoint-specific measurement error.

$$1/\sigma_k^2 \sim Gamma(0.1,0.1); k = 1:K.$$

Computation

The Bayesian model was computed in R version 4.1.2, using the rjags package. This package uses Markov Chain Monte Carlo (MCMC) to generate a sequence of dependent samples from the posterior distribution of the parameters. The MCMC had a burnin of 10,000 samples, followed by 100,000 samples.

Secondary analyses using estimated Disease Age

After building the DPMs, we extracted estimates of disease age for each observation. We then further explored the data in two different ways. For each endpoint, we first plotted raw values for mutation carriers and non-carriers as a function of disease age. For each measure, we provide mutation-specific estimates for the age at which that measure deviates from controls by one SD. Second, we binned mutation carriers and controls based on their disease age at baseline (i.e., Epoch 1: Disease Age = -40 to -10; Epoch 2: Disease Age = -10 to 0; Epoch 3: >0). Epochs were chosen for illustrative purposes and to allow for a frequentist statistical analysis. For the cross-sectional data, we first compared the three genetic groups within an epoch by fitting a linear regression with the clinical measure or biomarker as the outcome, and genetic group as a three-level categorical variable. Multiple comparisons were controlled for using the Tukey method. Within each epoch, we also compared carriers to controls. Using the first

available MRI scan for each participant, voxelwise mean W-scores for each bin were displayed for illustrative purposes. We also provide estimates of rates of change within each epoch based on the Bayesian DPM. Each Disease Age estimate is associated with a 95% credible interval. The mean of these credible intervals is presented for each epoch to provide an estimate of how the model accuracy varies as a function of Disease Age; we hypothesized greater uncertainty further away from onset as most measures will be in the normal range at this stage and thus the model is more reliant on prior knowledge (i.e., baseline age for presymptomatic cases).

Clinical Trial Simulation

Virtual clinical trial simulations are used to understand operating characteristics of proposed clinical trial designs. We simulated virtual patient outcomes under different assumptions for key design parameters to create simulated example trials. Within clinical trial simulation, generally, thousands of example trials are simulated under different sets of assumptions (scenarios) including trial sample size, randomization ratio, length of follow-up, targeted population, control progression rates and variability, and treatment effects. Overall average operating characteristics may then be summarized to quantify important characteristics of the proposed design (e.g. type I error, power, treatment effect estimates).

Clinical trial simulation requires assumptions to be made about the underlying data. Results from the disease progression model can be used to create evidence-based assumptions about rates of progression and variability of progression of each endpoint for a target population.

To create a single simulated clinical trial dataset of participant-level endpoint values over time we used the following approach for subject i at visits $\mathrm{j} = 1{:}\,\mathrm{N_j}$ for endpoints $\mathrm{k} = 1{:}\,\mathrm{K}$

- Simulate CDR®+NACC-FTLD global score at baseline given the mutation of the subject and distribution specified in Supplemental Table S9 (informed by natural history data).
- Simulate the disease age at baseline given the CDR®+NACC-FTLD global score and the mutation type from the distribution specified in Supplemental Table S9 (informed by natural history data).
- Simulate a subject-level random effect at normal for each endpoint k by first simulating the overall subject-level standard units from normal for each group of endpoints, $\mathrm{g} = 1{:}\,\mathrm{G}$

$$\mu^*_{\delta_{0,\mathrm{g,i}}} \sim \mathrm{N}(0,1);\, g = 1{:}\,G$$

and then simulating the subject and endpoint-specific effect using sampled subject-level standard units from above for each group, g, and posterior estimates from the DPM

$$\delta^*_{0,\mathrm{k,i}} \sim \mathrm{N}\left(\mu^*_{\delta_{0,\mathrm{g_k,i}}} * \widehat{\sigma}_{\delta_{0,\mathrm{k}}}, \widehat{\sigma}^2_{\delta_{0,\mathrm{k}}} * \widehat{\sigma}^2_{\mu_{\delta_{0,\mathrm{g(k)}}}}\right).$$

- Simulate observed value of endpoint k, at visit j, $Z_{i,j,k}$, from a normal distribution with a subject and endpoint-specific mean and endpoint-specific variance based on the posterior mean results DPM, the subject-level DA at each visit, $DA_{i,j}$, and the subject-level random effect at normal, $\delta^*_{0,k,i}$ simulated above:

$$Z_{i,j,k} \sim N\left(\hat{\mu}_{i,j,k}, \hat{\sigma}^2_k\right);$$

$$\hat{\mu}_{i,j,k} = \left(\hat{\delta}_{0,k} + \delta^*_{0,k,i}\right) + \frac{\hat{\delta}_{1,k} - \hat{\delta}_{0,k}}{1 + \exp\left(\hat{\theta}_{k,m_i} + \hat{\beta}_{k,m_i} * DA_{i,j}\right)}.$$

- Subject may additionally be accepted / rejected on enrollment into the simulated clinical trial based on inclusion/exclusion criteria for CDR®+NACC FTLD-global score, Disease Age at baseline, and/or NfL at baseline.

The expected change from baseline (mean and SD) over different timepoints for each endpoint for a placebo participant given a set of enrollment criteria are calculated using the above simulation strategy across 10,000 simulated datasets. The expected mean and SD of the change from baseline for a placebo participant is then used to calculate the sample size needed (N) to achieve 80% power for a 50% slowing in progression assuming 10% attrition rate per year and 1:1 randomization.

Enrollment criteria was defined based on baseline values of CDR®+NACC-FTLD Global, log(NfL), and estimated Disease Age. Presymptomatic trial designs consider only participants with a baseline CDR®+NACC-FTLD Global = 0 and explored inclusion criteria to define a subpopulation at heightened risk for symptom onset based on elevated NfL (log(NfL) > 3.0) or an estimated disease age within 5 years or 2.5 years of onset. The hypothesis was that enrolling those presymptomatic cases close to onset would reduce the sample size needed to detect an effect by increasing the likelihood that the participants change on the endpoints during the trial period. Early symptomatic trial designs (CDR®+NACC-FTLD = 0, 0.5, and 1) included all participants with a baseline Global score = 1. These simulations explored additional inclusion criteria for presymptomatic participants (Global score of 0 or 0.5) to define a high risk subpopulation based on NfL or an estimated Disease Age cutoff (-2.5 or 0).

Data Availability Statement:

The datasets analyzed for the current study reflect collaborative efforts of two research consortia: ALLFTD and GENFI. Each consortium provides clinical data access based on established policies for data use: processes for request are available for review at allftd.org/data for ALLFTD data and by emailing genfi@ucl.ac.uk. Certain data elements from both consortia (e.g. raw MRI images) may be restricted due to the potential for identifiability in the context of the sensitive nature of the genetic data. The deidentified combined dataset will be available for request through the FTD Prevention Initiative in 2023 (https://www.thefpi.org/).

Code Availability Statement:

Custom R code is available at 10.5281/zenodo.6687486.

Methods-only references

47. Boeve, B. *et al.* The longitudinal evaluation of familial frontotemporal dementia subjects protocol: Framework and methodology. in *Alzheimer's and Dementia* **16**, 22–36 (2020).
48. Ramos, E. M. *et al.* Genetic screening of a large series of North American sporadic and familial frontotemporal dementia cases. *Alzheimers. Dement.* **16**, 118–130 (2020).
49. Miyagawa, T. *et al.* Utility of the global CDR® plus NACC FTLD rating and development of scoring rules: Data from the ARTFL/LEFFTDS Consortium. *Alzheimers. Dement.* **16**, 106–117 (2020).
50. Staffaroni, A. M. *et al.* Longitudinal multimodal imaging and clinical endpoints for frontotemporal dementia clinical trials. *Brain* **142**, 443–459 (2019).
51. Miyagawa, T. *et al.* Use of the CDR® plus NACC FTLD in mild FTLD: Data from the ARTFL/LEFFTDS consortium. *Alzheimer's Dement.* **16**, 79–90 (2020).
52. Monsell, S. E. *et al.* Results From the NACC Uniform Data Set Neuropsychological Battery Crosswalk Study. *Alzheimer Dis. Assoc. Disord.* **30**, 134–139 (2016).
53. Jack, C. R. *et al.* Medial temporal atrophy on MRI in normal aging and very mild Alzheimer's disease. *Neurology* **49**, 786–94 (1997).
54. Olney, N. T. *et al.* Clinical and volumetric changes with increasing functional impairment in familial frontotemporal lobar degeneration. *Alzheimer's Dement.* **16**, 49–59 (2020).
55. Russell, L. L. *et al.* Social cognition impairment in genetic frontotemporal dementia within the GENFI cohort. *Cortex.* **133**, 384–398 (2020).
56. Sled, J. G., Zijdenbos, A. P. & Evans, A. C. A nonparametric method for automatic correction of intensity nonuniformity in MRI data. *IEEE Trans. Med. Imaging* **17**, 87–97 (1998).
57. Ashburner, J. & Friston, K. J. Unified segmentation. *Neuroimage* **26**, 839–51 (2005).
58. Ashburner, J. & Friston, K. J. Diffeomorphic registration using geodesic shooting and Gauss-Newton optimisation. *Neuroimage* **55**, 954–67 (2011).
59. Desikan, R. S. *et al.* An automated labeling system for subdividing the human cerebral cortex on MRI scans into gyral based regions of interest. *Neuroimage* **31**, 968–80 (2006).
60. Bocchetta, M. *et al.* Thalamic atrophy in frontotemporal dementia - Not just a C9orf72 problem. *NeuroImage. Clin.* **18**, 675–681 (2018).
61. Young, A. L. *et al.* Uncovering the heterogeneity and temporal complexity of neurodegenerative diseases with Subtype and Stage Inference. *Nat. Commun.* **9**, 4273 (2018).
62. Bocchetta, M. *et al.* Differential early subcortical involvement in genetic FTD within the GENFI cohort. *NeuroImage. Clin.* **30**, 102646 (2021).

Frontotemporal Prevention Initiative (FPI) Investigators

ALLFTD Investigators

Liana Apostolova,[70] Brian Appleby MD,[7] Sami Barmada,[71] Bradley Boeve MD,[5] Yvette Bordelon MD PhD,[8] Hugo Botha MD,[5] Adam L. Boxer MD PhD,[1] Andrea Bozoki,[19] Danielle Brushaber BS,[6] David Clark,[70] Giovanni Coppola,[8] Ryan Darby,[72] Bradford C. Dickerson MD,[9] Dennis Dickson,[4] Kimiko Domoto-Reilly MD,[10] Kelley Faber,[12] Anne Fagan,[14] Julie A. Fields PhD,[11] Tatiana Foroud PhD,[12] Leah Forsberg PhD,[5] Daniel Geschwind MD PhD,[8,13] Nupur Ghoshal MD PhD,[14] Jill Goldman MS MPhil,[15] Douglas R. Galasko,[20] Ralitza Gavrilova MD,[5] Tania F. Gendron PhD,[4] Jonathon Graff-Radford MD,[5] Neill Graff-Radford MD,[16] Ian M. Grant,[27] Murray Grossman MD EdD,[17] Matthew GH Hall MS,[1] Eric Huang,[1] Hilary W. Heuer PhD,[1] Ging-Yuek Hsiung MD MHSc,[18] Edward D. Huey MD,[15] David Irwin MD,[17] Kejal Kantarci MD,[5] Daniel Kaufer MD,[19] Diana Kerwin,[73] David Knopman MD,[5]John Kornak PhD,[69] Joel Kramer PsyD,[1] Walter Kremers PhD,[6] Maria Lapid,[5] Argentina Lario Lago PhD,[1] Suzee Lee,[1] Gabriel Leger,[20] Peter Ljubenkov MD,[1] Irene Litvan MD,[20] Diane Lucente MS,[9] Ian R. Mackenzie MD,[21] Joseph C. Masdeux,[74] Scott McGinnis,[9] Mario Mendez,[8] Carly Mester BA,[6] Bruce L. Miller MD,[1] Chiadi Onyike MD,[22] M. Belen Pascual,[74] Leonard Petrucelli PhD,[4] Peter Pressman,[75] Rosa Rademakers PhD,[4] Vijay Ramanan MD PhD,[5] Eliana Marisa Ramos PhD,[8] Meghana Rao MPH,[5] Katya Rascovsky PhD,[17] Katherine P. Rankin PhD,[1] Aaron Ritter,[76] Julio C. Rojas MD PhD,[1] Howard J. Rosen MD,[1] Rodolfo Savica MD PhD,[5] William W. Seeley,[1] Jeremy Syrjanen,[5] Adam M. Staffaroni PhD,[1] M. Carmela Tartaglia MD,[26] Jack C. Taylor,[1] Lawren VandeVrede MD PhD,[1] Sandra Weintraub PhD,[24] Bonnie Wong PhD [9]

[1] University of California, San Francisco, Weill Institute for Neurosciences, Department of Neurology, Memory and Aging Center, San Francisco, CA
[4] Mayo Clinic, Department of Neuroscience, Jacksonville, FL, USA
[5] Mayo Clinic, Department of Neurology, Rochester, MN, USA
[6] Mayo Clinic, Department of Quantitative Health Sciences, Rochester, MN, USA
[7] Case Western Reserve University, Department of Neurology, Cleveland, OH, USA
[8] University of California, Los Angeles, Department of Neurology, Los Angeles, CA, USA
[9] Department of Neurology, Massachusetts General Hospital and Harvard Medical School, Boston MA
[10] University of Washington, Department of Neurology, Seattle, WA, USA
[11] Mayo Clinic, Department of Psychiatry and Psychology, Rochester, MN, USA
[12] Indiana University School of Medicine, National Centralized Repository for Alzheimer's, IN, USA
[13] Institute for Precision Health, David Geffen School of Medicine, University of California, Los Angeles, Los Angeles, CA, USA
[15] Columbia University, Department of Neurology, New York, NY, USA
[16] Mayo Clinic, Department of Neurology, Jacksonville, FL, USA
[17] University of Pennsylvania, Department of Neurology, Philadelphia, PA, USA
[18] University of British Columbia, Division of Neurology, Vancouver, BC, CA
[19] University of North Carolina, Department of Neurology, Chapel Hill, NC, USA
[20] University of California, San Diego, Department of Neurosciences, La Jolla, CA, USA
[21] Department of Pathology, University of British Columbia. Vancouver, BC, CA
[22] Johns Hopkins University, Department of Psychiatry and Behavioral Sciences, Baltimore, MD, USA
[25] University of Alabama at Birmingham, Department of Neurology, Birmingham, AL
[26] Tanz Centre for Research in Neurodegenerative Diseases, Division of Neurology, University of Toronto, Toronto, Ontario, Canada
[27] Northwestern University, Department of Neurology, Chicago, IL, USA

[69] University of California, San Francisco, Department of Epidemiology and Biostatistics, San Francisco, CA
[70] Indiana University, Department of Neurology, Indianapolis, IN, USA
[71] University of Michigan, Department of Neurology, Ann Arbor, MI, USA
[72] Vanderbilt University, Department of Neurology, Nashville, TN, USA
[73] UT Southwestern, Department of Neurology, Dallas, TX, USA
[74] Houston Methodist, Department of Neurology, Houston, TX, USA
[75] University of Colorado, Department of Neurology, Aurora, CO, USA
[76] Lou Ruvo Center for Brain Health, Cleveland Clinic Las Vegas, Las Vegas, NV, USA

GENFI Investigators

Aitana Sogorb Esteve,[3,77] Annabel Nelson,[3] Arabella Bouzigues,[3] Carolin Heller,[3] Caroline V Greaves,[3] David Cash,[3] David L Thomas,[78] Emily Todd,[3] Hanya Benotmane,[77] Henrik Zetterberg,[77,79] Imogen J Swift,[3] Jennifer Nicholas,[80] Kiran Samra,[3] Martina Bocchetta,[3] Rachelle Shafei,[3] Rhian S Convery,[3] Carolyn Timberlake,[28] Thomas Cope,[28] Timothy Rittman,[28] Alberto Benussi,[29] Enrico Premi,[81] Roberto Gasparotti,[82] Silvana Archetti,[83] Stefano Gazzina,[84] Valentina Cantoni,[29] Andrea Arighi,[31] Chiara Fenoglio,[31] Elio Scarpini,[31] Giorgio Fumagalli,[31] Vittoria Borracci,[32] Giacomina Rossi,[32] Giorgio Giaccone,[32] Giuseppe Di Fede,[32] Paola Caroppo,[32] Pietro Tiraboschi,[32] Sara Prioni,[32] Veronica Redaelli,[32] David Tang-Wai,[85] Ekaterina Rogaeva,[26] Miguel Castelo-Branco,[86] Morris Freedman,[87] Ron Keren,[88] Sandra Black,[33] Sara Mitchell,[33] Christen Shoesmith,[34] Robart Bartha,[89,90] Rosa Rademakers,[23] Jackie Poos,[35] Janne M. Papma,[35] Lucia Giannini,[35] Rick van Minkelen,[35] Yolande Pijnenburg,[91] Benedetta Nacmias,[92] Camilla Ferrari,[92] Cristina Polito,[93] Gemma Lombardi,[92] Valentina Bessi,[92] Michele Veldsman,[38] Christin Andersson,[94] Hakan Thonberg,[40] Linn Öijerstedt,[40] Vesna Jelic,[95] Paul Thompson,[42] Tobias Langheinrich,[42] Albert Lladó,[46] Anna Antonell,[46] Jaume Olives,[46] Mircea Balasa,[46] Nuria Bargalló,[96] Sergi Borrego-Ecija,[46] Ana Verdelho,[97] Carolina Maruta,[98] Catarina B. Ferreira,[99] Gabriel Miltenberger,[47] Frederico Simões do Couto,[100] Alazne Gabilondo,[48] Ana Gorostidi,[49] Jorge Villanua,[99] Marta Cañada,[102] Mikel Tainta,[49] Miren Zulaica,[49] Myriam Barandiaran,[48,49] Patricia Alves,[48,49] Benjamin Bender,[103] Carlo Wilke,[51] Lisa Graf,[50] Annick Vogels,[104] Mathieu Vandenbulcke,[105] Philip Van Damme,[53] Rose Bruffaerts,[24] Koen Poesen,[106] Pedro Rosa-Neto,[107] Serge Gauthier,[108] Agnès Camuzat,[57] Alexis Brice,[57] Anne Bertrand,[57] Aurélie Funkiewiez,[109] Daisy Rinaldi,[109] Dario Saracino,[57] Olivier Colliot,[57] Sabrina Sayah,[57] Catharina Prix,[60] Elisabeth Wlasich,[60] Olivia Wagemann,[60] Sandra Loosli,[60] Sonja Schönecker,[60] Tobias Hoegen,[60] Jolina Lombardi,[63] Sarah Anderl-Straub,[63] Adeline Rollin,[66] Gregory Kuchcinski,[64,66] Maxime Bertoux,[66] Thibaud Lebouvier,[64,66] Vincent Deramecourt,[64,66] Beatriz Santiago,[110] Diana Duro,[111] Maria João Leitão,[68] Maria Rosario Almeida,[67] Miguel Tábuas-Pereira,[110] Sónia Afonso, [112] Annerose Engel,[113] Maryna Polyakova,[113,114]

[3] Dementia Research Centre, Department of Neurodegenerative Disease, UCL Queen Square London
[23] Applied and Translational Neurogenomics Group, VIB Center for Molecular Neurology, VIB, Antwerp, Belgium
[24] Department of Biomedical Sciences, University of Antwerp, Antwerp, Belgium
[26] Tanz Centre for Research in Neurodegenerative Diseases, Division of Neurology, University of Toronto, Toronto, Ontario, Canada
[28] Department of Clinical Neurosciences and Cambridge University Hospitals NHS Trust and Medical Research Council Cognition and Brain Sciences Unit, University of Cambridge, Cambridge, UK
[29] Centre for Neurodegenerative Disorders, Department of Clinical and Experimental Sciences, University of Brescia, Brescia, Italy
[31] Fondazione IRCCS Ca' Granda, Ospedale Maggiore Policlinico, Milan, Italy
[32] Fondazione IRCCS Istituto Neurologico Carlo Besta, Milano, Italy
[33] Division of Neurology, Department of Medicine, Sunnybrook Health Sciences Centre; Hurvitz Brain Sciences Program, Sunnybrook Research Institute; University of Toronto, Toronto, Canada

[34] Department of Clinical Neurological Sciences, University of Western Ontario, London, Ontario Canada
[35] Department of Neurology, Erasmus Medical Centre, Rotterdam, Netherlands
[38] Nuffield Department of Clinical Neurosciences, Medical Sciences Division, University of Oxford, Oxford, UK
[40] Center for Alzheimer Research, Division of Neurogeriatrics, Department of Neurobiology, Care Sciences and Society, Bioclinicum, Karolinska Institutet, Solna, Sweden
[42] Division of Neuroscience and Experimental Psychology, Wolfson Molecular Imaging Centre, University of Manchester, Manchester, UK.
[46] Alzheimer's disease and Other Cognitive Disorders Unit, Neurology Service, Hospital Clínic, Institut d'Investigacións Biomèdiques August Pi I Sunyer, University of Barcelona, Barcelona, Spain
[47] Faculty of Medicine, University of Lisbon, Lisbon, Portugal
[48] Cognitive Disorders Unit, Department of Neurology, Donostia University Hospital, San Sebastian, Gipuzkoa, Spain
[49] Neuroscience Area, Biodonostia Health Research Institute, San Sebastian, Gipuzkoa, Spain
[50] Department of Neurodegenerative Diseases, Hertie-Institute for Clinical Brain Research and Center of Neurology, University of Tübingen, Tübingen, Germany
[51] Center for Neurodegenerative Diseases (DZNE), Tübingen, Germany
[53] Neurology Service, University Hospitals Leuven, Belgium
[57] Sorbonne Université, Paris Brain Institute – Institut du Cerveau – ICM, Inserm U1127, CNRS UMR 7225, AP-HP - Hôpital Pitié-Salpêtrière, Paris, France
[60] Neurologische Klinik und Poliklinik, Ludwig-Maximilians-Universität, Munich, Germany
[63] Department of Neurology, University of Ulm, Ulm, Germany
[64] Univ Lille, France
[66] CHU, CNR-MAJ, Labex Distalz, LiCEND Lille, France
[67] University Hospital of Coimbra (HUC), Neurology Service, Faculty of Medicine, University of Coimbra, Portugal
[68] Center for Neuroscience and Cell Biology, Faculty of Medicine, University of Coimbra, Coimbra, Portugal
[77] UK Dementia Research Institute at University College London, UCL Queen Square Institute of Neurology, London, UK
[78] Neuroimaging Analysis Centre, Department of Brain Repair and Rehabilitation, UCL Institute of Neurology, Queen Square, London, UK
[79] Department of Psychiatry and Neurochemistry, the Sahlgrenska Academy at the University of Gothenburg, Mölndal, Sweden
[80] Department of Medical Statistics, London School of Hygiene and Tropical Medicine, London, UK
[81] Stroke Unit, ASST Brescia Hospital, Brescia, Italy
[82] Neuroradiology Unit, University of Brescia, Brescia, Italy
[83] Biotechnology Laboratory, Department of Diagnostics, ASST Brescia Hospital, Brescia, Italy
[84] Neurology, ASST Brescia Hospital, Brescia, Italy
[85] The University Health Network, Krembil Research Institute, Toronto, Canada
[86] Faculty of Medicine, University of Coimbra, Coimbra, Portugal
[87] Baycrest Health Sciences, Rotman Research Institute, University of Toronto, Toronto, Canada
[88] The University Health Network, Toronto Rehabilitation Institute, Toronto, Canada
[89] Department of Medical Biophysics, The University of Western Ontario, London, Ontario, Canada
[90] Centre for Functional and Metabolic Mapping, Robarts Research Institute, The University of Western Ontario, London, Ontario, Canada
[91] Amsterdam University Medical Centre, Amsterdam VUmc, Amsterdam, Netherlands
[92] Department of Neuroscience, Psychology, Drug Research and Child Health, University of Florence, Florence, Italy
[93] Department of Biomedical, Experimental and Clinical Sciences "Mario Serio", Nuclear Medicine Unit, University of Florence, Florence, Italy
[94] Department of Clinical Neuroscience, Karolinska Institutet, Stockholm, Sweden
[95] Division of Clinical Geriatrics, Karolinska Institutet, Stockholm, Sweden
[96] Imaging Diagnostic Center, Hospital Clínic, Barcelona, Spain

[97] Department of Neurosciences and Mental Health, Centro Hospitalar Lisboa Norte - Hospital de Santa Maria & Faculty of Medicine, University of Lisbon, Lisbon, Portugal
[98] Laboratory of Language Research, Centro de Estudos Egas Moniz, Faculty of Medicine, University of Lisbon, Lisbon, Portugal
[99] Laboratory of Neurosciences, Faculty of Medicine, University of Lisbon, Lisbon, Portugal
[100] Faculdade de Medicina, Universidade Católica Portuguesa
[101] OSATEK, University of Donostia, San Sebastian, Gipuzkoa, Spain
[102] CITA Alzheimer, San Sebastian, Gipuzkoa, Spain
[103] Department of Diagnostic and Interventional Neuroradiology, University of Tübingen, Tübingen, Germany
[104] Department of Human Genetics, KU Leuven, Leuven, Belgium
[105] Geriatric Psychiatry Service, University Hospitals Leuven, Belgium; Neuropsychiatry, Department of Neurosciences, KU Leuven, Leuven, Belgium
[106] Laboratory for Molecular Neurobiomarker Research, KU Leuven, Leuven, Belgium
[107] Translational Neuroimaging Laboratory, McGill Centre for Studies in Aging, McGill University, Montreal, Québec, Canada
[108] Alzheimer Disease Research Unit, McGill Centre for Studies in Aging, Department of Neurology & Neurosurgery, McGill University, Montreal, Québec, Canada
[109] Centre de référence des démences rares ou précoces, IM2A, Département de Neurologie, AP-HP - Hôpital Pitié-Salpêtrière, Paris, France; Sorbonne Université, Paris Brain Institute – Institut du Cerveau – ICM, Inserm U1127, CNRS UMR 7225, AP-HP - Hôpital Pitié-Salpêtrière, Paris, France
[110] Neurology Department, Centro Hospitalar e Universitario de Coimbra, Coimbra, Portugal
[111] Faculty of Medicine, University of Coimbra, Coimbra, Portugal
[112] Instituto Ciencias Nucleares Aplicadas a Saude, Universidade de Coimbra, Coimbra, Portugal
[113] Clinic for Cognitive Neurology, University Hospital Leipzig, Leipzig, Germany
[114] Department for Neurology, Max Planck Institute for Human Cognitive and Brain Sciences, University Hospital Leipzig, Leipzig, Germany

Figure 1

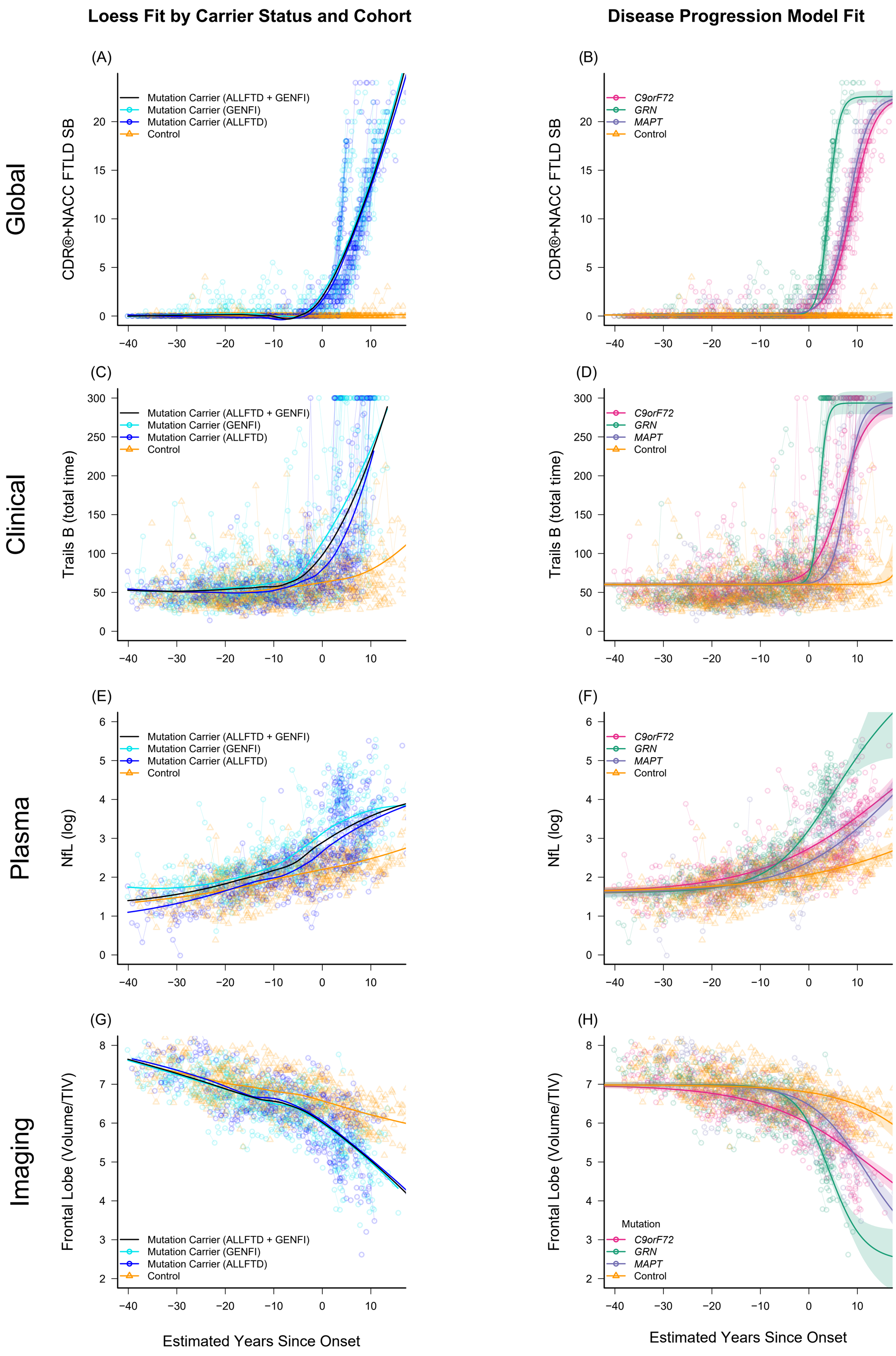
Loess Fit by Carrier Status and Cohort
Disease Progression Model Fit
Global
Clinical
Plasma
Imaging
(A)
(B)
(C)
(D)
(E)
(F)
(G)
(H)
CDR®+NACC FTLD SB
Trails B (total time)
NfL (log)
Frontal Lobe (Volume/TIV)
Mutation Carrier (ALLFTD + GENFI)
Mutation Carrier (GENFI)
Mutation Carrier (ALLFTD)
Control
C9orF72
GRN
MAPT
Mutation
Estimated Years Since Onset

Figure 2

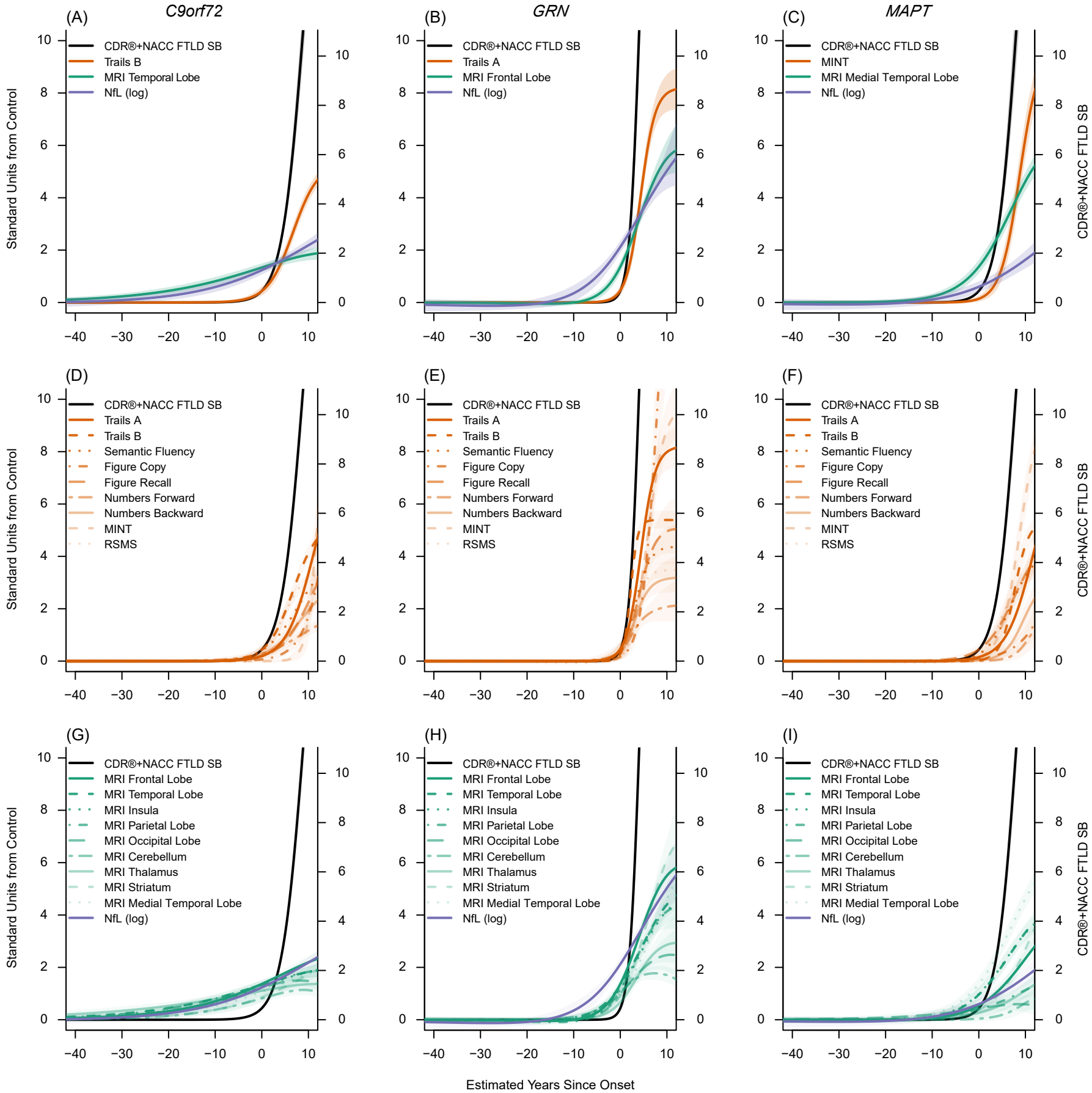
(A)
C9orf72
CDR®+NACC FTLD SB
Trails B
MRI Temporal Lobe
NfL (log)
(B)
GRN
CDR®+NACC FTLD SB
Trails A
MRI Frontal Lobe
NfL (log)
(C)
MAPT
CDR®+NACC FTLD SB
MINT
MRI Medial Temporal Lobe
NfL (log)
(D)
CDR®+NACC FTLD SB
Trails A
Trails B
Semantic Fluency
Figure Copy
Figure Recall
Numbers Forward
Numbers Backward
MINT
RSMS
(E)
CDR®+NACC FTLD SB
Trails A
Trails B
Semantic Fluency
Figure Copy
Figure Recall
Numbers Forward
Numbers Backward
MINT
RSMS
(F)
CDR®+NACC FTLD SB
Trails A
Trails B
Semantic Fluency
Figure Copy
Figure Recall
Numbers Forward
Numbers Backward
MINT
RSMS
(G)
CDR®+NACC FTLD SB
MRI Frontal Lobe
MRI Temporal Lobe
MRI Insula
MRI Parietal Lobe
MRI Occipital Lobe
MRI Cerebellum
MRI Thalamus
MRI Striatum
MRI Medial Temporal Lobe
NfL (log)
(H)
CDR®+NACC FTLD SB
MRI Frontal Lobe
MRI Temporal Lobe
MRI Insula
MRI Parietal Lobe
MRI Occipital Lobe
MRI Cerebellum
MRI Thalamus
MRI Striatum
MRI Medial Temporal Lobe
NfL (log)
(I)
CDR®+NACC FTLD SB
MRI Frontal Lobe
MRI Temporal Lobe
MRI Insula
MRI Parietal Lobe
MRI Occipital Lobe
MRI Cerebellum
MRI Thalamus
MRI Striatum
MRI Medial Temporal Lobe
NfL (log)
Standard Units from Control
CDR®+NACC FTLD SB
Estimated Years Since Onset
−40 −30 −20 −10 0 10
0 2 4 6 8 10

Domain	Measure	Mutation	Disease Age Epoch		
			-40 to -10 YSO	-10 to 0 YSO	0+ YSO
Global	CDR®+NACC FTLD SB	*C9orf72*	**0.07**	**0.10**	**0.41**
		GRN	**0.06**	**0.09**	**0.52**
		MAPT	**0.07**	**0.15**	**0.47**
Clinical	Trails B	*C9orf72*	**0.01**	**0.07**	**0.32**
	Trails A	*GRN*	**0.02**	**0.04**	**0.29**
	MINT	*MAPT*	0.00	0.02	**0.40**
Plasma	NfL (log)	*C9orf72*	**0.05**	**0.22**	**0.28**
		GRN	**0.04**	**0.15**	**0.69**
		MAPT	0.00	0.00	**0.28**
Imaging	Temporal Lobe	*C9orf72*	**0.08**	**0.34**	**0.27**
	Frontal Lobe	*GRN*	0.00	**0.08**	**0.41**
	Medial Temporal Lobe	*MAPT*	**0.02**	**0.07**	**0.57**

ω^2 0 0.2 0.4

Domain/Sub-Domain		Measure	Mutation	Disease Age Epoch		
				-40 to -10 YSO	-10 to 0 YSO	0+ YSO
Global	CDR®+NACC FTLD SB		*C9orf72*	**0.07**	**0.10**	**0.41**
			GRN	**0.06**	**0.09**	**0.52**
			MAPT	**0.07**	**0.15**	**0.47**
Clinical	EF/ Attention/ Speed	Numbers Forward	*C9orf72*	0.00	0.01	**0.10**
			GRN	0.00	0.01	**0.22**
			MAPT	0.00	0.00	0.01
		Numbers Backward	*C9orf72*	0.00	0.01	**0.24**
			GRN	0.00	0.01	**0.31**
			MAPT	**0.01**	0.00	**0.06**
		Trails A	*C9orf72*	**0.03**	**0.04**	**0.20**
			GRN	**0.02**	**0.04**	**0.29**
			MAPT	0.00	0.01	**0.11**
		Trails B	*C9orf72*	**0.01**	**0.07**	**0.32**
			GRN	0.00	**0.02**	**0.50**
			MAPT	0.00	0.01	**0.21**
	Language	Semantic Fluency	*C9orf72*	0.00	0.00	**0.34**
			GRN	0.00	0.01	**0.40**
			MAPT	0.00	0.01	**0.33**
		MINT	*C9orf72*	0.00	0.00	**0.16**
			GRN	0.00	0.00	**0.30**
			MAPT	0.00	0.02	**0.40**
	Memory	Figure Recall	*C9orf72*	**0.02**	0.00	**0.18**
			GRN	0.00	0.01	**0.34**
			MAPT	0.00	0.01	**0.28**
	Visuospatial	Figure Copy	*C9orf72*	0.00	0.01	**0.10**
			GRN	0.01	0.01	**0.12**
			MAPT	0.00	**0.04**	**0.03**
	Behavior	RSMS	*C9orf72*	0.00	0.01	**0.52**
			GRN	0.00	0.00	**0.39**
			MAPT	**0.01**	0.02	**0.40**
Plasma	NfL (log)		*C9orf72*	**0.05**	**0.22**	**0.28**
			GRN	**0.04**	**0.15**	**0.69**
			MAPT	0.00	0.00	**0.28**
Imaging	Frontal Lobe		*C9orf72*	**0.04**	**0.28**	**0.39**
			GRN	0.00	**0.08**	**0.41**
			MAPT	0.00	0.01	**0.20**
	Temporal Lobe		*C9orf72*	**0.08**	**0.34**	**0.27**
			GRN	0.00	**0.14**	**0.25**
			MAPT	**0.01**	0.00	**0.45**
	Medial Temporal Lobe		*C9orf72*	**0.02**	**0.26**	**0.21**
			GRN	0.00	**0.15**	**0.21**
			MAPT	**0.02**	**0.07**	**0.57**
	Parietal Lobe		*C9orf72*	**0.06**	**0.30**	**0.29**
			GRN	0.00	**0.08**	**0.21**
			MAPT	0.00	0.01	0.01
	Occipital Lobe		*C9orf72*	**0.06**	**0.25**	**0.22**
			GRN	0.01	**0.08**	**0.08**
			MAPT	0.00	0.01	0.01
	Insula		*C9orf72*	**0.05**	**0.23**	**0.29**
			GRN	**0.01**	**0.12**	**0.26**
			MAPT	0.01	0.01	**0.49**
	Striatum		*C9orf72*	0.01	**0.12**	**0.21**
			GRN	0.00	0.02	**0.37**
			MAPT	0.01	0.00	**0.25**
	Thalamus		*C9orf72*	**0.10**	**0.28**	**0.23**
			GRN	0.00	**0.06**	**0.15**
			MAPT	0.00	0.01	**0.06**
	Cerebellum		*C9orf72*	0.01	**0.12**	**0.09**
			GRN	0.00	**0.05**	**0.10**
			MAPT	**0.03**	**0.05**	0.01

ω^2 0 0.2 0.4

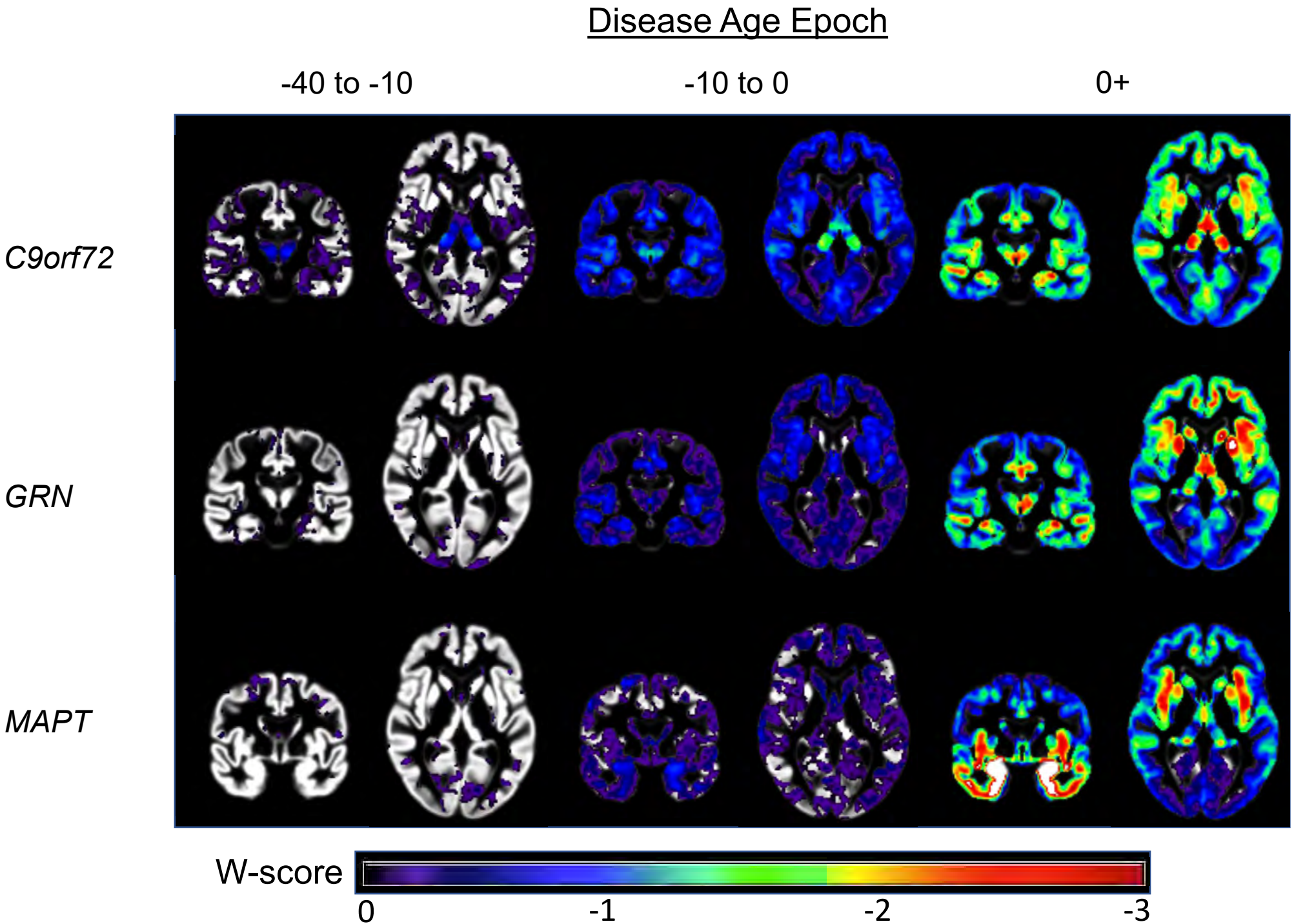
Disease Age Epoch
-40 to -10
-10 to 0
0+
C9orf72
GRN
MAPT
W-score
0
-1
-2
-3

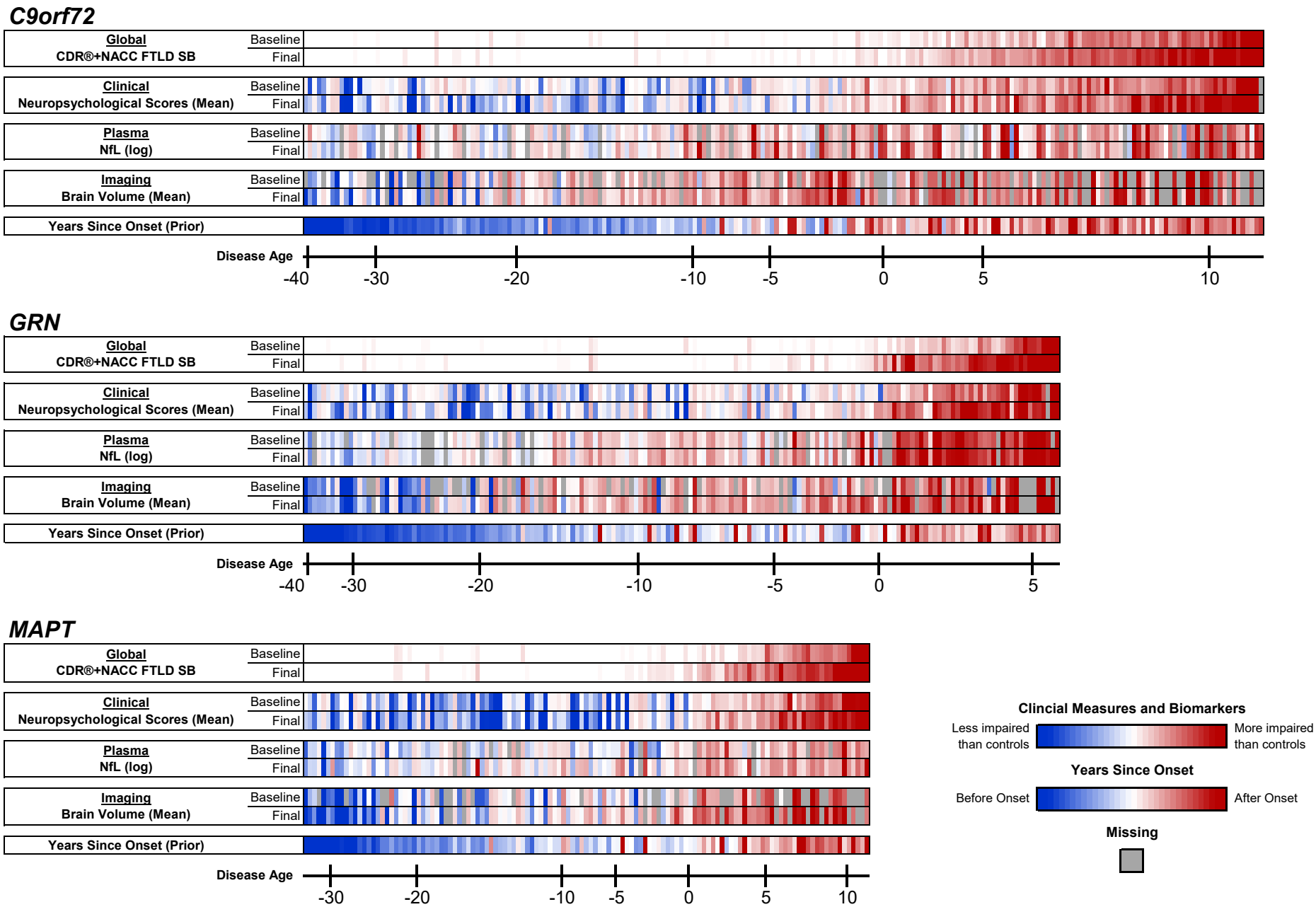
C9orf72
Global
CDR®+NACC FTLD SB
Baseline
Final
Clinical
Neuropsychological Scores (Mean)
Plasma
NfL (log)
Imaging
Brain Volume (Mean)
Years Since Onset (Prior)
Disease Age
-40
-30
-20
-10
-5
0
5
10
GRN
MAPT
Clincial Measures and Biomarkers
Less impaired than controls
More impaired than controls
Years Since Onset
Before Onset
After Onset
Missing

Supplementary Materials

Table of Contents

Supplementary Figure S1. Raw data points overlaid on model estimated fit for all measures

Supplemental Figure 1.1

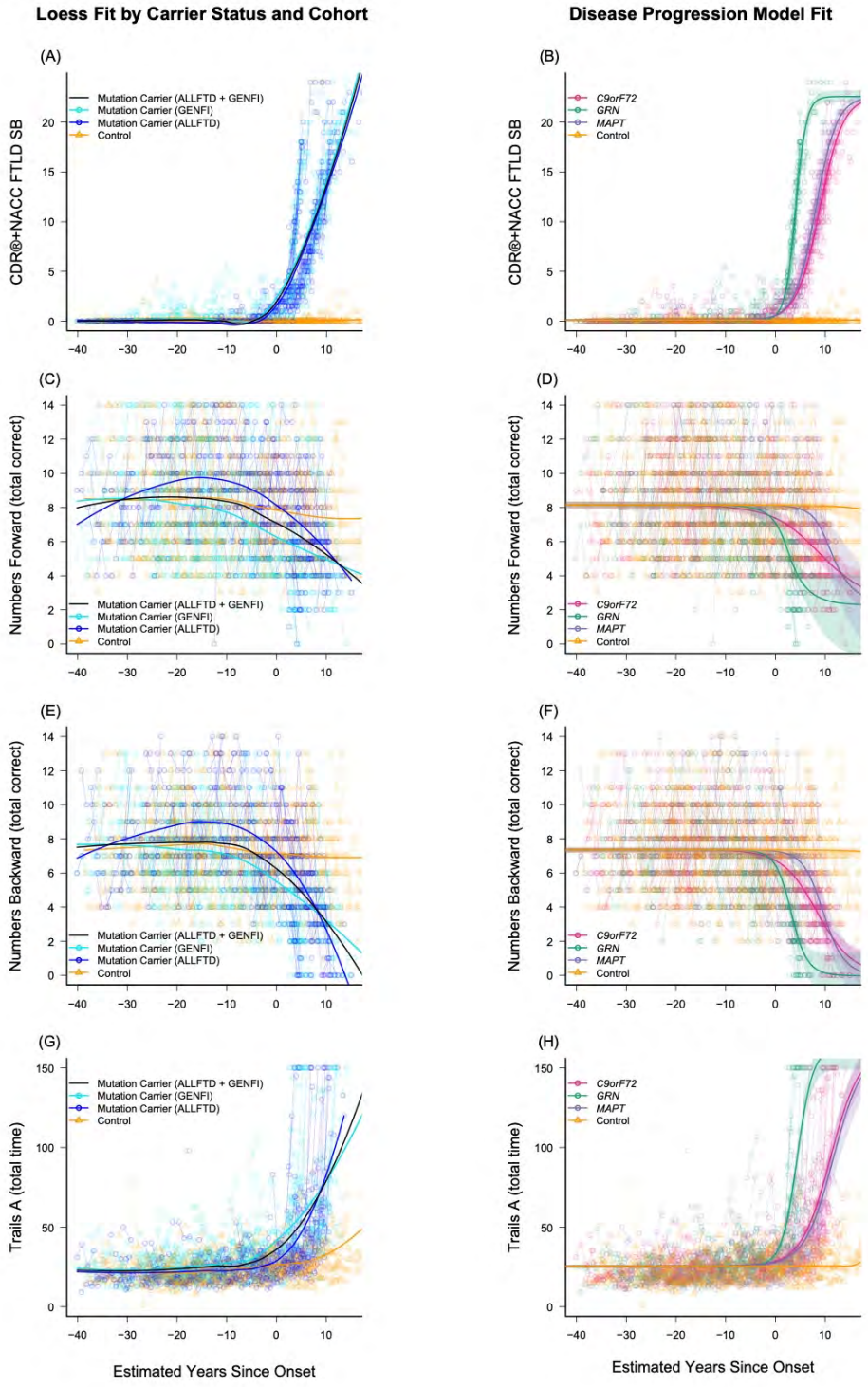

Supplemental Figure 1.2

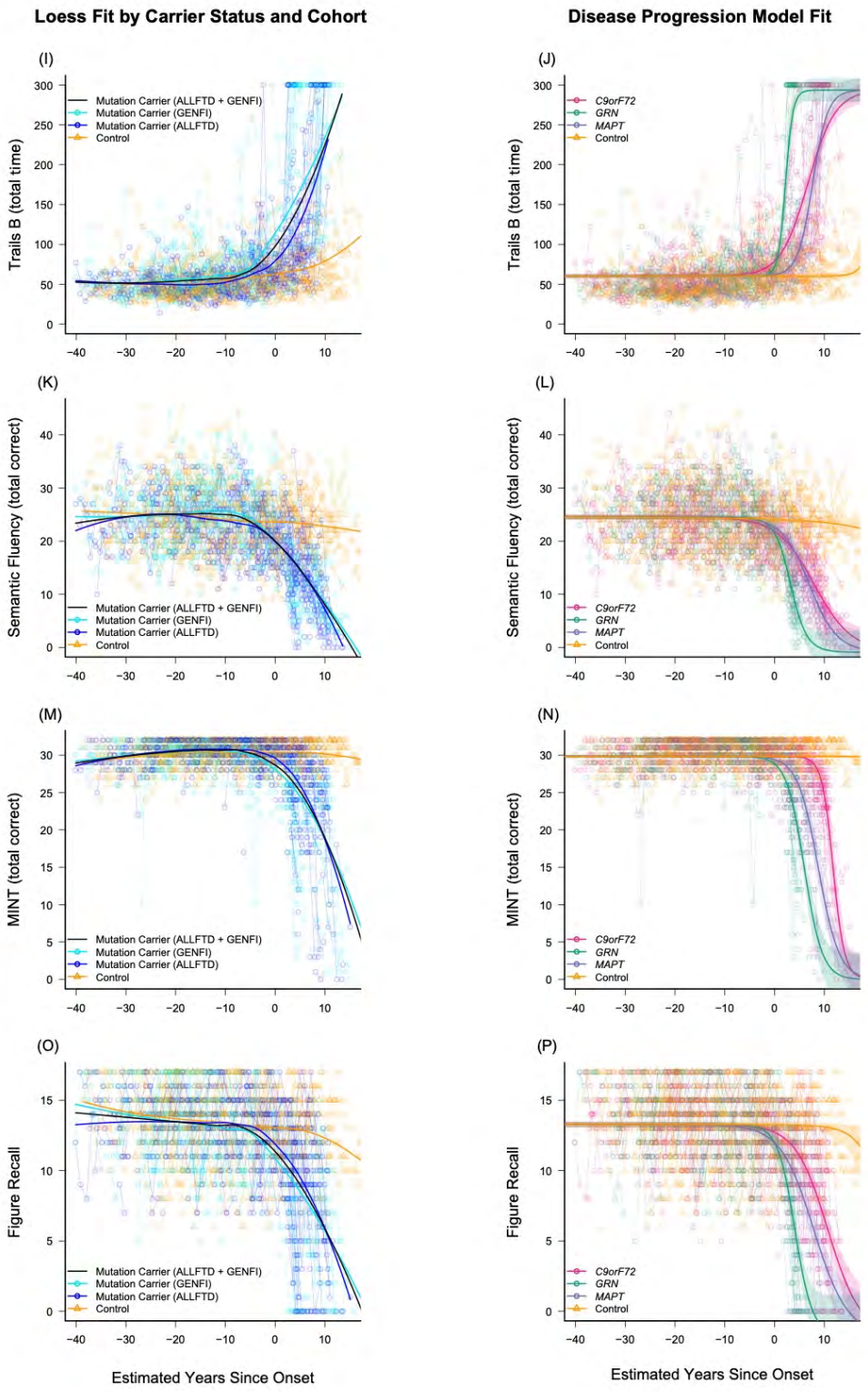

Supplemental Figure 1.3

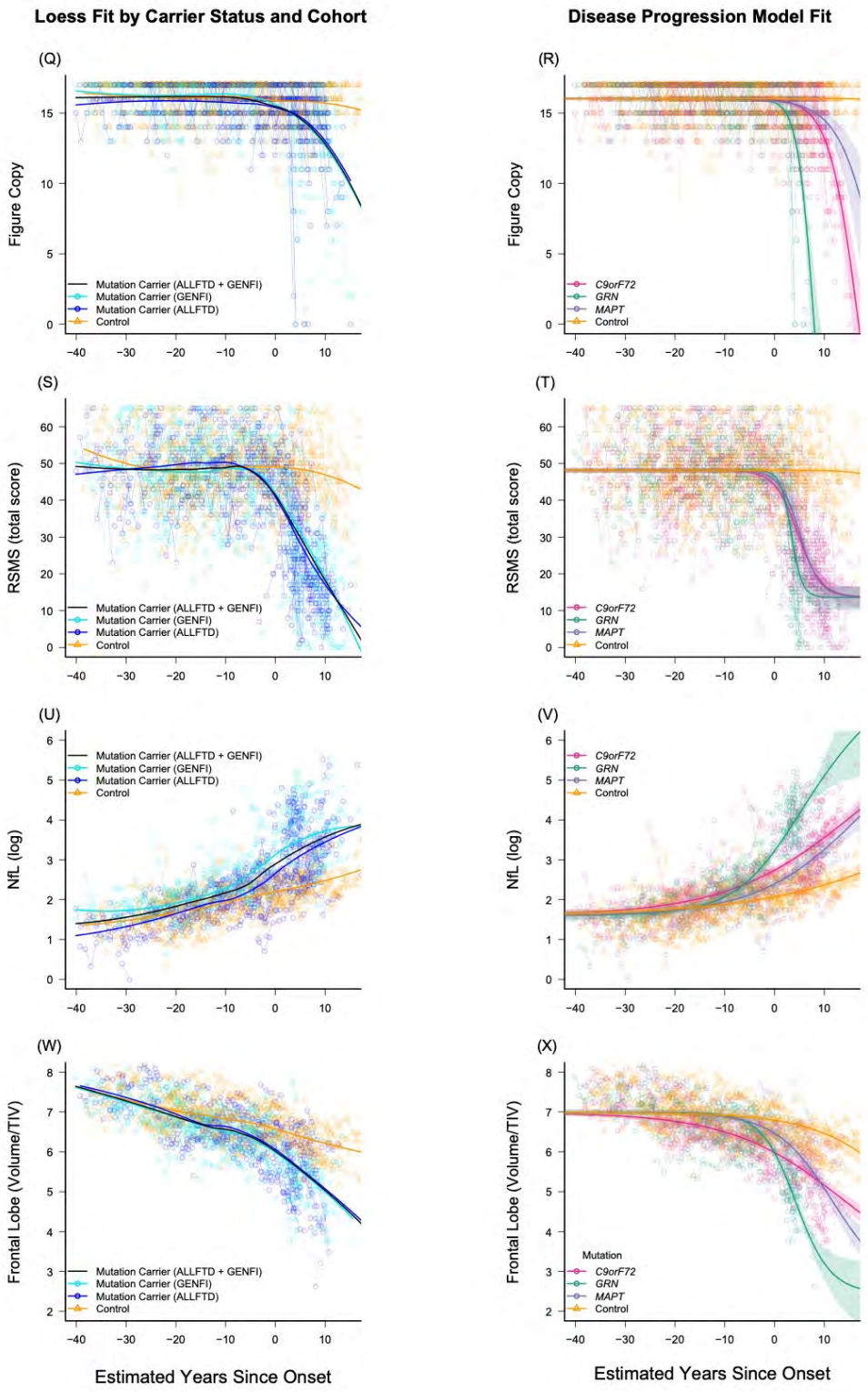

Supplemental Figure 1.4

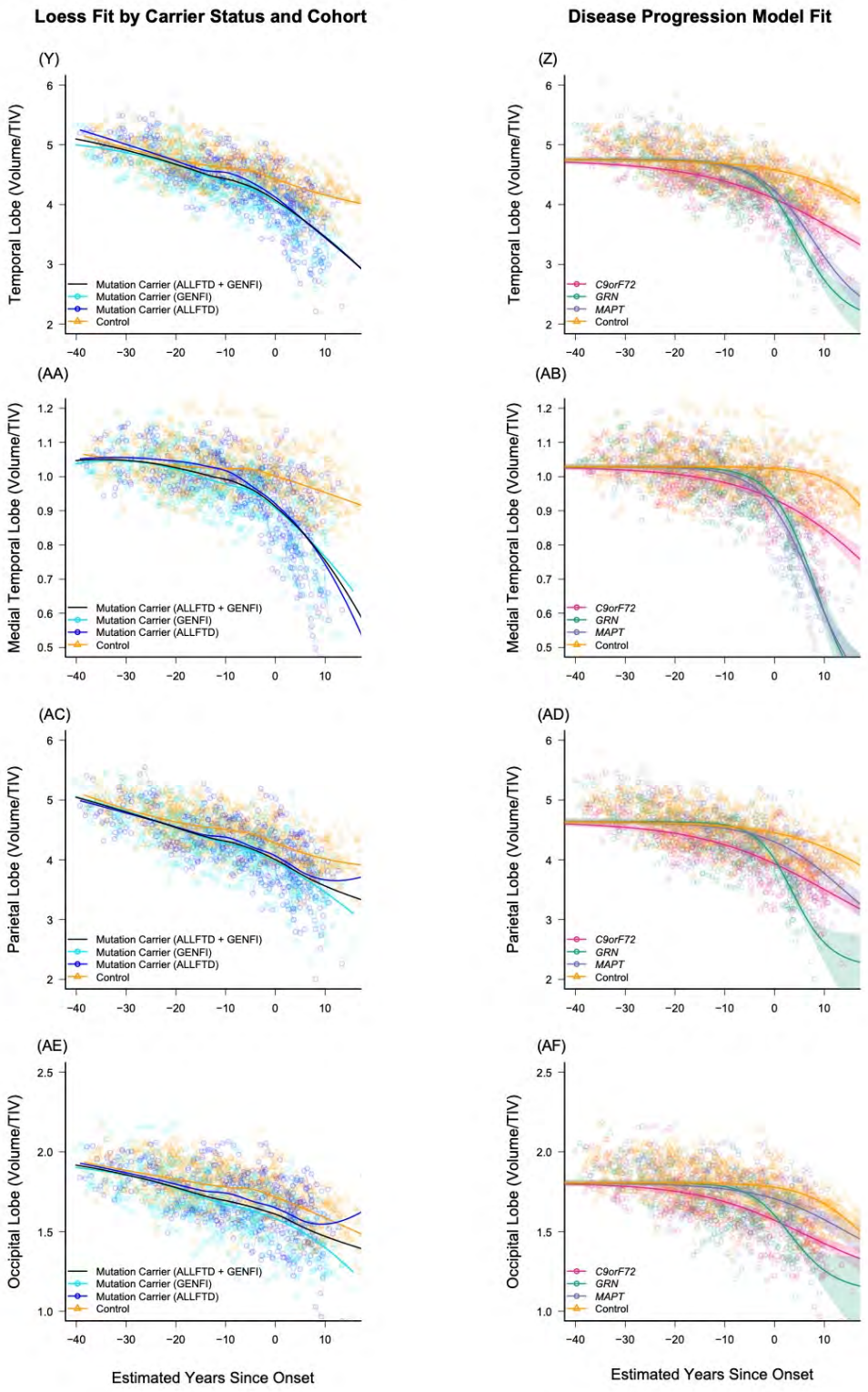

Supplemental Figure 1.5

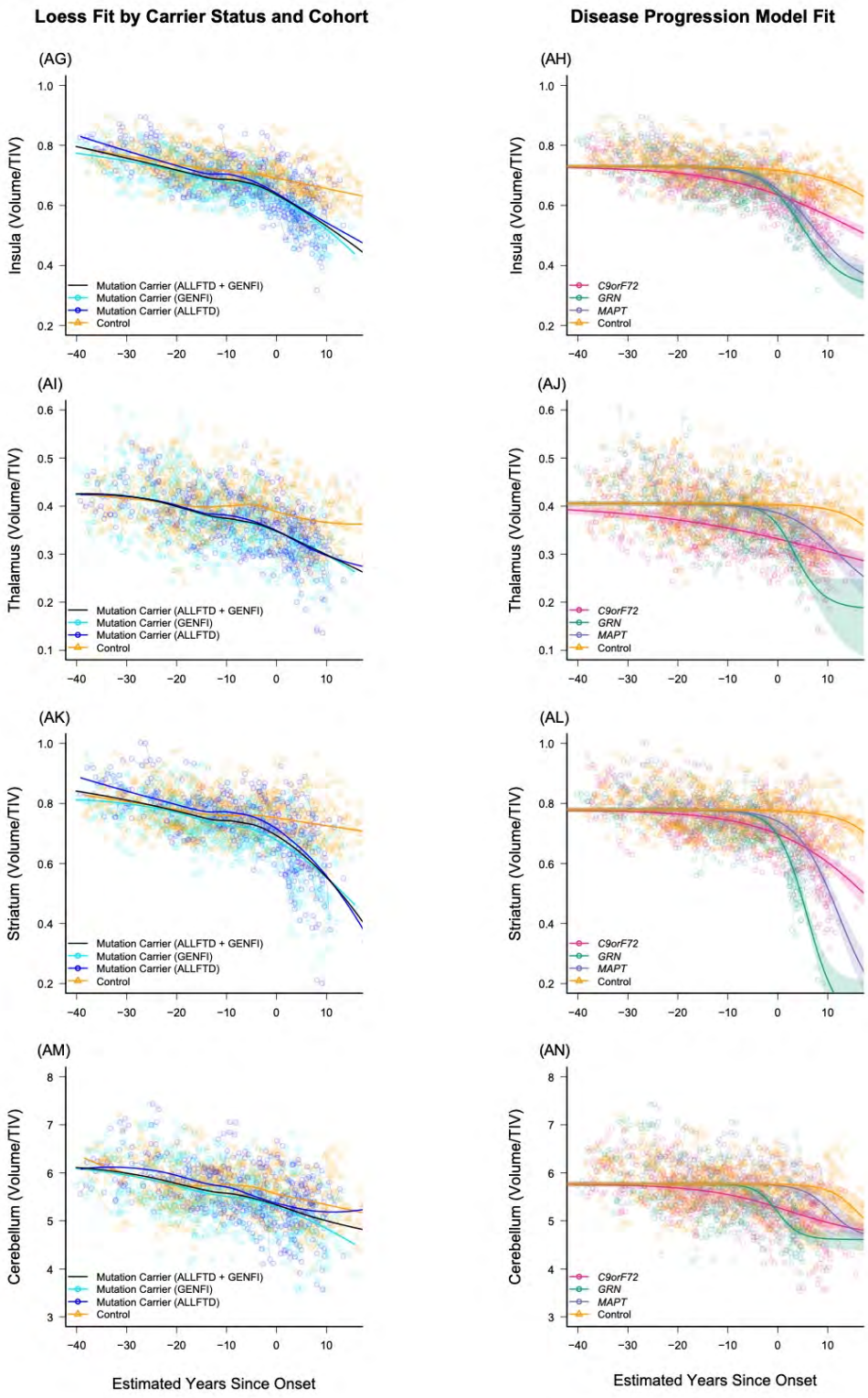

Note. For Supplemental Figures S1.1-1.5, the left columns present raw data points for mutation carriers (blue) and noncarrier controls (gold) for all measures as a function of model estimated Disease Age, with a loess fit to each group displayed using thick solid lines. In these panels, raw outcomes are plotted, and mutation carriers are color coded based on whether they were enrolled through ALLFTD or GENFI. These panels highlight the consistency in progression regardless of cohort. The right column of panels displays raw data points colored by mutation as a function of disease age. In these panels, the overall fit for each group was derived from the Bayesian disease progression model and is displayed using thick solid lines. Shaded areas indicate the 95% credible interval of the estimate.

Abbreviations: CDR®+NACC FTLD SB: Clinical Dementia Rating Scale plus National Alzheimer's Coordinating Center's Frontotemporal Lobar Degeneration Module Sum of Boxes; Trails B: Trail Making Test, Part B (total time displayed in seconds); NfL (log): Log-transformed plasma neurofilament light chain; TIV: Total intracranial volume.

Figure S2. Voxelwise atrophy in *C9orf72* repeat expansion carriers at three disease stages.

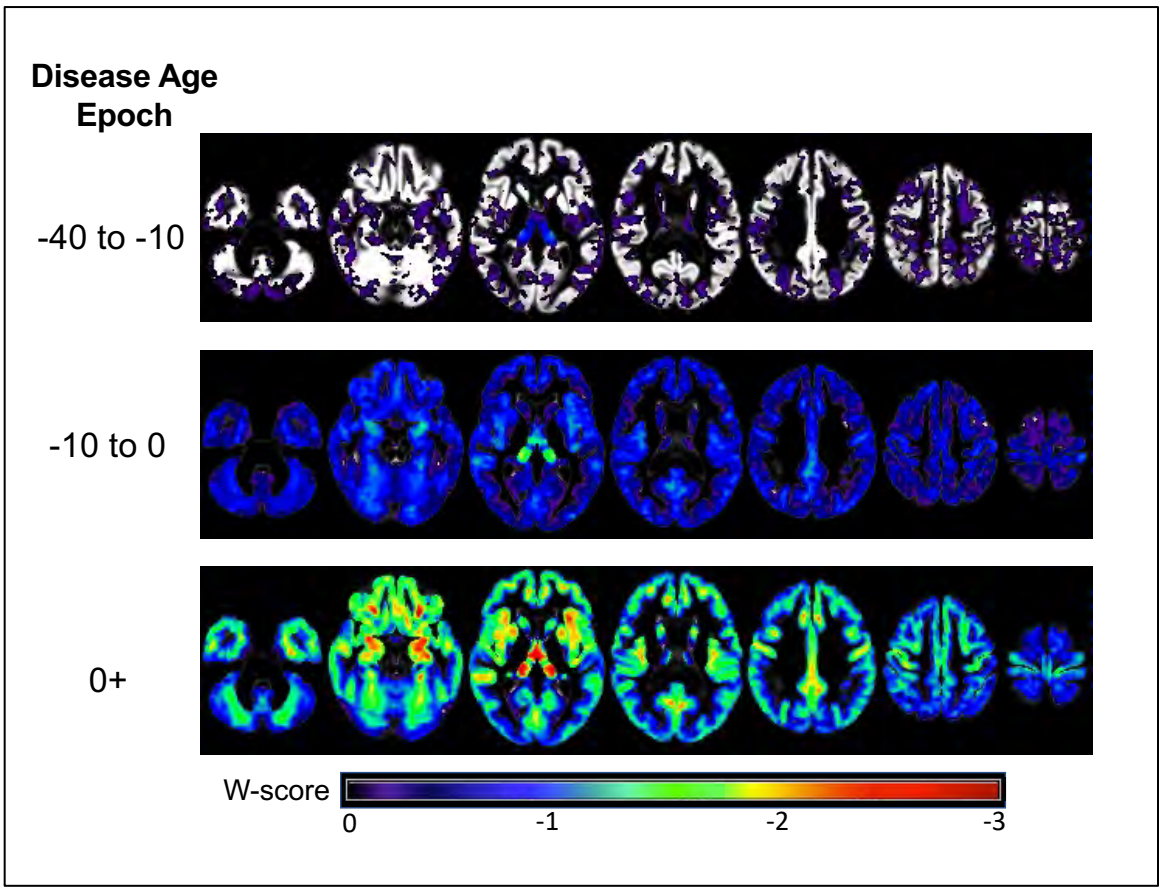

Note. Voxelwise atrophy maps in *C9orf72* were consistent with the region of interest findings. Images are presented in radiological orientation. W-scores indicate the number of standard deviations of atrophy compared to controls, controlling for total intracranial volume and scanner.

Figure S3. Voxelwise atrophy in *GRN* mutation carriers at three disease stages.

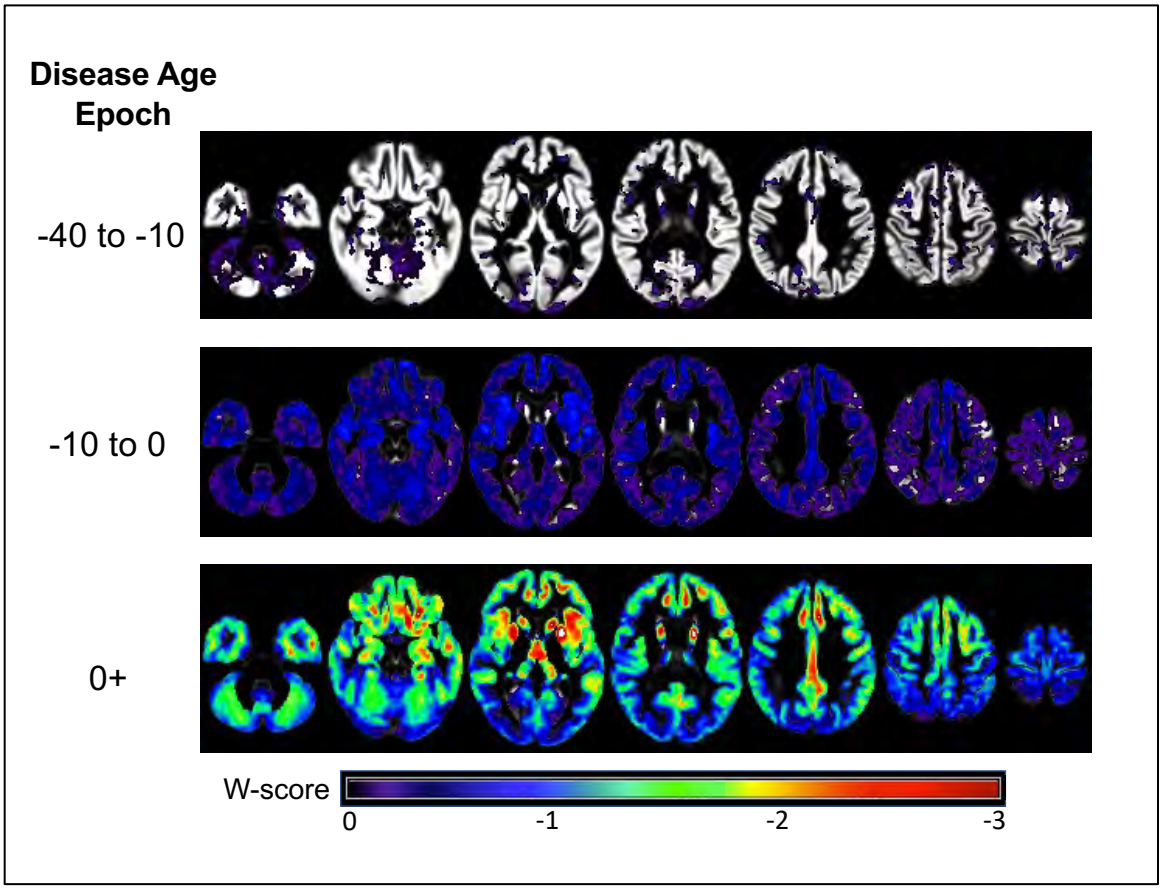

Note. Voxelwise atrophy maps in *GRN* were consistent with the region of interest findings. Images are presented in radiological orientation. W-scores indicate the number of standard deviations of atrophy compared to controls, controlling for total intracranial volume and scanner.

Figure S4. Voxelwise atrophy in *MAPT* mutation carriers at three disease stages.

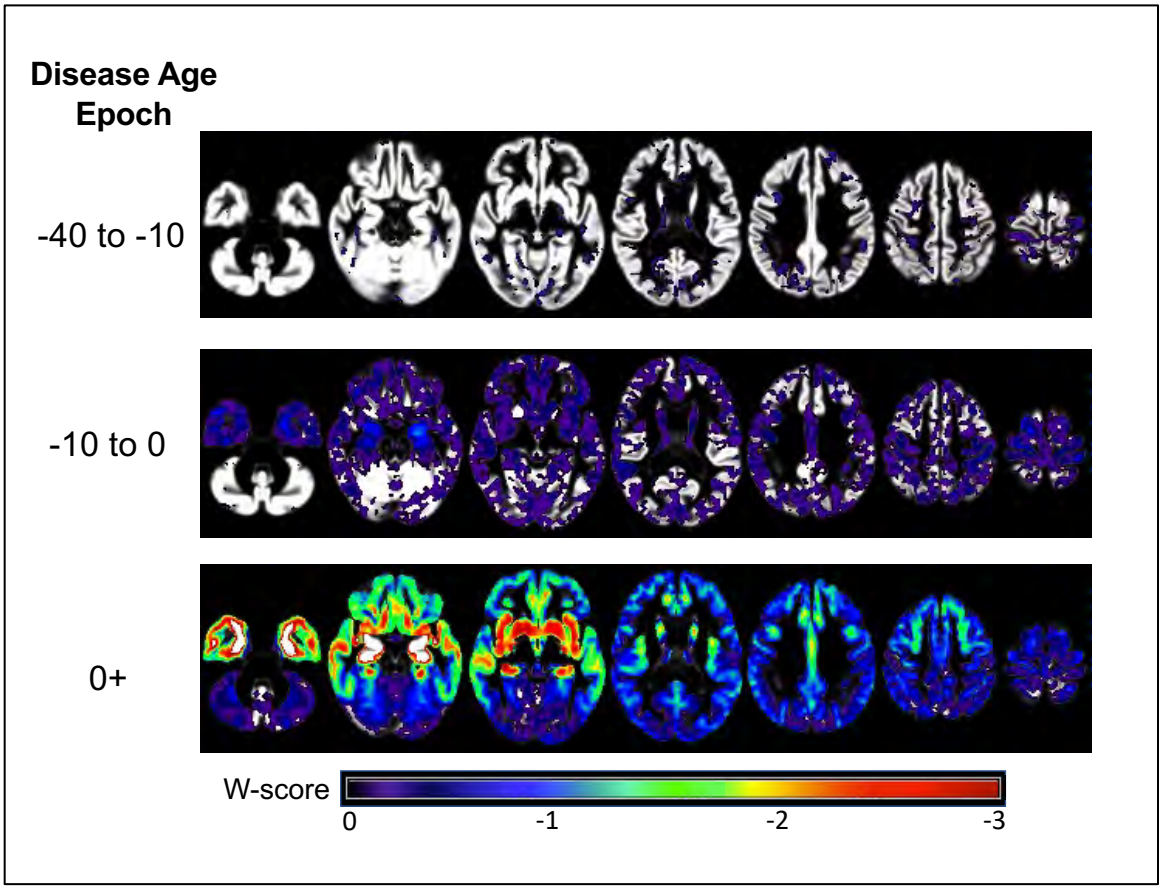

Note. Voxelwise atrophy maps in *MAPT* were consistent with the region of interest findings. Images are presented in radiological orientation. W-scores indicate the number of standard deviations of atrophy compared to controls, controlling for total intracranial volume and scanner.

Supplemental Figure S5. Disease progression model using covariate-adjusted neuropsychological and imaging endpoints

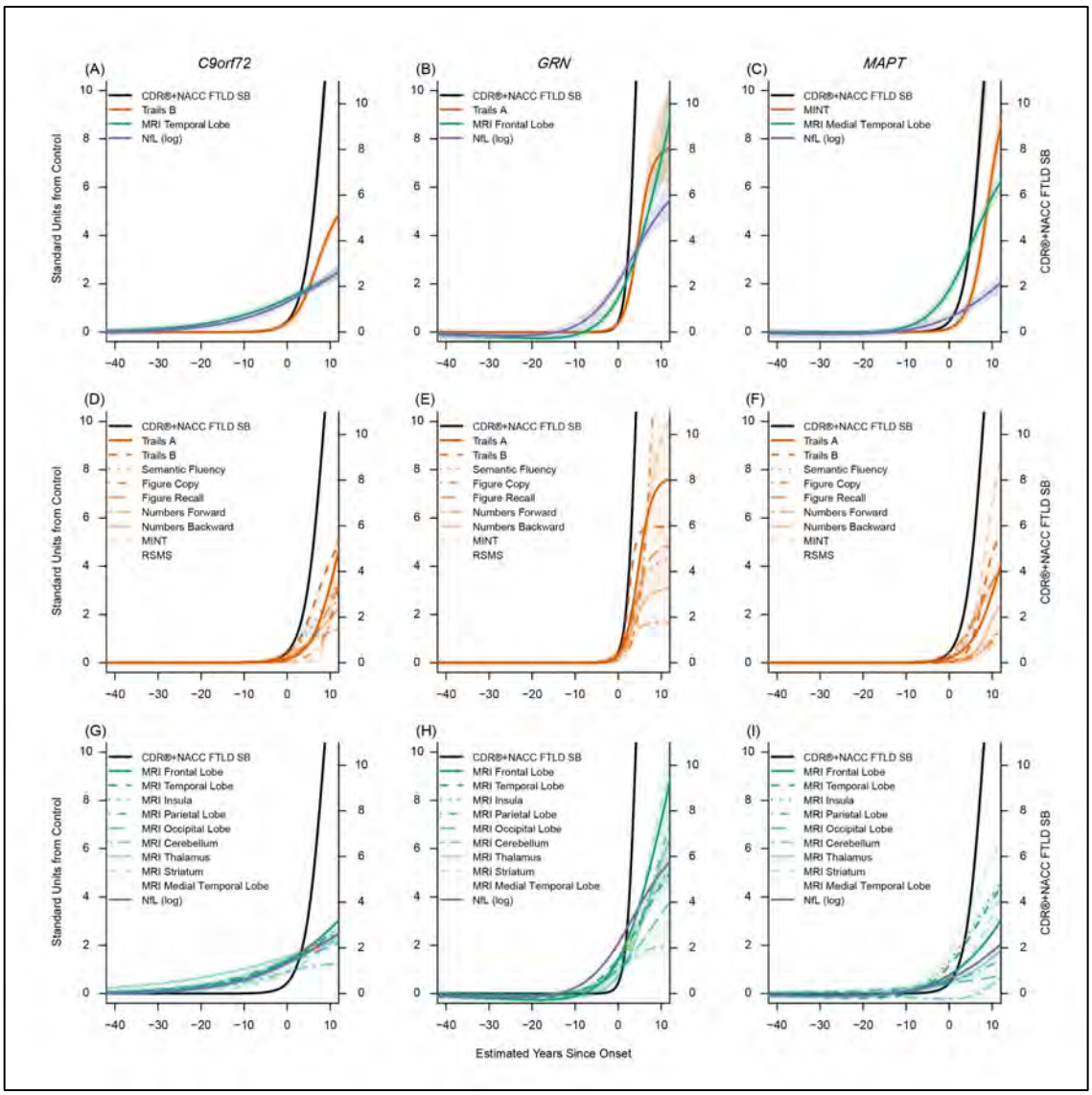

Note. These figures display the empirically derived model-estimated curves in each genetic group using covariate-adjusted neuropsychological scores and volumetric imaging estimates. This figure was created as a sensitivity analysis to complement Figure 2, as the primary disease progression models discussed in this paper included neuropsychological and neuroimaging metrics uncorrected for nuisance covariates. Here, imaging measures were adjusted for head size and scanner. Clinical measures were adjusted for sex, education, and language of test administration. In all figures, model estimated time from onset (years) is on the x-axis. The left y-axis indicates the number of standard deviations (SD) of abnormality compared to controls and the right y-axis indicates CDR®+NACC FTLD Box Score units. Panels A-C display the mean curves for the CDR®+NACC FTLD Box Score, NfL, and a selected imaging and clinical measure for each genetic group, based on which measure is first elevated by one standard deviation from controls and the rate of longitudinal progression. All clinical, imaging, and fluid biomarkers are displayed in the remaining panels (D-I). The shaded areas indicate the 95% credible interval of the estimate. These figures suggest that the results of the disease progression models are not substantively affected by demographic covariates.

Abbreviations: CDR®+NACC FTLD SB: Clinical Dementia Rating Scale plus National Alzheimer's Coordinating Center's Frontotemporal Lobar Degeneration Module Sum of Boxes; Trail B: Trail Making Test, Part B; MINT: Multilingual Naming Test; RSMS: Revised Self Monitoring Scale; MRI: magnetic resonance imaging; NfL (log): Log-transformed plasma neurofilament light chain; Stand: Standard

Supplemental Table S1. Characteristics of mutation carriers by consortium.

	All Carriers		*C9orf72* +		*GRN* +		*MAPT* +		Controls	
Characteristic	**ALLFTD**	**GENFI**	**ALLFTD**	**GENFI**	**ALLFTD**	**GENFI**	**ALLFTD**	**GENFI**	**ALLFTD**	**GENFI**
Sample Size	275	521	127	220	68	213	80	88	161	251
Age - yr (mean(SD))	50.4 (14.4)	50.1 (13.7)	51.2 (14.0)	51.2 (13.6)	55.9 (13.6)	51.0 (13.6)	44.5 (13.5)	45.3 (13.1)	46.9 (13.4)	45.3 (12.8)
Female - no. (%)	158 (57.5%)	289 (55.5%)	76 (59.9%)	112 (50.9%)	38 (55.9%)	129 (60.6%)	44 (55%)	48 (54.6%)	97 (60.3%)	142 (56.6%)
Education - yr	15.5 (2.6)	13.9 (3.3)	15.5 (2.4)	13.9 (3.2)	15.4 (3.0)	13.8 (3.5)	15.5 (2.6)	14.1 (3.3)	15.5 (2.4)	14.3 (3.1)
Visits (total number)	2.4 (1.1)	2.0 (1.1)	2.2 (1.0)	1.8 (0.9)	2.2 (1.0)	2.1 (1.1)	2.7 (1.3)	2.3 (1.0)	2.3 (1.0)	2.2 (1.1)
N with 1 visit	72	220	36	99	19	95	17	26	41	96
N with 2 visits	91	142	43	77	25	43	23	22	55	51
N with 3 visits	60	98	28	25	13	44	19	29	48	70
N with ≥4 visits	52	61	20	19	11	31	21	11	17	34
Total number of observations	649	1,046	286	404	152	440	212	202	365	545
Follow-up Length (if > 1 visit) -yrs	2.1 (0.9)	2.0 (0.9)	1.9 (0.9)	1.8 (0.9)	2.0 (0.9)	2.2 (0.9)	2.3 (1.0)	2.2 (0.7)	2.1 (0.8)	2.2 (0.8)
Race										
White (%)	266 (96.7%)	510 (97.9%)	124 (98.4%)	218 (99.1)	63 (92.7%)	211 (99.1%)	79 (98.8%)	81 (92.1%)	155 (96.3%)	249 (99.2%)
Non-White^	8 (2.9%)	11 (2.1%)	2 (1.6%)	2 (0.9%)	5 (7.4%)	2 (0.9%)	1 (1.3%)	7 (8.0%)	4 (2.5%)	2 (0.8%)
Unknown	1 (0.4%)	0	1 (0.8%)	0	0	0	0	0	2 (1.2%)	0
CDR® + NACC FTLD										
0	143 (52.0%)	290 (55.7%)	60 (47.2%)	111 (50.5%)	38 (55.9%)	130 (61.0%)	45 (56.3%)	49 (55.7%)	161 (100%)	251 (100%)
0.5	45 (16.4%)	82 (15.7%)	24 (18.9%)	37 (16.8%)	8 (11.8%)	31 (15.6%)	13 (16.3%)	14 (15.9%)	NA	NA
≥ 1	87 (31.6%)	149 (28.6%)	43 (33.9%)	72 (32.7%)	22 (32.4%)	52 (24.4%)	22 (27.5%)	25 (28.4%)	NA	NA
Estimated Years Since Onset*	5 (6)	4.3 (3.9)	5 (5)	4.8 (3.8)	3 (2)	2.7 (3.4)	6 (10)	6 (6)	NA	NA
Symptomatic Diagnoses (n)										
bvFTD	65 (74.7%)	97 (65.1%)	33 (76.7%)	52 (72.2%)	12 (54.6%)	26 (50.0%)	20 (90.9%)	19 (76.0%)	NA	NA
PPA	7 (8.1%)	23 (15.4%)	1 (2.3%)	3 (4.2%)	6 (27.3%)	19 (36.5%)	--	1 (4.0%)	NA	NA
CBS	1 (1.2%)	1 (0.7%)	--	--	1 (4.6%)	1 (1.9%)	--	--	NA	NA
PSP	--	3 (2.0%)	--	1 (1.4%)	--	1 (1.9%)	--	1 (4.0%)	NA	NA
ALS	2 (2.3%)	2 (1.3%)	2 (4.7%)	2 (2.8%)	--	--	--	--	NA	NA
FTD-MND	4 (4.6%)	7 (4.7%)	4 (9.3%)	7 (9.7%)	--	--	--	--	NA	NA
MCI	4 (4.6%)	--	2 (4.7%)	--	1 (4.6%)	--	1 (4.6%)	--	NA	NA
AD Dementia	4 (4.6%)	1 (0.7%)	1 (2.3%)	--	2 (9.1%)	1 (1.9%)	1 (4.6%)	--	NA	NA
Other**	--	5 (3.4%)	--	3 (4.2%)	--	1 (1.9%)	--	1 (4.0%)	NA	NA
Missing	--	9 (6.0%)	--	4 (5.6%)	--	2 (3.9%)	--	3 (12%)	NA	NA

Note. Demographics were calculated using baseline values. Symptomatic clinical diagnoses were calculated in those with a CDR®+NACC FTLD ≥ 1. Demographic variables and other participant characteristics were compared across genetic groups and controls using regression with pairwise group contrasts for most variables. Sex, race, CDR®+NACC-FTLD, and diagnostic categories were compared using chi-square with Bonferroni-adjusted pairwise comparisons when the omnibus test was significant. For chi-square tests in which any bins were < 10, the Fisher's exact test was used. All tests were two-sided.

^ Due to the small number of non-White participants in this sample, a single bin was used to protect participants' identities

* Median (IQR) of baseline values for symptomatic cases based on clinician report

** Other diagnoses include dementia NOS (n=2) or the clinician marked "other" without entering additional information.

Abbreviations: CDR®+NACC FTLD: Clinical Dementia Rating Scale plus National Alzheimer's Coordinating Center Frontotemporal Lobar Degeneration Module; bvFTD: Behavioral Variant Frontotemporal Dementia; PPA: Primary Progressive Aphasia; CBS: Corticobasal Syndrome; PSP: Progressive Supranuclear Palsy Syndrome; ALS: Amyotrophic Lateral Sclerosis; MND: Motor Neuron Disease; MCI: Mild Cognitive Impairment; AD: Alzheimer's Disease

Supplemental Table S2. Baseline raw and standardized values for all measures in controls

Age-Matched Controls		Disease Age Epoch		
		-40 to-10 YSO	-10 to 0 YSO	0+ YSO
	N (prop)	229 (0.56)	85 (0.21)	98 (0.24)
	Mean age (SD)	36.8 (7.7)	52.6 (6.7)	61.6 (7.7)
Outcome Measures				
Mean raw score (SD; Range)	CDR® + NACC FTLD SB	0 (0; 0-0)	0 (0; 0-0)	0 (0; 0-0)
	Numbers Forward	8.38 (2.92; 4-14)	7.72 (2.7; 3-14)	7.36 (2.33; 3-13)
	Numbers Backward	7.35 (2.33; 2-14)	7 (2.42; 2-14)	6.83 (2.26; 2-13)
	Trails A	22.76 (8.03; 8-78)	26.36 (9.39; 12-61)	31.07 (14.67; 12-89)
	Trails B	53.81 (21.93; 19-187)	62.06 (29.48; 27-202)	73.63 (30.43; 31-167)
	Semantic Fluency	24.94 (6.44; 10-45)	24.04 (5.71; 9-44)	22.76 (5.93; 9-36)
	MINT	29.92 (1.75; 24-32)	29.94 (1.62; 26-32)	29.95 (1.92; 25-32)
	Figure Recall	13.53 (2.55; 6-17)	12.94 (2.77; 6-17)	12.3 (2.66; 5-17)
	Figure Copy	16.15 (1.23; 9-17)	16.12 (1.1; 13-17)	15.8 (1.42; 11-17)
	RSMS	47.74 (8.76; 20-65)	46.54 (8.09; 27-65)	49 (9.27; 17-65)
	NfL (log)	1.67 (0.43; 0.38-3.27)	2.05 (0.38; 1.06-2.94)	2.42 (0.43; 1.71-3.76)
	Frontal	7.07 (0.48; 5.39-8.21)	6.68 (0.41; 5.83-7.55)	6.33 (0.45; 5.27-7.28)
	Temporal	4.76 (0.29; 3.76-5.62)	4.54 (0.22; 4.07-5.03)	4.24 (0.28; 3.46-4.79)
	Medial Temporal	1.03 (0.06; 0.81-1.22)	1.02 (0.06; 0.89-1.19)	0.97 (0.07; 0.8-1.13)
	Parietal	4.67 (0.32; 3.72-5.79)	4.41 (0.29; 3.72-5.04)	4.09 (0.31; 3.3-4.74)
	Occipital	1.83 (0.13; 1.43-2.17)	1.75 (0.13; 1.37-2.04)	1.62 (0.12; 1.28-1.95)
	Insula	0.74 (0.05; 0.58-0.89)	0.7 (0.05; 0.6-0.86)	0.67 (0.06; 0.52-0.8)
	Striatum	0.79 (0.07; 0.63-0.97)	0.76 (0.07; 0.63-0.94)	0.74 (0.07; 0.58-0.97)
	Thalamus	0.41 (0.06; 0.27-0.57)	0.4 (0.05; 0.29-0.51)	0.37 (0.05; 0.27-0.47)
	Cerebellum	5.82 (0.46; 4.43-7.21)	5.66 (0.44; 4.72-6.64)	5.38 (0.53; 3.95-6.54)

Note. Raw and standardized values for several measures are displayed for controls at three Disease Age epochs. Each participant was assigned to a Disease Age epoch based on the estimated Disease Age at their first visit. Raw imaging measures are presented as percentage of total intracranial volume to account for head size. Mean standardized units from controls indicates the number of standard deviations from the control group, based on the control mean and standard deviation.

Abbreviations: CDR®+NACC FTLD SB: Clinical Dementia Rating Scale plus National Alzheimer's Coordinating Center's Frontotemporal Lobar Degeneration Module Sum of Boxes; Trail A/B: Trail Making Test, Parts A & B; MINT: Multilingual Naming Test; MRI: magnetic resonance imaging; TIV: Total intracranial volume; NfL (log): Log-transformed plasma neurofilament light chain; Stand: Standard; RSMS: Revised Self-Monitoring Scale

Supplemental Table S3 (A-C). Baseline raw and standardized values for all measures in mutation carriers

A. *C9orf72* mutation carriers		Disease Age Epoch		
		-40 to-10 YSO	-10 to 0 YSO	0+ YSO
	N (prop)	135 (0.39)	63 (0.18)	149 (0.43)
	Mean age (SD)	38.3 (8.8)	54.6 (8.2)	61.5 (9)
	Outcome Measures			
Mean Raw Score (SD; Range)	CDR®+NACC FTLD SB	0.19 (0.57; 0-3)	0.31 (0.69; 0-3.5)	8.32 (6.23; 0-22)
	Numbers Forward	8.16 (2.5; 4-14)	7.62 (2.83; 4-14)	5.69 (2.46; 1-14)
	Numbers Backward	7.59 (2.11; 3-13)	7 (2.23; 3-12)	4.14 (2.41; 0-11)
	Trails A	26.3 (10.97; 12-98)	31.41 (12.9; 15-83)	59.06 (34.54; 16-150)
	Trails B	58.92 (21.85; 28-151)	84 (45.61; 23-300)	168.25 (88.4; 35-300)
	Semantic Fluency	24.13 (5.52; 10-39)	23 (5.46; 14-39)	13.07 (6.98; 0-37)
	MINT	29.93 (2.5; 10-32)	29.63 (2.32; 22-32)	24.68 (7.34; 0-32)
	Figure Recall	12.68 (2.63; 5-17)	12.68 (2.35; 6-17)	8.78 (4.17; 0-17)
	Figure Copy	16.15 (1.24; 11-17)	15.81 (1.34; 11-17)	13.88 (3.33; 0-17)
	RSMS	46.62 (9.97; 18-65)	46.42 (10.55; 20-65)	24.71 (12.63; 0-60)
	NfL (log)	1.89 (0.48; 0.94-3.89)	2.58 (0.6; 1.72-4.76)	3.31 (0.85; 1.54-5.54)
	Frontal	6.86 (0.5; 5.78-8.42)	6.12 (0.49; 5.04-7.29)	5.33 (0.72; 3.69-7.08)
	Temporal	4.58 (0.29; 3.95-5.22)	4.16 (0.32; 3.43-4.71)	3.76 (0.46; 2.29-4.78)
	Medial Temporal	1.01 (0.06; 0.87-1.13)	0.94 (0.07; 0.78-1.05)	0.86 (0.11; 0.61-1.08)
	Parietal	4.5 (0.34; 3.89-5.46)	3.97 (0.36; 3.17-4.56)	3.58 (0.45; 2.26-4.8)
	Occipital	1.76 (0.14; 1.44-2.15)	1.57 (0.16; 1.2-1.88)	1.44 (0.2; 0.94-1.95)
	Insula	0.71 (0.06; 0.61-0.83)	0.65 (0.05; 0.53-0.77)	0.58 (0.07; 0.43-0.77)
	Striatum	0.77 (0.07; 0.65-0.96)	0.7 (0.07; 0.57-0.85)	0.62 (0.13; 0.3-0.92)
	Thalamus	0.37 (0.05; 0.24-0.52)	0.33 (0.05; 0.24-0.47)	0.31 (0.06; 0.14-0.46)
	Cerebellum	5.71 (0.5; 4.2-6.93)	5.32 (0.47; 4.11-6.5)	5.01 (0.6; 3.54-6.38)
Mean Stand. Units from Control (SD; Range)	CDR®+NACC FTLD SB	---	---	---
	Numbers Forward	-0.08 (0.85; -1.5-1.92)	-0.04 (1.05; -1.38-2.33)	-0.72 (1.06; -2.73-2.85)
	Numbers Backward	0.1 (0.9; -1.87-2.42)	0 (0.92; -1.66-2.07)	-1.19 (1.07; -3.02-1.84)
	Trails A	0.44 (1.37; -1.34-9.37)	0.54 (1.37; -1.21-6.03)	1.91 (2.36; -1.03-8.11)
	Trails B	0.23 (1; -1.18-4.43)	0.74 (1.55; -1.32-8.07)	3.11 (2.91; -1.27-7.44)
	Semantic Fluency	-0.13 (0.86; -2.32-2.18)	-0.18 (0.96; -1.76-2.62)	-1.63 (1.18; -3.84-2.4)
	MINT	0 (1.43; -11.4-1.19)	-0.19 (1.43; -4.9-1.27)	-2.75 (3.83; -15.64-1.07)
	Figure Recall	-0.33 (1.03; -3.34-1.36)	-0.09 (0.85; -2.51-1.47)	-1.33 (1.57; -4.63-1.77)
	Figure Copy	0 (1.01; -4.19-0.69)	-0.29 (1.21; -4.64-0.8)	-1.36 (2.35; -11.16-0.84)
	RSMS	-0.13 (1.14; -3.39-1.97)	-0.02 (1.3; -3.28-2.28)	-2.62 (1.36; -5.29-1.19)
	NfL (log)	0.51 (1.11; -1.68-5.1)	1.37 (1.57; -0.85-7.06)	2.07 (1.96; -2.01-7.18)
	Frontal	-0.43 (1.03; -2.69-2.82)	-1.37 (1.18; -3.98-1.47)	-2.2 (1.6; -5.81-1.66)
	Temporal	-0.62 (1; -2.79-1.56)	-1.75 (1.43; -5.04-0.76)	-1.71 (1.65; -6.92-1.94)
	Medial Temporal	-0.33 (1.04; -2.72-1.75)	-1.35 (1.25; -4.2-0.53)	-1.38 (1.54; -4.81-1.56)
	Parietal	-0.56 (1.06; -2.46-2.46)	-1.51 (1.27; -4.29-0.52)	-1.67 (1.46; -5.94-2.31)
	Occipital	-0.57 (1.11; -3.15-2.51)	-1.29 (1.19; -4.16-1.01)	-1.45 (1.58; -5.53-2.67)
	Insula	-0.5 (1.01; -2.32-1.69)	-1.24 (1.21; -3.89-1.51)	-1.54 (1.33; -4.28-1.83)
	Striatum	-0.22 (1.06; -2.03-2.44)	-0.78 (1.06; -2.8-1.43)	-1.49 (1.69; -5.86-2.54)
	Thalamus	-0.69 (0.94; -2.88-1.92)	-1.27 (1; -3.13-1.42)	-1.27 (1.23; -4.48-1.76)
	Cerebellum	-0.25 (1.09; -3.53-2.42)	-0.77 (1.05; -3.52-1.91)	-0.7 (1.12; -3.45-1.87)

B. *GRN* mutation carriers		Disease Age Epoch		
Outcome Measure		-40 to-10 YSO	-10 to 0 YSO	0+ YSO
	N (prop)	125 (0.44)	72 (0.26)	84 (0.3)
	Mean age (SD)	41 (10.3)	58.2 (7.5)	63.7 (8.8)
	Outcome Measures			
Mean Raw Score (SD; Range)	CDR®+NACC FTLD SB	0.08 (0.26; 0-2)	0.31 (0.71; 0-3)	9.19 (6.53; 0-24)
	Numbers Forward	8 (2.67; 4-14)	7.08 (2.61; 2-14)	4.75 (2.47; 1-10)
	Numbers Backward	7.06 (2.25; 2-13)	6.47 (2.29; 2-14)	3.52 (2.65; 0-14)
	Trails A	25.37 (9.2; 9-63)	30.57 (10.73; 16-81)	72.12 (46.48; 23-150)
	Trails B	57.43 (21.27; 27-138)	72.42 (29.25; 34-230)	205.36 (97.09; 44-300)
	Semantic Fluency	25.11 (5.08; 15-40)	24.1 (6.36; 11-40)	11.82 (7.26; 0-32)
	MINT	29.88 (1.85; 23-32)	30.18 (1.92; 23-32)	23.78 (6.78; 3-32)
	Figure Recall	13.13 (2.55; 5-17)	12.31 (2.52; 7-17)	7.22 (4.32; 0-17)
	Figure Copy	16.38 (1.02; 13-17)	16.12 (1.35; 11-17)	13.6 (4.07; 0-17)
	RSMS	47.31 (8.75; 16-65)	45.35 (9.03; 25-65)	29.82 (14.32; 0-65)
	NfL (log)	1.87 (0.43; 0.82-3.34)	2.45 (0.56; 1.57-4.27)	4.04 (0.65; 2.14-5.35)
	Frontal	7.03 (0.52; 5.39-8.93)	6.4 (0.52; 5.25-7.48)	5.15 (0.92; 2.62-7.77)
	Temporal	4.74 (0.35; 3.84-6.08)	4.32 (0.32; 3.64-5.12)	3.77 (0.51; 2.21-4.75)
	Medial Temporal	1.02 (0.06; 0.87-1.18)	0.97 (0.07; 0.81-1.13)	0.87 (0.11; 0.61-1.11)
	Parietal	4.66 (0.37; 3.62-5.45)	4.22 (0.33; 3.24-4.97)	3.62 (0.59; 2-5.12)
	Occipital	1.8 (0.16; 1.35-2.18)	1.66 (0.15; 1.2-1.98)	1.52 (0.21; 0.87-1.94)
	Insula	0.73 (0.06; 0.59-0.85)	0.67 (0.05; 0.56-0.79)	0.58 (0.08; 0.32-0.76)
	Striatum	0.78 (0.06; 0.56-0.9)	0.73 (0.07; 0.59-0.88)	0.57 (0.13; 0.21-0.82)
	Thalamus	0.41 (0.06; 0.28-0.61)	0.37 (0.05; 0.3-0.5)	0.32 (0.07; 0.14-0.5)
	Cerebellum	5.74 (0.59; 4.15-7.41)	5.44 (0.48; 4.23-7.05)	5 (0.55; 3.91-6.82)
Mean Stand. Units from Control (SD; Range)	CDR®+NACC FTLD SB	---	---	---
	Numbers Forward	-0.13 (0.91; -1.5-1.92)	-0.23 (0.97; -2.12-2.33)	-1.12 (1.06; -2.73-1.13)
	Numbers Backward	-0.12 (0.97; -2.3-2.42)	-0.22 (0.95; -2.07-2.9)	-1.46 (1.17; -3.02-3.16)
	Trails A	0.33 (1.15; -1.71-5.01)	0.45 (1.14; -1.1-5.82)	2.8 (3.17; -0.55-8.11)
	Trails B	0.17 (0.97; -1.22-3.84)	0.35 (0.99; -0.95-5.7)	4.33 (3.19; -0.97-7.44)
	Semantic Fluency	0.03 (0.79; -1.54-2.34)	0.01 (1.11; -2.28-2.8)	-1.84 (1.22; -3.84-1.56)
	MINT	-0.03 (1.06; -3.96-1.19)	0.15 (1.18; -4.28-1.27)	-3.22 (3.54; -14.07-1.07)
	Figure Recall	-0.16 (1; -3.34-1.36)	-0.23 (0.91; -2.15-1.47)	-1.92 (1.63; -4.63-1.77)
	Figure Copy	0.18 (0.83; -2.56-0.69)	0 (1.23; -4.64-0.8)	-1.56 (2.88; -11.16-0.84)
	RSMS	-0.05 (1; -3.62-1.97)	-0.15 (1.12; -2.66-2.28)	-2.07 (1.55; -5.29-1.73)
	NfL (log)	0.46 (1; -1.95-3.84)	1.04 (1.45; -1.25-5.79)	3.74 (1.49; -0.62-6.75)
	Frontal	-0.08 (1.09; -3.49-3.89)	-0.68 (1.26; -3.46-1.92)	-2.59 (2.02; -8.18-3.18)
	Temporal	-0.09 (1.19; -3.17-4.53)	-1.02 (1.44; -4.09-2.61)	-1.66 (1.82; -7.21-1.83)
	Medial Temporal	-0.11 (1.02; -2.72-2.58)	-0.91 (1.16; -3.75-1.86)	-1.27 (1.44; -4.77-1.93)
	Parietal	-0.05 (1.18; -3.33-2.43)	-0.65 (1.16; -4.05-1.96)	-1.53 (1.9; -6.79-3.35)
	Occipital	-0.25 (1.27; -3.82-2.77)	-0.66 (1.13; -4.09-1.79)	-0.81 (1.67; -6.08-2.56)
	Insula	-0.27 (1.08; -2.75-1.97)	-0.82 (1.16; -3.15-1.85)	-1.49 (1.47; -6.23-1.6)
	Striatum	-0.17 (0.92; -3.31-1.58)	-0.34 (0.99; -2.46-1.84)	-2.15 (1.76; -7.01-1.08)
	Thalamus	0.1 (1.08; -2.3-3.48)	-0.54 (0.99; -1.94-2.11)	-0.99 (1.35; -4.4-2.39)
	Cerebellum	-0.17 (1.28; -3.64-3.47)	-0.5 (1.09; -3.24-3.16)	-0.71 (1.03; -2.76-2.7)

C. *MAPT* mutation carriers		Disease Age Epoch		
		-40 to-10 YSO	-10 to 0 YSO	0+ YSO
	N (prop)	69 (0.41)	37 (0.22)	62 (0.37)
	Mean Age (SD)	34.1 (9.2)	46.3 (9.5)	56.1 (8.6)
	Outcome Measures			
Mean Raw Score (SD; Range)	CDR®+NACC FTLD SB	0.15 (0.48; 0-2.5)	0.39 (0.76; 0-3)	7.9 (6.51; 0-24)
	Numbers Forward	8.74 (3.3; 0-14)	8.08 (2.66; 4-14)	7.23 (2.66; 3-14)
	Numbers Backward	8.04 (2.48; 3-13)	7.54 (2.56; 3-13)	5.54 (2.53; 0-11)
	Trails A	21.06 (7.56; 12-53)	27.03 (11.08; 12-53)	47.23 (31.07; 14-150)
	Trails B	50.81 (20.69; 23-134)	59.92 (29.95; 29-164)	135.96 (86.75; 36-300)
	Semantic Fluency	24.15 (5.48; 10-36)	24.27 (5.97; 13-37)	13.75 (6.63; 0-27)
	MINT	29.88 (1.8; 25-32)	29.16 (3; 17-32)	21.22 (8.04; 1-32)
	Figure Recall	13.69 (2.63; 5-17)	12.8 (2.19; 8-17)	7.13 (5.48; 0-15)
	Figure Copy	16.01 (1.11; 13-17)	15.57 (1.24; 13-17)	14.87 (3.25; 0-17)
	RSMS	50.47 (9.76; 28-65)	50.24 (10.89; 14-65)	26 (18.66; 0-64)
	NfL (log)	1.69 (0.45; 0.39-2.53)	1.98 (0.55; 0.93-3.44)	3.04 (0.55; 1.93-5.1)
	Frontal	7.07 (0.57; 5.9-8.07)	6.72 (0.45; 5.9-7.68)	5.68 (0.82; 3.96-7.02)
	Temporal	4.86 (0.34; 4.01-5.51)	4.5 (0.25; 4.04-5.03)	3.54 (0.49; 2.83-4.43)
	Medial Temporal	1.05 (0.06; 0.87-1.16)	0.98 (0.07; 0.77-1.08)	0.72 (0.14; 0.46-1.04)
	Parietal	4.68 (0.35; 3.84-5.43)	4.44 (0.32; 3.85-5.19)	4 (0.42; 2.99-5.02)
	Occipital	1.83 (0.14; 1.56-2.07)	1.75 (0.16; 1.36-2.04)	1.64 (0.16; 1.35-1.96)
	Insula	0.76 (0.06; 0.65-0.89)	0.71 (0.06; 0.62-0.84)	0.54 (0.08; 0.43-0.73)
	Striatum	0.81 (0.07; 0.64-1)	0.77 (0.07; 0.64-0.9)	0.62 (0.13; 0.24-0.82)
	Thalamus	0.41 (0.05; 0.32-0.53)	0.4 (0.05; 0.3-0.53)	0.34 (0.05; 0.24-0.47)
	Cerebellum	6.03 (0.5; 4.95-7.44)	5.89 (0.42; 4.76-6.52)	5.52 (0.45; 4.61-6.67)
Mean Stand. Units from Control (SD; Range)	CDR®+NACC FTLD SB	---	---	---
	Numbers Forward	0.12 (1.13; -2.87-1.92)	0.13 (0.98; -1.38-2.33)	-0.06 (1.14; -1.87-2.85)
	Numbers Backward	0.3 (1.07; -1.87-2.42)	0.22 (1.06; -1.66-2.48)	-0.57 (1.12; -3.02-1.84)
	Trails A	-0.21 (0.94; -1.34-3.77)	0.07 (1.18; -1.53-2.84)	1.1 (2.12; -1.16-8.11)
	Trails B	-0.14 (0.94; -1.4-3.66)	-0.07 (1.02; -1.12-3.46)	2.05 (2.85; -1.24-7.44)
	Semantic Fluency	-0.12 (0.85; -2.32-1.72)	0.04 (1.04; -1.93-2.27)	-1.52 (1.12; -3.84-0.72)
	MINT	-0.02 (1.03; -2.82-1.19)	-0.48 (1.85; -7.98-1.27)	-4.56 (4.2; -15.12-1.07)
	Figure Recall	0.06 (1.03; -3.34-1.36)	-0.05 (0.79; -1.78-1.47)	-1.95 (2.07; -4.63-1.02)
	Figure Copy	-0.11 (0.91; -2.56-0.69)	-0.5 (1.13; -2.83-0.8)	-0.66 (2.29; -11.16-0.84)
	RSMS	0.31 (1.11; -2.25-1.97)	0.46 (1.35; -4.02-2.28)	-2.48 (2.01; -5.29-1.62)
	NfL (log)	0.04 (1.03; -2.95-1.98)	-0.19 (1.45; -2.91-3.63)	1.45 (1.26; -1.11-6.17)
	Frontal	0 (1.19; -2.43-2.09)	0.08 (1.09; -1.88-2.41)	-1.43 (1.8; -5.21-1.54)
	Temporal	0.33 (1.18; -2.6-2.56)	-0.19 (1.15; -2.27-2.19)	-2.47 (1.75; -5.02-0.68)
	Medial Temporal	0.41 (1.04; -2.7-2.15)	-0.69 (1.29; -4.46-1.15)	-3.33 (1.86; -6.87-1.04)
	Parietal	0.02 (1.1; -2.62-2.37)	0.12 (1.13; -1.93-2.74)	-0.29 (1.36; -3.59-3.03)
	Occipital	-0.05 (1.13; -2.18-1.85)	0.03 (1.24; -2.91-2.24)	0.12 (1.29; -2.23-2.72)
	Insula	0.27 (1.07; -1.7-2.84)	0.12 (1.29; -1.85-3.08)	-2.34 (1.35; -4.23-1.03)
	Striatum	0.28 (1.04; -2.12-3.07)	0.18 (0.99; -1.74-2.16)	-1.58 (1.72; -6.58-1.08)
	Thalamus	0.09 (0.85; -1.5-2.16)	0.01 (1; -2.02-2.55)	-0.54 (0.93; -2.47-1.95)
	Cerebellum	0.45 (1.09; -1.9-3.52)	0.52 (0.95; -2.04-1.95)	0.27 (0.85; -1.45-2.42)

Note. Raw and standardized values for several measures are displayed for mutation carriers (A-C) at three Disease Age epochs. Each participant was assigned to a Disease Age epoch based on the estimated Disease Age at their first visit. Raw imaging measures are presented as percentage of total intracranial volume to account for head size. Mean standardized units from controls indicates the number of standard deviations from the control group, based on the control mean and standard deviation.

Abbreviations: CDR®+NACC FTLD SB: Clinical Dementia Rating Scale plus National Alzheimer's Coordinating Center's Frontotemporal Lobar Degeneration Module Sum of Boxes; Trail A/B: Trail Making Test, Parts A & B; MINT: Multilingual Naming Test; MRI: magnetic resonance imaging; TIV: Total intracranial volume; NfL (log): Log-transformed plasma neurofilament light chain; Stand: Standard; RSMS: Revised Self-Monitoring Scale

Supplemental Table S4. Estimates extracted from the Bayesian disease progression model: Disease Age at which each endpoint deviates from controls and standardized rates of annual decline per epoch.

Endpoint	Raw value that is 1 SD worse than controls	*C9orf72*				*GRN*				*MAPT*			
		DA 1 SD Worse than Control *Mean (95% CI)*	Standardized Rate of Change			DA 1 SD Worse than Control *Mean (95% CI)*	Standardized Rate of Change			DA 1 SD Worse than Control *Mean (95% CI)*	Standardized Rate of Change		
			-40 to -10 Epoch	-10 to 0 Epoch	0+ Epoch		-40 to -10 Epoch	-10 to 0 Epoch	0+ Epoch		-40 to -10 Epoch	-10 to 0 Epoch	0+ Epoch
CDR®+NACC FTLD SB	1.18	2.0 (1.9, 2.2)	0.00	-0.04	-1.25	0.9 (0.9, 1.0)	0.00	-0.04	-2.06	1.8 (1.7, 2.0)	0.00	-0.04	-1.45
Numbers Forward	5.43	8.5 (6.9, 10.4)	0.00	-0.02	-0.09	2.5 (1.4, 3.3)	0.00	-0.04	-0.17	11.2 (9.4, 15.5)	0.00	0.00	-0.07
Numbers Backward	5.04	5.7 (4.7, 6.7)	0.00	-0.02	-0.17	2.0 (1.0, 2.6)	0.00	-0.04	-0.28	8.1 (7.1, 9.2)	0.00	0.00	-0.17
Trails A	42.17	5.3 (4.5, 6.1)	0.00	-0.02	-0.32	***1.4 (0.9, 1.9)***	**0.00**	***-0.05***	***-0.75***	6.0 (5.1, 6.9)	0.00	-0.01	-0.28
Trails B	103.99	***2.7 (1.9, 3.6)***	**0.00**	***-0.04***	***-0.37***	1.2 (0.7, 1.6)	0.00	-0.03	-0.51	5.5 (4.6, 6.3)	0.00	0.00	-0.44
Semantic Fluency	18.31	3.8 (2.7, 4.7)	0.00	-0.04	-0.23	1.4 (0.7, 2.0)	0.00	-0.05	-0.39	3.9 (2.7, 5.0)	0.00	-0.03	-0.30
MINT	26.59	9.4 (8.5, 10.3)	0.00	0.00	-0.17	2.2 (1.6, 2.6)	0.00	-0.03	-0.85	***4.3 (3.5, 5.2)***	**0.00**	***-0.01***	***-0.61***
Figure Copy	14.33	8.4 (7.5, 9.2)	0.00	-0.01	-0.16	3.2 (2.5, 3.8)	0.00	-0.02	-1.48	10.4 (8.7, 12.6)	0.00	-0.01	-0.08
Figure Recall	10.29	6.2 (5.2, 7.1)	0.00	-0.02	-0.21	1.7 (0.9, 2.4)	0.00	-0.04	-0.45	3.2 (2.1, 4.3)	0.00	-0.04	-0.29
RSMS	37.96	2.7 (1.7, 3.5)	0.00	-0.04	-0.27	2.4 (1.9, 2.9)	0.00	-0.02	-0.33	3.3 (2.3, 4.3)	0.00	-0.03	-0.29
NfL (log)	2.55	-3.0 (-0.7, -5.8)	-0.01	-0.06	-0.10	-4.9 (-3.4, -7)	-0.01	-0.18	-0.29	4.6 (7.1, 2.4)	0.00	-0.05	-0.10
MRI Frontal	6.27	-4.9 (-7.5, -2.7)	-0.02	-0.07	-0.08	***-1.1 (-1.9, -0.3)***	**0.00**	***-0.14***	***-0.41***	3.6 (1.6, 5.2)	0.00	-0.05	-0.18
MRI Temporal	4.29	***-6.1 (-9.4, -3.2)***	**-0.02**	***-0.05***	***-0.05***	-1.2 (-2.2, -0.3)	0.00	-0.12	-0.31	0.3 (-1.3, 1.6)	0.00	-0.09	-0.24
MRI MTL	0.94	-0.9 (-3.5, 1.5)	-0.01	-0.05	-0.07	0.0 (-1.0, 0.9)	0.00	-0.09	-0.36	***-1.8 (-3.2, -0.5)***	**-0.01**	***-0.11***	***-0.33***
MRI Parietal	4.14	-6.1 (-9.2, -3.2)	-0.02	-0.05	-0.05	-0.5 (-1.3, 0.3)	0.00	-0.12	-0.30	8.6 (5.8, 13.1)	0.00	-0.03	-0.07
MRI Occipital	1.62	-3.9 (-6.9, -1.0)	-0.02	-0.06	-0.02	-0.2 (-1.3, 0.9)	0.00	-0.09	-0.14	>21 (>21, >21)	0.00	-0.02	-0.02
MRI Insula	0.66	-3.9 (-7.0, -1.3)	-0.02	-0.06	-0.06	-0.8 (-1.8, 0.2)	0.00	-0.11	-0.30	0.1 (-1.4, 1.6)	0.00	-0.09	-0.23
MRI Striatum	0.68	2.0 (-0.3, 4)	-0.01	-0.05	-0.09	0.3 (-0.4, 1.0)	0.00	-0.09	-0.52	4.5 (2.9, 5.8)	0.00	-0.03	-0.23
MRI Thalamus	0.34	-3.1 (-7.4, 1.1)	-0.02	-0.03	-0.03	1.5 (0.6, 2.4)	0.00	-0.06	-0.22	9.0 (6.6, 12.6)	0.00	-0.02	-0.08
MRI Cerebellum	5.15	3.9 (0.3, >21)	-0.01	-0.04	-0.03	0.1 (-0.9, 1.2)	0.00	-0.10	-0.07	>21 (10.5, >21)	0.00	0.00	-0.06

Note. For each endpoint, the raw value corresponding to one standard deviation (SD) worse than controls is displayed. For MRI values, these values indicate the percentage of total intracranial volume that is one SD lower than controls. For each genetic group, the Disease Age at which each endpoint's curve reaches one standard deviation from controls is displayed, with lower values indicating earlier deviations from controls. For each Disease Age epoch, the annualized rate of change from the model fit was then standardized relative to the rate of change observed in controls from the corresponding epoch. The age at which measures deviated by one SD from controls and the standardized rates of change were used to select the neuropsychological test and brain regions included in the figures and tables of the main text (bolded here).

Abbreviations: SD: Standard Deviation; DA: Disease Age; CI: Credible Interval; CDR®+NACC FTLD SB: Clinical Dementia Rating Scale plus National Alzheimer's Coordinating Center's Frontotemporal Lobar Degeneration Module Sum of Boxes; Trails A/B: Trail Making Test, Parts A & B; MINT: Multilingual Naming Test; RSMS: Revised Self-Monitoring Scale; NfL(log): Log-transformed plasma neurofilament light chain; MRI: magnetic resonance imaging

Supplemental Table S5. Baseline comparisons of mutation carriers and controls

			Disease Age Epoch								
			-40 to -10			-10 to 0			0+		
Mutation	Domain	Measure	Estimate	p	95%CI	Estimate	p	95%CI	Estimate	p	95%CI
C9orf72	Global	CDR® NACC FTLD SB	**0.19**	**< 0.001**	**(0.12,0.27)**	**0.31**	**< 0.001**	**(0.16,0.46)**	**8.32**	**< 0.001**	**(7.08,9.56)**
	Clinical	Trails A	**-3.54**	**0.001**	**(-5.52,-1.56)**	**-5.05**	**0.007**	**(-8.67,-1.43)**	**-27.99**	**< 0.001**	**(-35.36,-20.62)**
		Trails B	**-5.11**	**0.034**	**(-9.83,-0.38)**	**-21.94**	**0.001**	**(-34.20,-9.69)**	**-94.62**	**< 0.001**	**(-113.68,-75.56)**
		Numbers Forward	-0.22	0.456	(-0.82,0.37)	-0.10	0.830	(-1.00,0.81)	**-1.68**	**< 0.001**	**(-2.31,-1.05)**
		Numbers Backward	0.23	0.345	(-0.25,0.71)	0.00	1.000	(-0.77,0.77)	**-2.70**	**< 0.001**	**(-3.31,-2.08)**
		MINT	0.00	0.997	(-0.44,0.44)	-0.31	0.346	(-0.95,0.33)	**-5.27**	**< 0.001**	**(-6.79,-3.75)**
		Animals	-0.82	0.220	(-2.12,0.49)	-1.04	0.268	(-2.88,0.81)	**-9.69**	**< 0.001**	**(-11.42,-7.96)**
		Figure Recall	**-0.85**	**0.003**	**(-1.42,-0.28)**	-0.26	0.551	(-1.13,0.60)	**-3.53**	**< 0.001**	**(-4.50,-2.55)**
		Figure Copy	0.00	0.990	(-0.27,0.27)	-0.32	0.124	(-0.72,0.09)	**-1.92**	**< 0.001**	**(-2.65,-1.20)**
		RSMS	-1.11	0.297	(-3.22,0.99)	-0.13	0.940	(-3.45,3.20)	**-24.29**	**< 0.001**	**(-27.42,-21.16)**
	Plasma	NfL (Log)	**0.22**	**< 0.001**	**(0.11,0.33)**	**0.53**	**< 0.001**	**(0.35,0.70)**	**0.90**	**< 0.001**	**(0.70,1.09)**
	Imaging	Frontal	**-0.21**	**0.001**	**(-0.32,-0.09)**	**-0.57**	**< 0.001**	**(-0.73,-0.40)**	**-1.00**	**< 0.001**	**(-1.20,-0.80)**
		Temporal	**-0.18**	**< 0.001**	**(-0.25,-0.11)**	**-0.39**	**< 0.001**	**(-0.48,-0.29)**	**-0.48**	**< 0.001**	**(-0.61,-0.35)**
		Medial Temporal	**-0.02**	**0.010**	**(-0.03,0.00)**	**-0.08**	**< 0.001**	**(-0.10,-0.05)**	**-0.10**	**< 0.001**	**(-0.13,-0.07)**
		Parietal	**-0.18**	**< 0.001**	**(-0.26,-0.10)**	**-0.43**	**< 0.001**	**(-0.55,-0.32)**	**-0.51**	**< 0.001**	**(-0.64,-0.39)**
		Occipital	**-0.07**	**< 0.001**	**(-0.10,-0.04)**	**-0.17**	**< 0.001**	**(-0.22,-0.12)**	**-0.18**	**< 0.001**	**(-0.23,-0.12)**
		Insula	**-0.03**	**< 0.001**	**(-0.04,-0.01)**	**-0.06**	**< 0.001**	**(-0.07,-0.04)**	**-0.09**	**< 0.001**	**(-0.11,-0.07)**
		Striatum	-0.02	0.080	(-0.03,0.00)	**-0.05**	**< 0.001**	**(-0.08,-0.03)**	**-0.11**	**< 0.001**	**(-0.15,-0.08)**
		Thalamus	**-0.04**	**< 0.001**	**(-0.05,-0.03)**	**-0.06**	**< 0.001**	**(-0.08,-0.05)**	**-0.07**	**< 0.001**	**(-0.08,-0.05)**
		Cerebellum	-0.11	0.053	(-0.23,0.00)	**-0.34**	**< 0.001**	**(-0.50,-0.18)**	**-0.37**	**< 0.001**	**(-0.56,-0.19)**
GRN	Global	CDR® NACC FTLD SB	**0.08**	**< 0.001**	**(0.05,0.11)**	**0.31**	**< 0.001**	**(0.16,0.46)**	**9.19**	**< 0.001**	**(7.89,10.49)**
	Clinical	Trails A	**-2.61**	**0.006**	**(-4.48,-0.75)**	**-4.20**	**0.010**	**(-7.38,-1.03)**	**-41.05**	**< 0.001**	**(-51.02,-31.08)**
		Trails B	-3.62	0.138	(-8.41,1.17)	**-10.36**	**0.030**	**(-19.69,-1.03)**	**-131.73**	**< 0.001**	**(-153.33,-110.12)**
		Numbers Forward	-0.38	0.231	(-1.00,0.24)	-0.63	0.139	(-1.48,0.21)	**-2.61**	**< 0.001**	**(-3.34,-1.88)**
		Numbers Backward	-0.29	0.261	(-0.80,0.22)	-0.53	0.165	(-1.27,0.22)	**-3.31**	**< 0.001**	**(-4.07,-2.56)**
		MINT	-0.05	0.817	(-0.44,0.35)	0.24	0.398	(-0.32,0.80)	**-6.17**	**< 0.001**	**(-7.62,-4.72)**
		Animals	0.16	0.807	(-1.16,1.49)	0.06	0.949	(-1.84,1.97)	**-10.93**	**< 0.001**	**(-12.99,-8.88)**
		Figure Recall	-0.40	0.173	(-0.97,0.18)	-0.63	0.155	(-1.49,0.24)	**-5.09**	**< 0.001**	**(-6.19,-3.99)**
		Figure Copy	0.22	0.092	(-0.04,0.49)	0.00	0.990	(-0.40,0.40)	**-2.20**	**< 0.001**	**(-3.11,-1.30)**
		RSMS	-0.43	0.674	(-2.43,1.58)	-1.19	0.431	(-4.19,1.80)	**-19.18**	**< 0.001**	**(-22.90,-15.45)**
	Plasma	NfL (Log)	**0.20**	**< 0.001**	**(0.09,0.31)**	**0.40**	**< 0.001**	**(0.24,0.56)**	**1.63**	**< 0.001**	**(1.45,1.80)**
	Imaging	Frontal	-0.04	0.530	(-0.16,0.08)	**-0.28**	**0.001**	**(-0.44,-0.12)**	**-1.17**	**< 0.001**	**(-1.43,-0.92)**
		Temporal	-0.03	0.487	(-0.10,0.05)	**-0.23**	**< 0.001**	**(-0.32,-0.13)**	**-0.47**	**< 0.001**	**(-0.61,-0.32)**
		Medial Temporal	-0.01	0.369	(-0.02,0.01)	**-0.05**	**< 0.001**	**(-0.07,-0.03)**	**-0.09**	**< 0.001**	**(-0.13,-0.06)**
		Parietal	-0.02	0.719	(-0.10,0.07)	**-0.19**	**0.001**	**(-0.29,-0.08)**	**-0.47**	**< 0.001**	**(-0.63,-0.30)**
		Occipital	-0.03	0.076	(-0.07,0.00)	**-0.09**	**0.001**	**(-0.14,-0.04)**	**-0.10**	**0.001**	**(-0.16,-0.04)**
		Insula	**-0.01**	**0.035**	**(-0.03,0.00)**	**-0.04**	**< 0.001**	**(-0.05,-0.02)**	**-0.08**	**< 0.001**	**(-0.11,-0.06)**
		Striatum	-0.01	0.160	(-0.03,0.00)	-0.02	0.057	(-0.05,0.00)	**-0.16**	**< 0.001**	**(-0.20,-0.12)**
		Thalamus	0.01	0.424	(-0.01,0.02)	**-0.03**	**0.003**	**(-0.04,-0.01)**	**-0.05**	**< 0.001**	**(-0.07,-0.03)**
		Cerebellum	-0.08	0.234	(-0.20,0.05)	**-0.22**	**0.008**	**(-0.38,-0.06)**	**-0.38**	**< 0.001**	**(-0.58,-0.18)**
MAPT	Global	CDR® NACC FTLD SB	**0.15**	**< 0.001**	**(0.09,0.21)**	**0.39**	**< 0.001**	**(0.23,0.55)**	**7.90**	**< 0.001**	**(6.61,9.20)**
	Clinical	Trails A	1.70	0.120	(-0.45,3.85)	-0.66	0.737	(-4.57,3.24)	**-16.15**	**< 0.001**	**(-23.54,-8.77)**
		Trails B	3.00	0.316	(-2.87,8.86)	2.14	0.714	(-9.41,13.69)	**-62.33**	**< 0.001**	**(-82.12,-42.53)**
		Numbers Forward	0.36	0.388	(-0.46,1.17)	0.36	0.494	(-0.69,1.41)	-0.13	0.749	(-0.95,0.68)
		Numbers Backward	**0.69**	**0.035**	**(0.05,1.33)**	0.54	0.266	(-0.42,1.50)	**-1.30**	**0.001**	**(-2.08,-0.51)**
		MINT	-0.04	0.868	(-0.52,0.44)	-0.78	0.066	(-1.61,0.05)	**-8.73**	**< 0.001**	**(-10.43,-7.02)**
		Animals	-0.80	0.357	(-2.49,0.90)	0.23	0.837	(-2.02,2.49)	**-9.01**	**< 0.001**	**(-11.09,-6.93)**
		Figure Recall	0.16	0.647	(-0.54,0.87)	-0.14	0.793	(-1.18,0.91)	**-5.17**	**< 0.001**	**(-6.51,-3.84)**
		Figure Copy	-0.14	0.414	(-0.47,0.19)	**-0.55**	**0.019**	**(-1.01,-0.09)**	**-0.93**	**0.018**	**(-1.70,-0.16)**
		RSMS	**2.73**	**0.038**	**(0.16,5.31)**	3.70	0.067	(-0.27,7.66)	**-23.00**	**< 0.001**	**(-27.63,-18.37)**
	Plasma	NfL (Log)	0.02	0.764	(-0.11,0.15)	-0.07	0.453	(-0.26,0.12)	**0.63**	**< 0.001**	**(0.46,0.80)**
	Imaging	Frontal	0.00	0.997	(-0.15,0.15)	0.03	0.713	(-0.15,0.22)	**-0.65**	**< 0.001**	**(-0.89,-0.41)**
		Temporal	**0.10**	**0.041**	**(0.00,0.19)**	-0.04	0.400	(-0.14,0.06)	**-0.69**	**< 0.001**	**(-0.84,-0.55)**
		Medial Temporal	**0.02**	**0.010**	**(0.01,0.04)**	**-0.04**	**0.005**	**(-0.07,-0.01)**	**-0.25**	**< 0.001**	**(-0.29,-0.21)**
		Parietal	0.01	0.892	(-0.09,0.11)	0.03	0.599	(-0.10,0.17)	-0.09	0.211	(-0.23,0.05)
		Occipital	-0.01	0.739	(-0.05,0.03)	0.00	0.914	(-0.06,0.07)	0.02	0.587	(-0.04,0.07)
		Insula	0.01	0.085	(0.00,0.03)	0.01	0.626	(-0.02,0.03)	**-0.13**	**< 0.001**	**(-0.16,-0.11)**
		Striatum	0.02	0.072	(0.00,0.04)	0.01	0.403	(-0.02,0.04)	**-0.12**	**< 0.001**	**(-0.16,-0.08)**
		Thalamus	0.01	0.547	(-0.01,0.02)	0.00	0.961	(-0.02,0.02)	**-0.03**	**0.007**	**(-0.05,-0.01)**
		Cerebellum	**0.21**	**0.005**	**(0.06,0.35)**	**0.23**	**0.019**	**(0.04,0.42)**	0.15	0.158	(-0.06,0.35)

Note. Each participant was assigned to a Disease Age epoch based on the estimated Disease Age at their first visit. For each mutation, baseline values of each measure were compared to controls at the three epochs using linear regression; the statistical tests were two-sided and no adjustments for multiple comparisons were applied. Bolded text indicates statistically significant differences ($p < .05$). The estimates represent the difference between carriers and controls. The units for CDR®NACC FTLD SB are raw box scores, with a positive contrast representing greater impairment in carriers. Similarly, for log NfL values, higher positive values represent higher levels in carriers. Raw values on clinical measures were used, with negative contrasts indicating poorer performance in mutation carriers compared to controls. Brain volume was estimated at percentage of total intracranial volume, with negative contrasts indicating lower volume (relative to head size) in mutation carriers. Note that statistical comparisons for the CDR®+NACC FTLD SB should be interpreted with caution given that controls were defined as having a baseline CDR®+NACC-FTLD=0 and thus have no variance due to this selection process. These parameters complement the effect sizes displayed in Extended Figure 1.

Abbreviations: CI: Confidence Interval; CDR®+NACC FTLD SB: Clinical Dementia Rating Scale plus National Alzheimer's Coordinating Center's Frontotemporal Lobar Degeneration Module Sum of Boxes; Trails A/B: Trail Making Test, Parts A & B; MINT: Multilingual Naming Test; RSMS: Revised Self-Monitoring Scale; NfL(log): Log-transformed plasma neurofilament light chain

Supplemental Table S6. Cross-sectional statistical comparison of baseline measures among the three f-FTLD genetic groups

		Disease Age Epoch								
		-40 to -10			-10 to 0			0+		
Domain	**Measure**	**Model F**	**p**	**Posthoc Comparison**	**Model F**	**p**	**Posthoc Comparison**	**Model F**	**p**	**Posthoc Comparison**
Global	**CDR®NACC FTLD SB**	2.03	0.133	--	0.19	0.829	--	0.82	0.44	--
Clinical	**Trails A**	6.99	0.001	(C=G)<M	1.71	0.184	--	6.58	0.002	(C=G), (C=M), G<M
	Trails B	3.39	0.035	(C=G), (G=M), C<M	5.23	0.006	(C=G), (G=M), C<M	7.57	0.001	G<(C=M)
	Animals	1.26	0.286	--	0.76	0.469	--	1.24	0.29	--
	Figure Copy	2.43	0.089	--	2.13	0.122	--	2.19	0.114	--
	Figure Recall	3.43	0.034	(C=G), (G=M), C<M	0.61	0.546	--	3.92	0.021	--
	Numbers Forward	1.67	0.19	--	1.77	0.173	--	15.6	< 0.001	G<C<M
	Numbers Backward	4.45	0.012	(C=G), (C=M), G<M	2.67	0.072	--	10.53	< 0.001	(C=G)<M
	MINT	0.02	0.982	--	2.48	0.087	--	4.29	0.015	(C=G), (G=M), M<C
	RSMS	3.52	0.031	(C=G), (G=M), C<M	2.38	0.096	--	2.86	0.059	--
Plasma	**NfL (Log)**	4.23	0.016	M<(C=G)	11.19	< 0.001	M<(C=G)	29.33	< 0.001	(C=M)<G
Imaging	**Frontal**	3.81	0.023	(C=G), (G=M), C<M	14.03	< 0.001	C<G<M	4.68	0.01	(C=G), (C=M), G<M
	Temporal	13.79	< 0.001	C<(G=M)	12.13	< 0.001	C<G<M	3.08	0.049	--
	Medial Temporal	8.97	< 0.001	(C=G)<M	3.24	0.042	--	23.27	< 0.001	M<(C=G)
	Parietal	7.17	0.001	C<(G=M)	18.22	< 0.001	C<G<M	10.45	< 0.001	(C=G)<M
	Occipital	3.88	0.022	(C=G), (G=M), C<M	12.06	< 0.001	C<G<M	13.56	< 0.001	(C=G)<M
	Insula	9.47	< 0.001	(C=G)<M	11.71	< 0.001	(C=G)<M	5.18	0.007	M<(C=G)
	Thalamus	19.9	< 0.001	C<(G=M)	16.7	< 0.001	C<G<M	4.73	0.01	(C=G), (G=M), C<M
	Striatum	4.96	0.008	(C=G)<M	8.54	< 0.001	(C=G), (G=M), C<M	2.42	0.092	--
	Cerebellum	6.93	0.001	(C=G)<M	14.71	< 0.001	(C=G)<M	13	< 0.001	(C=G)<M

Note. Each participant was assigned to a Disease Age epoch based on the estimated Disease Age at their first visit. For each measure at each epoch, baseline values were compared across the three carrier groups by fitting a linear regression model with a three-level categorical predictor; the statistical tests were two-sided. CDR®NACC FTLD SB units, log NfL values, raw clinical scores, and brain volume as a percentage of total intracranial volume were modeled as the outcomes. If the overall model was statistically significant, pairwise comparisons were conducted with Tukey correction for multiple comparisons. For clinical and imaging measures, the directionality of the pairwise comparisons is such that lower values (i.e., to the left of the < sign) represent more impairment, whereas higher values (i.e., to the right of the < sign) represent more impairment for CDR®+NACC FTLD SB and NfL. For example, for thalamic atrophy in Disease Age epoch -50 to -10, *C9orf72*+ carriers have statistically less thalamic volume compared to the other two groups and *GRN*+ have statistically higher log NfL compared to the other groups in the symptomatic 0+ epoch.

Abbreviations: CDR®+NACC FTLD SB: Clinical Dementia Rating Scale plus National Alzheimer's Coordinating Center's Frontotemporal Lobar Degeneration Module Sum of Boxes; Trails A/B: Trail Making Test, Parts A & B; MINT: Multilingual Naming Test; RSMS: Revised Self-Monitoring Scale; NfL(log): Log-transformed plasma neurofilament light chain

Supplemental Table S7. Scanner distribution by genetic group and consortium.

A. All Participants with at least one scan that passed quality control

Sample	Prisma Fit	Achieva	TrioTim	Discovery MR750	Prisma	Intera	Achieva dStream	Skyra fit	Skyra	Biograph mMR	Signa HDxt	Total
Reference Group	79	68	46	34	16	9	9	8	44	4	0	317
C9orf72	66	62	39	10	9	10	16	4	23	0	0	239
GRN	44	46	50	9	8	7	0	1	33	1	6	205
MAPT	39	17	12	23	5	0	1	1	17	6	0	121

B. ALLFTD Participants with at least one scan that passed quality control

Sample	Prisma Fit	Achieva	TrioTim	Discovery MR750	Prisma	Intera	Achieva dStream	Skyra fit	Skyra	Biograph mMR	Signa HDxt	Total
Reference Group	40	11	9	34	0	9	0	0	7	4	0	114
C9orf72	25	14	6	10	0	10	0	0	1	0	0	66
GRN	16	0	9	9	0	7	0	0	2	1	2	46
MAPT	22	2	1	23	0	0	0	0	4	6	0	58

C. GENFI Participants with at least one scan that passed quality control

Sample	Prisma Fit	Achieva	TrioTim	Discovery MR750	Prisma	Intera	Achieva dStream	Skyra fit	Skyra	Biograph mMR	Signa HDxt	Total
Reference Group	39	57	37	0	16	0	9	8	37	0	0	203
C9orf72	41	48	33	0	9	0	16	4	22	0	0	173
GRN	28	46	41	0	8	0	0	1	31	0	4	159
MAPT	17	15	11	0	5	0	1	1	13	0	0	63

Note. This table presents the number of scanners at baseline used for each group in the overall sample (A) and the ALLFTD (B) and GENFI (C) cohorts.

Supplemental Table S8. Model priors: Endpoint-specific expected best and worst values and grouping structure for correlation of subject-specific random effects across similar endpoints

Endpoint	Value at normal	Expected Worst Value	Grouping
CDR®+NACC FTLD SB	0	24	1
Trails A	20	150	2
Trails B	50	300	2
Animals	25	0	3
Figure Copy	17	0	4
Figure Recall	17	0	4
Number Span Forward	14	0	5
Number Span Backward	14	0	5
MINT	32	0	6
RSMS	65	0	7
NfL (log)	1.5	6	8
MRI Frontal	8	2	9
MRI Temporal	5	2	9
MRI Insula	1	0	9
MRI Parietal	5	2	9
MRI Occipital	2	0	9
MRI Cerebellum	6	2	9
MRI Thalamus	0.4	0	9
MRI Striatum	1	0	9
MRI MTL	1	0	9

Note. Presented here are the measures that were simultaneously modeled in the disease progression models, along with the values at normal and the expected worst value, both of which were incorporated into the model priors. All measures are presented in raw units; MRI measures are presented as percentage of total intracranial volume. Variables that share a Grouping number were specified to have correlated subject and endpoint-specific random effects based on shared characteristics of the measures (e.g., all MRI measures were grouped).

Abbreviations: CDR®+NACC FTLD SB: Clinical Dementia Rating Scale plus National Alzheimer's Coordinating Center's Frontotemporal Lobar Degeneration Module Sum of Boxes; Trail A/B: Trail Making Test, Parts A & B; MINT: Multilingual Naming Test; RSMS: Revised Self-Monitoring Scale; NfL (log): Log-transformed plasma neurofilament light chain; MRI: magnetic resonance imaging

Supplemental Table S9. Clinical trial simulation assumptions

CDR®+NACC FTLD Global	*C9orf72*	*GRN*	*MAPT*
Percentage of Population			
0	62%	70%	69%
0.5	25%	15%	20%
1	13%	15%	11%
Mean (SD) YSO per* CDR®+NACC-FTLD *Global Score			
0	-16.0 (10.0)	-14.0 (11.0)	-14.0 (10.0)
0.5	1.5 (2.8)	-0.3 (2.8)	0.4 (3.1)
1	5.8 (1.8)	3.1 (0.5)	5.7 (1.1)

Note. This table displays the assumptions for the clinical trial simulations. For each genetic group, CDR®+NACC-FTLD Global distribution and mean Disease Age given CDR®+NACC-FTLD Global are displayed. These estimates were based on the natural history data.

Abbreviations: *CDR®+NACC FTLD SB: Clinical Dementia Rating Scale plus National Alzheimer's Coordinating Center's Frontotemporal Lobar Degeneration Module Global Score; SD: Standard Deviation; YSO: Years since onset.*